The role of *miR-154* in early lung development

Inauguraldissertation
zur Erlangung des Grades eines Doktors der Medizin
des Fachbereichs Medizin
der Justus-Liebig-Universität Gießen

vorgelegt von Kolck, Johannes,
aus Bielefeld

Gießen 2019

Aus der Medizinischen Klinik und Poliklinik II
unter der Leitung von Prof. Dr. Werner Seeger,
des Fachbereichs Medizin der Justus-Liebig-Universität Gießen

Gutachter: Prof. Dr. Bellusci
Gutachter: Prof. Dr. Savai

Tag der Disputation: 22. Juni, 2020

Erklärung zur Dissertation

„Hiermit erkläre ich, dass ich die vorliegende Arbeit selbständig und ohne unzulässige Hilfe oder Benutzung anderer als der angegebenen Hilfsmittel angefertigt habe. Alle Textstellen, die wörtlich oder sinngemäß aus veröffentlichten oder nichtveröffentlichten Schriften entnommen sind, und alle Angaben, die auf mündlichen Auskünften beruhen, sind als solche kenntlich gemacht. Bei den von mir durchgeführten und in der Dissertation erwähnten Untersuchungen habe ich die Grundsätze guter wissenschaftlicher Praxis, wie sie in der „Satzung der Justus- Liebig-Universität Gießen zur Sicherung guter wissenschaftlicher Praxis“ niedergelegt sind, eingehalten sowie ethische, datenschutzrechtliche und tierschutzrechtliche Grundsätze befolgt. Ich versichere, dass Dritte von mir weder unmittelbar noch mittelbar geldwerte Leistungen für Arbeiten erhalten haben, die im Zusammenhang mit dem Inhalt der vorgelegten Dissertation stehen, oder habe diese nachstehend spezifiziert. Die vorgelegte Arbeit wurde weder im Inland noch im Ausland in gleicher oder ähnlicher Form einer anderen Prüfungsbehörde zum Zweck einer Promotion oder eines anderen Prüfungsverfahrens vorgelegt. Alles aus anderen Quellen und von anderen Personen übernommene Material, das in der Arbeit verwendet wurde oder auf das direkt Bezug genommen wird, wurde als solches kenntlich gemacht. Insbesondere wurden alle Personen genannt, die direkt und indirekt an der Entstehung der vorliegenden Arbeit beteiligt waren. Mit der Überprüfung meiner Arbeit durch eine Plagiatserkennungssoftware bzw. ein internetbasiertes Softwareprogramm erkläre ich mich einverstanden.“

_____ _____

Ort, Datum Unterschrift

Table of Content

List of figures

List of tables

Abbreviations

ACTA2/α-SMA	Smooth muscle actin
AECI	Alveolar epithelial cell type I
AECII	Alveolar epithelial cell type II
AGO	Argonaute protein
AMF	Alveolar myofibroblast
AQP5	Aquaporin 5
BMP	Bone morphogenetic protein
BMPR	Bone morphogenetic protein receptor
BPD	Bronchopulmonary dysplasia
CC10	Clara cell-specific 10 kDA protein or Scgb1a1
CCSP	Clara cell secretory protein 16 kDA
cDNA	Complementary DNA
COPD	Chronic obstructive pulmonary disease
DAPI	4',6'-diamidino-2-phenylindole, dihydrochloride
DGCR8	DiGeorge critical region 8
DMEM	Dulbecco´s Modified Eagle Medium
DNA	Deoxyribonucleic acid
DOX	Doxycycline
ECM	Extracellular matrix
EGF	Epidermal growth factor
EMT	Epithelial to mesenchymal transition
EpCam	Epithelial cell adhesion molecule
ERK	Extracellular signal-regulated kinase
Etv4/5	ETS translocation variant 4/5
FGF	Fibroblast growth factor
FGFR	Fibroblast growth factor receptor
FMPR1	Fragile X mental retardation protein 1
FSTL1	Follistatin like 1
GAG	Glycosaminoglycan
HBL-1	Hunchback like 1
H&E	Hematoxylin and Eosin stain

HBS	Heparin sulphate glycosaminoclycan binding site
Hox	Homebox transcription factor
HPRT	Hypoxanthine-guanine phosphoribosyltransferase
HMGA2	High mobility group A2
HSGAG	Heparin sulphate glycosaminoclycan
HVC	Hepatitis C virus
IGF	Insulin like growth factor
IPF	Idiopathic pulmonary fibrosis
LIF	Lipofibroblast
miR	Micro RNA
MIRG	miRNA-containing gene
MLI	Mean linear intercept
MYF	Myofibroblasts
NHLF	Normal human lung fibroblast
NKX2.1	NK homeobox 1 or TTF1
NMYC	N-myc proto-oncogene protein or basic helix-loop-helix protein 37 (bHLHe37)
NSCLC	Non-small lung cancer
PABP	Poly A bindin protein
PAI-1	Plasminogen activator inhibitor-1
PAH	Pulmonary hypertension
PBS	Phosphate buffered saline
PFA	Parafromaldehyde
PCR	Polymerase chain reaction
PDGF-A	Platelet-derived growth factor A
PDGFR-α	Platelet-derived growth factor receptor alpha
qPCR	Quantitative real-time PCR
RA	Retinoic acid
RISC	RNA-induced silencing complex
RNA	Ribonucleic acid
RT	Room Temperature
siRNA	Small interfering RNA
SPA	Surfactant protein A

SPB	Surfactant protein B
SPC	Surfactant protein C
SPD	Surfactant protein D
snoRNA	Small nuclear RNA
SPRY 2	Sprouty homolog 2
SPRY 4	Sprouty homolog 4
tet(O)	Tetracycline binding site
TGF-ß	Transforming growth factor beta
Tgf-ßR	Transforming growth factor beta receptor
TRBP	TAR RNA binding protein
TTF-1	Thyroid transcription factor 1 or NKX2.1
IL1-β	Interleukin 1 beta
µm	Micrometer
µl	Microliter
UTR	Untranslated region
WT	Wild type
WNT	Wingless/integrated

The role of *miR-154* in early lung development

1 Introduction

1.1 The Lung

In all mammals and terrestrial vertebrates, the lung is responsible for the vital gas exchange between blood and air. The Human lung lies within the thoracic cavity and is divided into two by the mediastinum. The left lung is comprised of two lobes, and the right lung has three lobes. From the outside, the lung is surrounded by the visceral pleura, which closely fits the lung. The visceral pleura lies within the parietal pleura, which is attached to the thoracic cavity. The thin fluid filled space between the two pleurae is called the pleural cavity. The diaphragm is a skeletal muscle, which lies caudally on the lung and separates the thoracic and the abdominal cavity. It performs inhalation and exhalation by contraction and relaxation. The human lung has a dual blood supply. The vasa privata are arteries that branch off the aorta and supply lung tissue with oxygen. The vasa publica serve the whole organism. They transport systemic oxygen-poor blood to the lung, where it is oxygenated and conduct the oxygen rich blood back to the heart. In that way, the lung provides essential oxygen to the body.
Functionally, the lung can be subdivided into the conducting and respiratory zones. Nose, pharynx, larynx, trachea, bronchi, bronchioles and terminal bronchioles are considered as conducting airways. The trachea constitutes the connection between pharynx and lung. It consists of cartilaginous rings, which are joined by fibrous connective tissue and smooth muscle. The inside of the trachea is lined with pseudo stratified ciliated columnar epithelium and mucine-secreting goblet cells. The mucus helps to intercept foreign particles, which then are transported upwards to the larynx and pharynx to be coughed up or swallowed. The cricoid cartilage serves to connect the

trachea to the larynx. Dorsally the trachea divides into the right and left primary bronchus. The average tracheal diameter lies in between 8 and 12 mm. As the right lung comprises three lobes, the right main bronchus further divides into three lobar bronchi. Accordingly, the left does into two. The lobar bronchi further subdivide, the right into 10 and the left into 9 segmental bronchi. The next divisional unit is called bronchiole and is characterized by the loss of cartilage and goblet cells. Here the average diameter is less then 1 mm. Each bronchiole is divided into 4 to 5 terminal bronchioles. As the number of goblet cells is reduced in the further course, the number of Club-cells, also known as Clara cells, increases. These cells secrete surfactant-like proteins, or Clara cell secretory protein, CCSP, and lysozyme, which serve unspecific immune defense. Elastic fibers prevent the lumen from collapsing, which was before achieved by cartilage tissue. At this point the respiratory zone begins. This functional unit is responsible for sufficient gas exchange and consists of respiratory bronchioles, alveolar ducts and the alveoli. The respiratory bronchioles and the ducti alveolaris connect the alveolar sacs to the conductive system. Their wall already shows isolated alveoli. Alveoli account for roughly 70% of lung surface. For this exchange a huge surface is obligatory. In human, lung surface comprises about 100 square meters. About 300 million alveoli perform 90% of blood oxygenation and release of carbon dioxide. Alveoli have a roundish form with a diameter of approximately 200 µm, which fluctuates depending on inhalation and exhalation. Alveoli consist of two types of alveolar cell. 95% of the surface is made up of alveolar epithelial cells type I (AECI, or Pneumocytes type I), which form the structure of alveoli and represent the epithelial side of the air-blood-barrier. These cells are flat and extraordinary thin, sometimes only 25nm. This facilitates the exchange of carbon dioxide and oxygen between alveoli and blood. The passive diffusion is dependent on partial pressure levels. Alveolar epithelial cells type II (AECII, also Pneumocytes type II) only constitute about 5% of the alveolar surface. However, they account for 60% of all alveolar epithelial cells. AECII are able to give rise to AECI by mitosis and therefore play an important role in injury repair. Moreover, they are involved in immune defence. Here the secretion of products, such as surfactant protein A and D (SPA, SPD) play an important role. Those proteins are able to bind pathogens, which are then destroyed by alveolar macrophages. The surface active agent (surfactant) is composed of phospholipids, cholesterol and proteins in a ratio of 10:1:1 and functions in preventing the alveoli from collapsing at the end of expiration and in increasing

pulmonary compliance by reduction of surface tension (Macklin 1954; Pison et al. 1994; Hoffman and Ingenito 2012).

Expansion and collapse of the alveoli during respiration mean great stress for the alveolar structure. The framework of AECI and AECII cells is therefore strengthened by extracellular matrix (ECM) and interstitial fibroblasts. Collagen types I and III, elastin, fibronectin, laminin and glycosaminoglycans (GAGs) are major components of the ECM (Pelosi et al. 2007). Myofibroblasts (also known as alveolar smooth muscle cells) are located at the tip of new forming septa and synthesize elastin. Lipofibroblasts are situated at the base of septa and strike through their lipid-filled cytoplasm. They are also involved in generating ECM proteins and assist the AECII cells in the production of surfactant (McGowan and Torday 1997; Vaccaro and Brody 1978).

1.2 Embryonic lung development

Morphologically there are some differences between mouse and human lung. Although the mice lung is also divided into two, the right side consists of a cranial, a medial, a caudal and an accessory lobe and the left lung only comprises one single lobe. Embryonic lung development in mice is a very well documented process and therefore presents itself as suitable basis for developmental research. A rough overview will be pictured in the following:

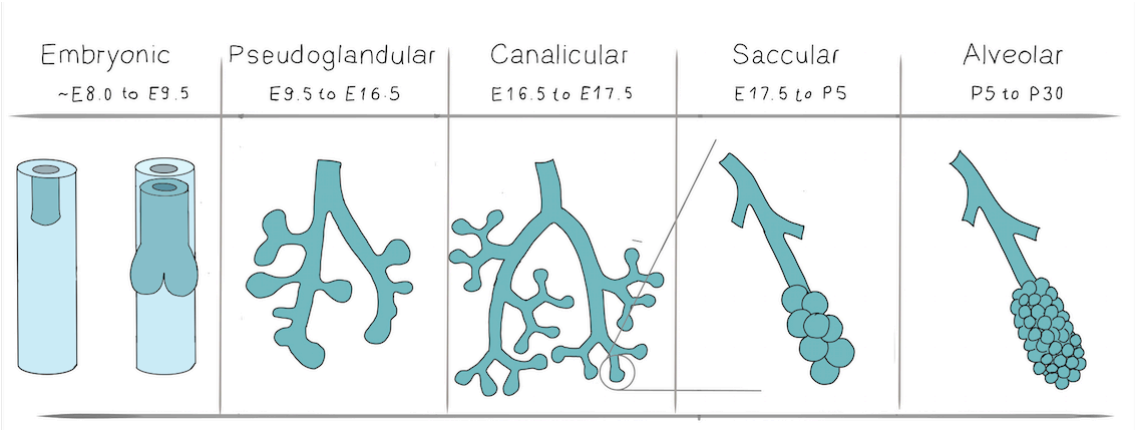

Figure 01. Overview of embryonic lung development.
Depicted are the embryonic and the four subsequent histological stages of embryonic lung development in mice from E8.0 to P30.

During embryonic day 9 (E9) until E 11.5 the primitive lung anlage arises from the ventral wall of the foregut, an endodermal tube, which is surrounded by mesenchyme and mesothelium. Here the laryngotracheal groove forms, initiating the emergence of the laryngotracheal diverticulum. This protrusion further separates dorsoventrally building the primitive trachea and the first two bronchial branches. Foregut, or embryonic esophagus, and trachea separate from each other, as more branching at each side of the first bronchial branches takes place (Spooner and Wessells 1970). The epithelial elements of trachea and lung derive from dorsal esophageal endoderm. Distal lung mesenchyme emerges from somatopleura. In contrast, splanchnic mesoderm gives rise to trachea-bronchiolar mesenchyme. Visceral pleura later on arises out of the mesothelium, which is associated with lung buds (Brown and James 2009). Both mesoderm and endoderm express regulatory molecules, such as homeobox transcription factors (Hox), retinoic acid (RA) and other growth factors or transcription factors. Those orchestrate the further organogenesis. NKX2.1 (thyroid transcription factor 1, TFT1) for instance has been recognized as fundamental to early lung development. It is an early marker of lung endoderm, which is also expressed in emerging thyroid and brain. Although *Nkx2.1* knock out mice are able to grow trachea and lung buds, branching morphogenesis is diminished and endodermal as well as epithelial differentiation are lacking (Minoo et al. 1999).

The consecutive development can be differentiated into four histological stages: The pseudoglandular stage starts with embryonic day 11.5 (E11.5) and lasts until E16.5. It is than followed by the canalicular stage, which spreads from 16.5 to 17.5. The third (saccular) stage occurs from E17.5 to postnatal day 5 (P5) and merges into the alveolar stage. By the end of P30, all histological stages are completed.

During the pseudoglandular stage intense epithelial branching forms a gland like lung structure. The epithelium and mesenchyme are the two main germ layers of the developing lung. The epithelium is organized in basal, ciliated, secretory and neuroendocrine cells. Endothelial, chondrocytic, smooth muscle, nerve and lymphatic cells are found in the mesenchyme. At this time point the fluid-filled terminal bronchioles are still incapable of gas exchange. In the canalicular stage the conducting airway system further extends. Here respiratory bronchioles and alveolar ducts emerge. At the cellular level, the epithelial airway cells develop into immature alveolar type I and type II cells (AEC I and II). This enables the epithelium to perform gas exchange

for the first time. At about the same time, lipofibroblasts (LIF) arise in the mesenchyme and the capillary and lymphatic systems begin to form.
Further landmarks in sufficient lung function are reached within the saccular stage. Here apoptosis and further differentiation of the mesenchyme lead to a considerable thinning of the interstitium (Kresch et al. 1998). AECII start to efficiently produce surfactant and further air sacs arise. Also, lymphatic and capillary vessels further evolve.
The alveolar stage is the last step of lung development. Here a further subdivision of air sacs into alveoli takes place. This process, also known as alveolarization or alveologenesis, signifies an enormous increase of gas-exchanging surface.

1.3 Epithelial Mesenchymal crosstalk

During early lung development a number of signaling molecules orchestrates the epithelial-mesenchymal crosstalk. These are attributed great importance in organ patterning and differentiation. In the following section a selection of key regulators is presented.

1.3.1 Fgf10/Fgf9

Fgf10 is a member of the fibroblast growth factor (Fgf) family. These signaling molecules can be found amongst vertebrates and invertebrates. They influence processes such as limb development, brain patterning and branching morphogenesis (Beenken and Mohammadi 2009). Fgfs can be differentiated into 23 subgroups on the basis of protein sequence homology. The growth factors bind specifically to their respective receptors, thus activating them. These fibroblast growth factor receptors (Fgfrs) are transmembrane tyrosine kinase receptors, which can be subdivided into four groups (Fgfr1 – Fgfr4) (Ornitz and Itoh 2001).
The molecular structure of each growth factor is determinant for its binding specificity and functional mechanism. The sequence variations of the N- and C-terminal tails of the ligands are, for example, responsible for their different biology (Mohammadi, Olsen, and Ibrahimi 2005). Moreover, the constitution of the Fgfs heparan sulphate

glycosaminoglycan (Hsgag) binding site (Hbs) determinates whether the growth factor acts in a paracrine or endocrine manner (Goetz et al. 2007).

In 1998, Min et al. (Min et al. 1998) underlined the crucial role of Fgf10 in lung development. The absence of Fgf10 during organogenesis in mice resulted in an incomplete development of the distal lung, larynx and trachea. The animals died shortly after birth. Moreover, the lack of Fgfr2IIIb, which mainly mediates the effects of Fgf10, led to disrupted lung development (De Moerlooze et al. 2000). For proper lung development, the presence of Fgf10 expression and dosage of *Fgf10* expression level is vital. Mice with only 20% expression of *Fgf10* compared to wild type animals (WT) grew hypo-plastic lungs with reduced vascular development, diminished alveolar smooth muscle cell formation and inhibited formation of secondary septae. Moreover, the authors revealed epithelial differentiation defects by evaluating the presence of cells positive for epithelial cell markers. Surfactant proteins A, B and C (SpA, SpB, SpC) and thyroid-specific transcription factor (Ttf-1or Nkx2.1) played the overriding role here. The observed reduction of marker positive cells in the mutant group was attributed to Fgf10's impact on peripheral epithelial progenitor amplification. Most mutant animals died within the first 24-48 hours after birth (Ramasamy et al. 2007; Warburton et al. 2008).

In 1997, Bellusci at al. reported the presence of Fgf10 during early lung development. *Fgf10* RNA is already detectable at E9.75. At E11.5 high levels of *Fgf10* expression could be located in the mesenchyme at the very distal tips of all lung lobes, except the right cranial lobe. During bud outgrowth into the mesenchyme, increased *Fgf10* expression levels were found in the region where the next bud was forming. This suggests, that cells in the mesenchyme adjacent to the mesothelium influence branching morphogenesis. They secrete Fgf10, which binds to the epithelial cells expressing Fgfr2b (Bellusci, Grindley, et al. 1997). Subsequently Park et al. could outline Fgf10's ability to chemotactically guide the nearby epithelium to the formation of buds, as epithelial tips migrate and proliferate toward Fgf10 (Park et al. 1998). Lü et al. could identify target genes of Fgf10 during the period of bud formation. In response to local application of Fgf10, they discovered an up-regulation of genes associated with cell rearrangement and migration, as well as inflammatory processes and lipid metabolism

(Lu et al. 2005). Also, Fgf10 is involved in controlling the mitotic spindle angle via a Ras-regulated Erk1/2 signaling pathway. It is therefore essential for the general shaping the of the lung tube (Tang et al. 2011). More recent investigations suggest, that Fgf10 has a regulatory function for the differentiation of epithelial progenitor cells. In a bronchopulmonary dysplasia (BPD) simulating mouse model, Chao et al. observed altered emergence of AECII cells due to reduced *Fgf10* expression (Chao et al. 2017).

Another Fibroblast growth factor involved in branching morphogenesis is Fgf9. Although Fgf9 and Fgf10 belong to the same protein family, there are some differences between them. In opposition to Fgf10, Fgf9 is only temporary expressed in the bronchial epithelium. At E10.5 it can be detected in both the visceral pleura and the bronchial epithelium. However, in further development (At E12.5 and E14.5) Fgf9 expression only persists in the visceral pleura. Moreover, it has only poor affinity to Fgfr2IIIb and rather activates Fgfr2IIIc. These two receptors are located differently. Fgfr2IIIb is usually expressed in the epithelium, whereas Fgfr2IIIC is expressed in lung mesenchyme. Therefore, Fgf9 signals from pleura and epithelium towards the mesenchyme and thus vice versa to Fgf10, which signals from mesenchyme to epithelium via Fgfr2IIIb (Colvin et al. 1999). Colvin at al. examined Fgf9's influence on lung development in 2001. The authors observed lung hypoplasia in *Fgf9*-null mice, which died shortly after birth. The lungs showed decreased mesenchyme and branching of airways. However, the formation of distal airspace and the differentiation of alveolar epithelial cell types I and II stayed intact. In addition, the authors highlighted the complementary roles of Fgf10 and Fgf9 during lung organogenesis, as Fgf9 controls the amount of lung mesenchyme and thereby the amount of Fgf10 expression (Colvin et al. 2001). In 2011, Yin, Wang and Ornitz presented Fgd9's different modes of action depending on its localization. Epithelial expressed Fgf9 functions in epithelial proliferation. Mesothelial expressed Fgf9, in contrast, stimulates mesenchymal proliferation by affecting Wnt2a expression and mesenchymal Wnt/b-catenin signaling, but not Fgf10 signaling (Yin, Wang, and Ornitz 2011).

The Fgf-Fgfr pathway itself is tightly regulated. One of the key modulators is the Sprouty family (Spry). Those molecules inhibit Fgf-induced MAPK (mitogen-activated protein kinase) activity in a highly cell and context dependent manner and are triggered

by the Fgf cascade itself (Cabrita and Christofori 2008). Four Sprouty genes (*mSpry1-4*) are known in mice. Spry 2 can be found within the embryonic lung epithelium, whereas Spry 4 is expressed in the mesenchyme. Overexpression of *Spry2* leads to a decrease in branching morphogenesis and epithelial cell proliferation (Mailleux et al. 2001; Tefft et al. 2002). Vice versa Tefft et al. reached a 72% gain of branching by reduction of *mSpry2* expression level (Tefft et al. 1999).

1.3.2 Tgf-ß/Bmp family

The Tgf-ß superfamily is involved in many developmental processes. Proliferation, transformation, apoptosis, as well as extracellular matrix (ECM) deposition and remodeling are to be mentioned here in particular (Sporn and Roberts 1990). The Tgf family comprises three isoforms: Tgf-ß1, 2 and 3. Moreover there are structurally related polypeptides such as Bmp. Tgf-ß ligands activate the signaling pathway by binding to the Tgf-ß receptor type II (Tgf-ßr2 or TßrII). TßrII recruits a Tgf-ß receptor type I (Tgf-ßr1, also known as activin-like kinase (Alk-1)). This in turn mediates signals within the cell via second messenger proteins (Smads) or in a smad-independent manner. Both activation of type I receptor and Smad proteins is due to phosphorylation (Chen et al. 1998; Massague 1998). Smad2 and Smad3 proteins activated by the Tgf-ß receptor type I form an oligomer with Smad4. This Smad complex is able to enter the nucleus and alter DNA transcription (Heldin, Miyazono, and ten Dijke 1997). Smad7 has been identified as an inducible antagonist of Tgf-ß signaling. It competitively binds the Tgf-ß1 receptor more stable and thereby prevents Smad2 and Smad3 activation (Nakao et al. 1997).

The presence of Tgf-ß1, 2 and 3 in embryonic mouse lung and of Tgf-ß receptor type I and II in embryonic rat lung were documented previously (Pelton et al. 1991; Zhao and Young 1995; Zhao and Shah 2000). Tgf-ß2 is mainly expressed in the distal epithelium, whereas Tgf-ß3 can be temporarily found in the proximal epithelium of the respiratory tract and in the lung mesothelium at all stages (Millan et al. 1991). Furthermore, Tgf-ß signaling has been identified as a key player in fetal lung morphogenesis, injury repair and remodeling. It has also been linked to lung pathologies such as bronchopulmonary dysplasia (BPD) and pulmonary fibrosis (Zhao et al. 2002; Gauldie et al. 2003; Jankov

and Keith Tanswell 2004). Knock out of each *Tgf-ß1, 2* and *3* caused either abnormal lung morphogenesis or inordinate post-natal lung inflammation (Kulkarni et al. 1993; Sanford et al. 1997; Shi et al. 1999).

Various studies have determined Tgf-ß signaling as inhibiting to airway branching during early lung development. Correspondingly down regulation of either *Tgfßr2* or *Smad2*, *Smad3* or *Smad4* and over expression of *Smad7* caused intensified branching morphogenesis (Zhao et al. 1996; Zhao et al. 1998; Zhao et al. 2000). Interestingly however, diminished Tgf-ß signaling in late lung development (P7 – P28) equally caused impaired alveolarization (Chen et al. 2005). During late human lung development TGF-ß signaling was found involved in formation of airway and alveolar epithelium as well as vascular and airway smooth muscle emergence (Alejandre-Alcazar et al. 2008).

In 2008, Chen et al. examined the effects of TßrII abrogation in epithelium and mesenchyme during early and late lung development. At E11.5 TßrII is only expressed in airway epithelial cells, later at E14.5 the receptor was localized within epithelium and mesenchyme. Postnatally TßrII was detected in septal structures at P14. No significant changes in lung phenotype were found in mice with epithelial lack of TßrII function during early lung development. However, abolished TßrII expression in epithelium during post-natal alveogenesis caused changes in cell composition. The authors observed a noticeable reduction of Aqp5 positive cells representative for the AECIs, but unimpaired presence of SpC positive cells, reflecting the AECII population. Apart from cell differentiation, diminished proliferation was discovered at days P14 and P28. Remarkably, mesenchymal knock out of *TßrII* expression during early lung development resulted in significant decrease of terminal branching. Therefore, embryonic lung branching is affected by mesenchymal instead of epithelial TßrII mediated signaling (Chen et al. 2008). In summary, the adequate expression of TGF-ß in the respective developmental stages appears to be essential for regular organogenesis. At different times both overexpression and deficiency lead to pathological changes in this process (Saito, Horie, and Nagase 2018).

Tgf-ß signaling itself is regulated in multiple ways. One of the most striking positive modulator is the auto- or cross induction of Tgf-ß isoforms (Kim et al. 1990; Bascom et al. 1989). On the downside, Tgf-ß activity can be regulated extracellularly, as its

precursor molecules have to be activated by cleavage before becoming signaling ligands (Miyazono, Ichijo, and Heldin 1993). Moreover, Smad6 and Smad7 inhibit the signaling pathway. *Smad7* expression was found provoked by Tgf-ß1 itself (Nakao et al. 1997), but also by mechanical stress (Topper et al. 1997) and cross talk with epidermal growth factor (Egf) (Afrakhte et al. 1998).

Bone morphogenetic proteins (Bmps) are Tgf-ß related growth factors. They orchestrate the morphogenesis of various tissues, including the lung. The Bmp family comprises over 20 ligands. It was originally discovered as inductor for cartilage and bone formation (Hogan 1996; Reddi and Reddi 2009). Similar to Tgf-ß ligands Bmp ligands bind heteromeric serine/threonine kinase receptors. The binding activates Bmp receptor type II, which in turn activates Bmp receptor type I via phosphorylation. Receptor-bound Smad proteins are subsequently activated by Bmp receptor type I. Smad1, Smad5 and Smad8 are known Bmp specific second messengers. If they are in active state, these form complexes with already mentioned Smad4. The further signaling cascade is carried out just like the Tgf-ß signaling pathway (Massague 1998; Shi and Massague 2003).

Four Bmps were found present in embryonic mouse lung, namely Bmp3, Bmp4, Bmp5 and Bmp7. Bmp5 is expressed in the mesenchyme of mouse lung from E10.5 until at least E16.5 (King et al. 1994). Sountoulidis et al investigated the activation of Bmp4 pathway during lung development and adult lung tissue repair. During the pseudoglandular stage the Bmp pathway was mainly involved in vascularization and airway smooth muscle formation. When branching comes to completion, the Bmp pathway activity rises in airway and alveolar epithelium. The activity level reaches its peak around birth, thereupon returning to a lower level. Furthermore, a reactivation of Bmp pathway was observed after lung tissue injury in adult mouse lung. In addition, the authors underlined Bmp's crucial role for managing and sustaining the pool of alveolar and epithelial progenitor cells (Sountoulidis et al. 2012).

To this day, three Bmp type I receptors, Alk2, Alk3 and Alk6, have been discovered. Alk3, also known as Bmpr-Ia, is expressed in distal epithelial cells throughout lung development (E12.5, E14.5 and E14.5). Mice with *Alk3* knock out died early (E7.5 – E9.5.) before lung organogenesis (Mishina et al. 1995). Arrogations of Alk3 in lung epithelium from E7.5, E17.5 or E18.5 were all followed by respiratory distress. All

animals died after birth. However, mice with postnatal *Alk3* knock out developed morphologically normal lungs. Mice with an early *Alk3* knock out grew lungs with enlarged airspace and lack of saccular formation. This phenotype was accompanied by abnormal distal cell proliferation, differentiation and apoptosis. On the genetic level, *Ccsp*, *SpC* and *Aqp5* expression levels were found significantly reduced. A late knock out of *Alk3* resulted in significant epithelial apoptosis and diminished surfactant secretion (Sun et al. 2008).

Bragg et al. investigated Bmp4's effects on the branching program. On the one hand, the authors injected Bmp4 directly into the lumen of embryonic lung explants; on the other hand, they added Bmp4 only to the surrounding medium. Interestingly proliferation and branching morphogenesis were not affected by the injection, whereas the addition of Bmp4 to the medium enhanced branching processes (Bragg, Moses, and Serra 2001). Bmp4 addition to cultured embryonic lung endoderm, which was isolated at E11.5, led to diminished outgrowth. Correspondingly, the reduction of endogenous produced Bmp4 via antagonist Noggin resulted in increased budding. Moreover, it could be highlighted, that Bmp4 counteracts Fgf10 –induced growth of lung endoderm (Weaver, Dunn, and Hogan 2000). Bellusci et al. located high levels of *Bmp4* expression in the tips of distal bud epithelium and nearby mesenchyme and investigated the influence of modified *Bmp4* expression on lung organogenesis. The over expression of *Bmp4* in the distal epithelium of transgenic lungs led to outgrowth of significantly smaller lungs with cystic terminal air sacs and enhanced cell death in the mesenchyme. Furthermore, the epithelial cell differentiation was investigated at E16.5 and E18.5. This revealed limited expression levels of *SpC* in the transgenic mice lungs (Bellusci et al. 1996). The interaction of Bmp and its antagonists in lung development has also been investigated in several studies. One of these antagonists is Follistatin-Like 1 (Fstl1). Mice with lack of Fstl1 grew dysplastic lungs with hypoplastic tracheal rings, irregular shaped lobes, enlarged proximal bronchioles and enclosed distal sacs. The animals also presented disrupted limb- and axial skeleton patterning and died shortly after birth, due to respiratory distress (Sylva et al. 2011). The Overexpression of *Gremlin*, another Bmp antagonist, caused a disruption of proximal-distal lung patterning (Lu et al. 2001).

1.3.3 Pdgfs

Platelet-derived growth factors belong to a family of growth factors, which have been subject to intense research over the last decades. Five ligands, Pdgf-a, Pdgf-b, Pdgf-c, Pdgf-d and Pdgf-ab, have been investigated so far. They form either homodimers (aa, bb, cc or dd) or heterodimeres (ab) and act via two receptors. Pdgf receptor types α and ß are transmembrane Tyrosinkinase receptors. Their extracellular activation with Pdgf ligands is followed by dimerization and autophosphorylation (Claesson-Welsh, Ronnstrand, and Heldin 1987; Heldin 1997). Although Pdgfrs are expressed in most cells, there is a notable high expression in fibroblasts and smooth muscle cells. The Pdgf-signaling pathway is involved in many crucial biological processes. Besides development of organs like the kidney or eye, it has also been found involved in lung organogenesis.

In 1996, Bostrom et al. examined *Pdgf*-a null mice. The animals died during embryogenesis or shortly after birth. The mutant mouse lungs showed emphysema, associated with a lack of alveolar septation due to loss of alveolar myofibroblasts (Bostrom et al. 1996). Furthermore, the authors created an experimental setup with mice lacking Pdgfr-α. These animals developed smaller lungs, however early branching morphogenesis appeared to be intact (Bostrom, Gritli-Linde, and Betsholtz 2002). The dysplastic lung phenotype of *Pdgf-a* (-/-) mice was further investigated in 1997. Lindahl et al. concluded, that the failure of alveogenesis in mutant mice is linked to insufficient spreading of Pdgf-Ra$^+$ cells, which are progenitors to tropoelastin-positive alveolar smooth muscle cells (Lindahl et al. 1997). Li and Hoyle overexpressed *Pdgf-a* in mouse lung epithelium. They recognized an increase of mesenchymal cells, dilated airspaces and a decreased number of bronchioles at E16.5. At E18.5 the transgenic mice showed thickened mesenchyme, lacking deposition of elastin within the parenchyma and still cuboidal respiratory epithelium. Hence, the usual down regulation of *Pdgf-a* is necessary for the transition from canalicular into saccular stage of lung development (Li and Hoyle 2001).

Moreover, PDGF signaling has been linked to certain human lung diseases. Amongst pulmonary arterial hypertension (PAH) and lung cancer, pulmonary fibrosis was one of the main topics. Abdollahi et al., for instance, found that PDGF-signaling is substantial

in the pathogenesis of lung fibrosis and pathway inhibition. Therefore, it might in turn become a therapeutic option (Abdollahi et al. 2005).

1.4 MicroRNAs

In the past decade, small non-coding mRNA strands have aroused the particular interest of research. These microRNAs (miRNAs) are about 21 nucleotides long and are increasingly associated with lung development. In general, this family of regulatory molecules is attributed an important role in post-transcriptional gene expression, developmental timing, growth control and differentiation. In 1993 Lee, Feinbaum and Ambros discovered the first microRNAs. It were transcripts of *lin-4*, which negatively regulate *lin-14* (Lee, Feinbaum, and Ambros 1993). Later, Reinhart et al. revealed the role of a microRNA, *let-7,* in developmental timing in C. elegans. Both over and under expression of *let-7* caused irritation of developmental processes (Reinhart et al. 2000). Micro RNAs can be found in viruses, eukaryotes, fungi, plants and animals (Cullen 2011; Lee et al. 2010; Molnar et al. 2007; Huang et al. 2012; Ambros 2001). Approximately 50% of all protein-coding genes are influenced by miRNAs in mammals. As miRNAs regulate a broad number of processes they themselves are regulated in a tight and dynamic manner (Krol, Loedige, and Filipowicz 2010). All so far known miRNAs are catalogued in an online accessible data base called miRBase (Griffiths-Jones et al. 2006).

1.4.1 MicroRNA biogenesis

In 2004 Rodriguez et al. identified the genomic localization and context of 232 mammalian microRNAs. Roughly 39% were found within introns of protein-coding genes and about 28% were found located in non-coding introns and exons (Rodriguez et al. 2004). The first transcript of miRNAs arises within the nucleus. Here, RNA Polymerase II or RNA Polymerase III transcribe miRNA genes or introns (Lee et al. 2004). The resulting pri-miRNA consist of a 33 base-pair hairpin stem with two single-stranded flanking regions at the 5’ and 3’ end and a terminal loop (Winter et al. 2009).

Next, the microprocessor complex performs cleavage of the pri-microRNA into around 70 nucleotide long pre-microRNA (Kim 2005). This enzyme complex consists of Drosha, an RNase III enzyme, and Pasha, also known as DGCR8 (DiGeorge critical region 8) protein (Lee et al. 2003; Gregory et al. 2004). Pasha precisely binds the pri-miRNA, thus defining the cleavage site at which Drosha cleaves 11 base pairs off the hairpin stem (Han et al. 2004; Han et al. 2006; Zeng and Cullen 2003 2005). In contrast, the emergence of microRNAs out of small nuclear RNAs (snoRNA) is not dependent on Drosha, but Dicer processing (Hutzinger et al. 2009). The correctly processed pre-microRNAs are thereupon exported from the nucleus into the cytoplasm. The transferring complex comprises Exportin-5 and Ran-GTP, which also withdraw the pre-microRNAs from nuclear degradation (Yi et al. 2003 Y., Macara, I. G. & Cullen, B. R., 2003; Bohnsack, Czaplinski, and Gorlich 2004 K. & Gorlich, D., 2004). In the cytoplasm, the pre-microNRA passes further processing. This is mainly performed by the RLC, RISC loading complex, which is composed of RISC (RNA-induced silencing complex), the RNase Dicer, the double-stranded RNA binding protein TRBP and Argonaute2 (Ago2) (Gregory et al. 2004 T. P., Cooch, N., Shiekhattar R., 2005). RISC itself contains a single-stranded microRNA or small interfering RNA (siRNA), which complementary binds the target miRNA (McManus et al. 2002). MiRNAs that reveal a high degree of complementarity within the hairpin stem are first cleaved by Ago2, before Dicer-mediated cleavage (Diederichs and Haber 2007). The RNase III Dicer then carries out the main-cleavage. The loop of the pre-miRNA is cut off, giving rise to a roughly 22-nucleotide miRNA duplex with two protruding nucleotides at each 3' end (Ketting et al. 2001). Bernstein et al. underlined the vital role of this endonuclease in miRNA processing. The deletion of the enzyme in mice caused lethality in early development (Bernstein et al. 2003). As cleavage is executed, Dicer and TRBP dissociate from the miRNA double-strand.

The unwinding of the duplex is performed by helicases. Yet there was no universal helicase found responsible. In mice p68 in complex with *let-7* unwind the double-strand (Salzman, Shubert-Coleman, and Furneaux 2007). Although the separation of the duplex gives rise to two different mature miRNAs, mostly only one strand is loaded into RISC (Schwarz et al. 2003). This leads to the differentiation into functional (miRNA) and passenger strand (miRNA*)(Czech and Hannon 2011). The latter is degraded after the unwinding. Unlike the passenger strand, functional strands, which will be

incorporated into RISC, usually have a less stable 5' end (Khvorova, Reynolds, and Jayasena 2003 A. & Jayasena, S. D., 2003). The current nomenclature divides microRNAs into 3-prime ('3p) and 5-prime ('5p) strands, since both are in principle functional. MicroRNA processing and maturation are regulated in many ways. A few will be presented in the following.

1.4.2 Regulation of microRNA

MicroRNAs are regulated at levels of transcription, processing and decay. There are many parallels between the regulation of miRNA transcription and the transcription of protein-coding genes. Both mostly have promoter regions comprising transcription factor binding sites (TATA box sequences) and a binding site for RNA polymerases. This indicates a gene expression regulation of miRNAs by transcription factors (Corcoran et al. 2009). Proto-oncogene c-Myc and cellular tumor antigen p53 for instance are positive effectors of microRNA transcription (O'Donnell et al. 2005; He et al. 2007).

Apart from direct stimulation and inhibition of microRNA expression, regulating feedback loops have been found participating in those processes. The reciprocal negative feedback loop in C. elegans is just one representative example. Here HBL-1 (Hunchback like-1) a target of *let-7*, antagonizes the expression of its own repressor, *let-7* (Roush and Slack 2009).

Regulation of microRNA processing is another common control mechanism. P53, which has already been mentioned as direct initiator of transcription, can also intervene at levels of miRNA processing. P53 was observed facilitating the maturation of growth suppressive *miR-16-1*, *miR-143* and *miR-145* by interacting with Drosha. Correspondingly inactivation of p53 led to a slowdown of miRNA processing (Suzuki et al. 2009). Davis et al. revealed another Drosha-dependent regulation of miRNA processing. They found increased mature *miR-21* levels promoted by TGF-ß and BMP signaling due to interaction of downstream signaling molecules, SMADs, and the Drosha microprocessor complex (Davis et al. 2008).

Besides Drosha, Dicer plays an important role in processing microRNA maturation. Ma et al. showed that a component of Dicer, the helicase domain DExD/H-box, might disturb Dicer functionality. This was concluded, as removal of DExD/H-box led to an increased processing activity of Dicer (Ma et al. 2008). Moreover, Dicer expression can

be reduced by miRNAs. *Let-7* microRNA, for instance, targets Dicer mRNA. This can be considered as an auto regulatory negative feedback loop, which regulates miRNA processing (Forman, Legesse-Miller, and Coller 2008). Furthermore, protein factors are able to diminish maturation of specific microRNAs. *Lin-28* codes for a RNA-binding protein, that facilitates the transcription of insulin like growth factor 2 (IGF-2). This protein was investigated and exhibited the ability to selectively inhibit the pri-miRNA processing of *let-7*g microRNA (Viswanathan, Daley, and Gregory 2008).

Control of microRNA decay is a further way to regulate activity levels. Although miRNA degradation has not been as well examined as biogenesis, microRNAs are generally considered as stable molecules. Krol et al. observed the half-lives of a number of micro RNAs. Due to the inhibition of miRNA transcription or processing, certain miRNAs lasted many hours or even days (Krol et al. 2010; van Rooij et al. 2007). Another study examined the turnover of roughly 200 miRNAs. Most of them showed half-life periods greater than 24 hours. However 61 miRNAs were degraded within the first 12 hours (Marzi et al. 2016). Several developmental and controlling processes involve fluctuating activity levels of miRNAs, therefore miRNA decay is occasionally being expedited. This was observed in neuronal cells during dark adaption of mice retina, and human post-mortem brain tissue (Krol et al. 2010; Sethi and Lukiw 2009). Katoh et al. determined the role of poly(A) polymerase GLD-2 in stabilizing microRNAs (Katoh et al. 2009). Vice versa deadenylation of miR-122 caused its accelerated turnover (Katoh, Hojo, and Suzuki 2015).

1.4.3 MicroRNA functional mechanisms

The functional unit around the specific microRNA is named RISC - RNA-induced silencing complex. It is composed of Dicer, an Argonaute protein (AGO), the P-body protein PW182, the human immunodeficiency virus trans activating response RNA-binding protein (TRBP), the fragile X mental retardation protein (FMPR1) and a specific miRNA (Redfern et al. 2013; Liu et al. 2005; Chendrimada et al. 2005; Jin et al. 2004). This complex acts in three different ways: mRNA target cleavage, mRNA deadenylation and translational repression. In mammals, microRNAs are usually thought to be more active in inhibiting translation than degradating their targets. However, Farh et al. observed a reduction of target mRNAs, due to an increase of

microRNAs (Farh et al. 2005). Moreover, Vasudevan et al. revealed a switch of miRNAs from translational repressor to activator under conditions of serum starvation. Those findings suggest, that functional mechanisms are dependent on the individual microRNAs, their specific targets and cell background (Vasudevan, Tong, and Steitz 2007 Y & Steitz, J. A., 2007).

Most target mRNAs are imperfectly base-paired within their three-prime untranslated region (3'-UTR). However, with nucleotides 2 to 8, also known as the seed region, miRNAs bind their targets complementary (Bagby et al. 2009). For the target cleavage the RISC complex needs to almost perfectly complementary base-pair with an encountered mRNA, which is then degraded (Carthew and Sontheimer 2009; Song et al. 2004).

The exact mechanics of miRNA-mediated translational repression are not yet understood. However, it is known, that both 5'-cap and poly(A) tail are needed for accurate translation, and therefore are potential targets of translational repressors. Mathonnet et al revealed the prevention of the 5'-cap recognition during translation by microRNAs. As the 80S ribosomal complex assembly is dependent on cap recognition, translation initiation was found inhibited (Mathonnet et al. 2007). Moreover Argonaute proteins, Ago1 and Ago2, both have been found involved in translational repression in Drosophila. Ago1-RISC shortens the poly(A) tail of its mRNA targets in a ATP-dependent manner. Whereas Ago2 comprises a cap-binding domain and therefore competes with eIF4E, an eukaryotic initiation factor of translation, in binding eIF4G, also disrupting the initiation process (Iwasaki, Kawamata, and Tomari 2009).

Deadenylation of mRNA is mediated by glycine-tryptophan protein of 182 kDA, GW182 proteins. Deadenylases CCR4 and CAF1 are recruited by the cobroxy-terminal part of GW 182 proteins, which also interacts with the poly(A) binding protein (PABP) (Chekulaeva and Filipowicz 2009 W. & Parker R,, 2009). The deadenylated mRNAs are commonly less stable and will be digested by exonucleases (Chen et al. 2009 D., Xia, Z., Shyu, A. B., 2009).

1.5 Role of microRNAs in early lung development and disease

1.5.1 Current knowledge of miR-154

Since the first verification of microRNAs in 1993 there has been a great increment in knowledge about the function and impact of these regulatory molecules. The role of microRNAs in developmental processes and their role in human diseases are two fields of interest that have become subject of intense scientific research. Thereby the need for decrypting the physiologies of specific microRNAs is constantly growing.

MicroRNA-154 (*miR-154*) is a 22-nucleotide long RNA molecule, which has already been linked to certain diseases and alterations in lung structure. The coding gene for *miR-154* is located at human chromosome 14q32.31 and mouse chromosome 12F2. The *miR-154* family is part of a cluster – the second largest human microRNA cluster (Seitz et al. 2004). The stem loop sequence and the sequences for the functional (miRNA) and passenger strand (miRNA*) of *miR-154* are identical in the genomes of "Homo sapiens" and "Mus musculus":

Table 1

RNA molecule	Sequence
Stem loop	GUGGUACUUGAAGAUAGGUUAUCCGUGUUGCCUU CGCUUUAUUUGUGACGAAUCAUACACGGUUGACC UAUUUUUCAGUACCAA
miR-154-5p (*miR-154*)	UAGGUUAUCCGUGUUGCCUUCG
miR-154-3p (*miR-154**)	AAUCAUACACGGUUGACCUAUU

So far *miR-154* has been subject to a number of studies, most of which investigated *miR-154*s role in human diseases. *MiR-154* was, inter alia, found involved in small cell lung carcinoma (Lin et al. 2015), glioblastoma (Yang et al. 2016), hepatocellular carcinoma (Pang et al. 2015), colorectal cancer (Xin, Zhang, and Liu 2014), prostate cell cancer (Formosa et al. 2014), (Zhu et al. 2013) and pulmonary fibrosis (Milosevic et al. 2012). Prior to the clinical value of *miR-154*, Lagos-Quintana et al. examined

microRNA expression levels in mouse brain (midbrain, cortex and cerebellum), heart, liver, small intestine and colon. They detected 34 novel microRNAs and localized *miR-154* expression in midbrain mouse tissue (Lagos-Quintana et al. 2002). Two years later, Suh et al. analysed several microRNAs in human embryonic stem cells by cDNA cloning. Here *miR-154** was identified amongst fifteen other microRNAs for the first time (Suh et al. 2004). In 2007, Williams et al. compared expression levels of microRNAs, which are potentially involved in human and mouse lung development. They found significant similarities of certain microRNA expression levels between human and mouse. Amongst others, *miR-154* is first highly expressed at P1 in both human and mouse lung, however shows diminished expression levels at P14 and P60. The further analysis of those microRNAs, which are highly expressed shortly after birth, revealed adjacent genomic locations. *MiR-134*, *miR-154*, *miR-299*, *miR-323*, *miR-337* and *miR-370* are all located within the Gtl2-Dio3 domain at human chromosome 14q32.31, or mouse chromosome 12F2. Notably, two clusters within the Gtl2-Dio3 domain are only expressed from the maternal chromosome. One cluster is situated within a retro transposon-like gene, namely *Rtl1*. The miRNA-containing gene (*Mirg)* is located 150 kb further upstream and comprises the other cluster, which includes *miR-154*.

In addition, the authors applied in situ hybridization in order to detect the spatial expression of microRNAs. The perceived presence of *miR-154* was concordant with the expression levels determined by RT-PCR. In fetal mouse lung, *miR-154* was observed throughout epithelium and stroma. In adult mouse lung however, *miR-154* is expressed especially within alveolar and airway epithelium (Williams et al. 2007).

1.5.2 MicroRNAs in early lung development

Future studies have revealed microRNAs as important modulators in embryonic development. The complete loss of Dicer, which implies a lack of microRNA processing, led to lethality of mouse embryos before gastrulation (Bernstein et al. 2003). Harris et al. abrogated Dicer in the mouse lung epithelium. As a consequence, Mutant mice showed large epithelial pouches compared to WT mice. This phenotype was observed before increasing epithelial cell death. Thus Dicer appears to be vital for

epithelial branching morphogenesis, independently of its role in cell survival (Harris et al. 2006).

Not only was the general influence of microRNAs, represented by Dicer activity, investigated, but also the function of single microRNAs. So for instance the overexpression of the miR-17-92 cluster, which caused increased proliferation and inhibition of differentiation in lung epithelial progenitor cells (Lu et al. 2007). Also, *microRNA-142-3p* was found to influence proliferation and differentiation of mesenchymal cells during lung development (Carraro et al. 2014). M*iR-127* (Bhaskaran et al. 2009), the *miR-200* family (Benlhabib et al. 2015), *miR-124* (Wang et al. 2015), *miR-375* (Wang et al. 2013), *miR-221* and *miR-130a* (Mujahid, Nielsen, and Volpe 2013) are, amongst others, further examples for microRNAs associated with early lung development. However, the total number of investigated microRNAs is still quite manageable compared to the hundreds of known human microRNAs (Bentwich et al. 2005).

1.5.3 MicroRNAs in lung disease

As the lung mediates the essential gas exchange between outside air and blood, pathologies of this organ are associated with high mortality. Although therapeutic treatments have improved over the last decades, most are still imperfect. Hence there is an eager scientific interest in detailed understanding of lung diseases. Various microRNAs are already known to be involved in human pathologies. Here lung-, liver- and kidney diseases, but also infectious diseases and Sickle Cell disease are to be mentioned (Ha 2011). In addition, changes in MicroRNA expression levels have been found related to lung diseases such as adenocarcinoma, small and non-small cell lung cancer, cystic fibrosis, idiopathic pulmonary fibrosis and inflammatory lung diseases like asthma and chronic obstructive pulmonary disease (COPD) (Haigl et al. 2014; Nadal et al. 2013; Perry, Adcock, and Chung 2015; Szymczak, Wieczfinska, and Pawliczak 2016; Li et al. 2016).

With the growing understanding of specific microRNA-mediated processes, the interest in transforming this knowledge into promising clinical application increases steadily. Liang et al. identified *miR-26a* as a therapeutic option in idiopathic pulmonary fibrosis (Liang et al. 2014). The same applies for *miR-199a-5p* and idiopathic cystic fibrosis (Zhang et al. 2015). Moreover microRNAs could act as biomarkers in lung disease

(Vencken, Greene, and McKiernan 2015). *MiR-92a-2* for instance, was perceived as such for small cell lung cancer (Yu et al. 2017), or *miR-145-5p*, *miR-338-3p* and *miR-3620-3p* for chronic obstructive pulmonary disease (Wang, Huang, et al. 2016). Lanford et al. achieved a long-lasting depression of viral load in hepatitis C virus (HVC) infected chimpanzees by treatment with locked nucleic acid complementary to *miR-122* (Lanford et al. 2010). These findings give an insight of the therapeutic potential of microRNAs.

1.5.3.1 IPF

In 2012 Milosevic et al. examined the function of 43 up-regulated microRNAs in idiopathic pulmonary fibrosis (IPF). Twenty-four of these, including *miR-154*, are located within the chromosome 14q32 cluster. Half of the up-regulated microRNAs within the 14q32 cluster belong to the *miR-154* family. The stimulation of normal human lung fibroblast (NHLF) with Tgf-ß1, a key regulator of lung fibrosis, caused up-regulation of seven microRNAs. These were equally found in up-regulated in IPF and also belong to the *miR-154* family. In order to understand the effects of those up-regulated microRNAs, the authors transfected NHLFs with *miR-154*, as a representative of the *miR-154* family. They observed increased migration and proliferation. Also, the transfection led to an up-regulation of the Wnt pathway activators and a down-regulation of pathway inhibitors. Moreover, the *miR-154* dependent proliferation could be prevented by transfecting NHLFs with Icg-001 or Xav939, both inhibitors of the Wnt/ß-Catenin pathway. Consequentially Milosevic et al. assumed, that *miR-154* might alter NHLF proliferation through the Wnt/ß-Catenin pathway (Milosevic et al. 2012).

1.5.3.2 Lung cancer

Cazzoli et al. examined the presence of 742 microRNAs in 30 samples of patient plasma, in order to identify potential biomarkers for lung adenocarcinoma and lung granuloma. *MiR-154*-3p was amongst the fourteen most promising microRNAs, which were further evaluated. Thereby the authors observed up-regulation of *miR-154*-3p in both lung adenocarcinoma and lung granuloma (Cazzoli et al. 2013).

One year later Huang et al. recognized an association of *miR-154*-5p expression levels with smoking and lung cancer. They analyzed the microRNA expression within the serum samples of smokers, lung-cancer patients and non-smokers. Interestingly, *miR-154*-5p was, concurrently with *let-7i-3p*, down regulated in smoker and lung-cancer serum. However, the differences between these two groups were not statistically substantiated. Via target gene prediction, five promising targets of *miR-154*-5p were identified. ABCC9, ROS, ATG7, TNFAIP3 and CUL2 are all associated with morphogenesis and metastasis of lung cancer, suggesting that *miR-154*-5p is linked to the emergence of cigarette-smoke induced lung cancer (Huang et al. 2014).

As *miR-154* has been described as tumor suppressive in colorectal (Xin, Zhang, and Liu 2014) and prostate cancer (Zhu et al. 2013), Lin et al. explored *miR-154*'s value in the suppression of non-small cell lung cancer (NSCLC). Compared to normal lung cells, *miR-154* was generally down regulated in NSCLC tissue. In addition, low expression levels of *miR-154* were found associated with advanced tumor progression (TNM staging, tumor size and metastasis) and reduced survival rates. Subsequently, the authors transfected A549 (adenocarcinomic human alveolar basal epithelial) cells with *miR-154* and recognized inhibited cell proliferation, colony formation, cell migration and invasion, as well as induction of cell cycle arrest and apoptosis. Furthermore, the over expression of *miR-154* caused a reduction of N-cadherin, vimentin and increased E-cadherin expression, indicating a regulatory role of *miR-154* in epithelial to mesenchymal transition (EMT). In vivo, mice with high *miR-154* expression showed significantly smaller tumors in comparison to controls with lower *miR-154* levels, suggesting a inhibitory role of miR154 in NSCLC tumor growth (Lin et al. 2015). Based on these results the authors could determine zink finger E-box binding homebox 2 (ZEB2) as specific target of *miR-154* in NSCLC. Down regulation of *ZEB2* in NSCLC cells resulted in changes similar to the effects of overexpressing *miR-154*. Especially EMT is affected by *miR-154* mediated targeting of ZEB2, which results in inhibited migration and invasion of NSCLC cells (Lin et al. 2016). Zhou at al. identified another target of *miR-154* in NSCLC cells, namely high mobility group A2 protein (HMGA2) and equally observed the cancer-suppressing effects of *miR-154*. *MiR-154* therefore might be considered as potential agent for the treatment of NSCLC (Zhuo et al. 2016).

2 *Material and Methods*

2.1 Transgenic mice

Mice given by J. Whitsett were selected to generate Control and Experimental genotypes. We chose the *CCSP-rtTA*, Clara Cell Secretory Protein, promoter to selectively target the airway epithelium, as previously described (Perl, Zhang, and Whitsett 2009). In combination with the *tet(O)mir154* transgene, this allowed us to perform a doxycycline-inducible overexpression of *miR-154* in this specific tissue layer. Moreover, we aimed to generate equal numbers of Control and Experimental pups within the same litter. The crossing mates were chosen accordingly. In this way, all pups would be exposed to the exact same conditions. Therefore, a *Tg(CCSP-rtTA)/?;Tg(tet(O)miR-154/+* female and a male with the same genotype were crossed. (**Figure 01)** shows all potential genotypes of pups that might result from this mating.

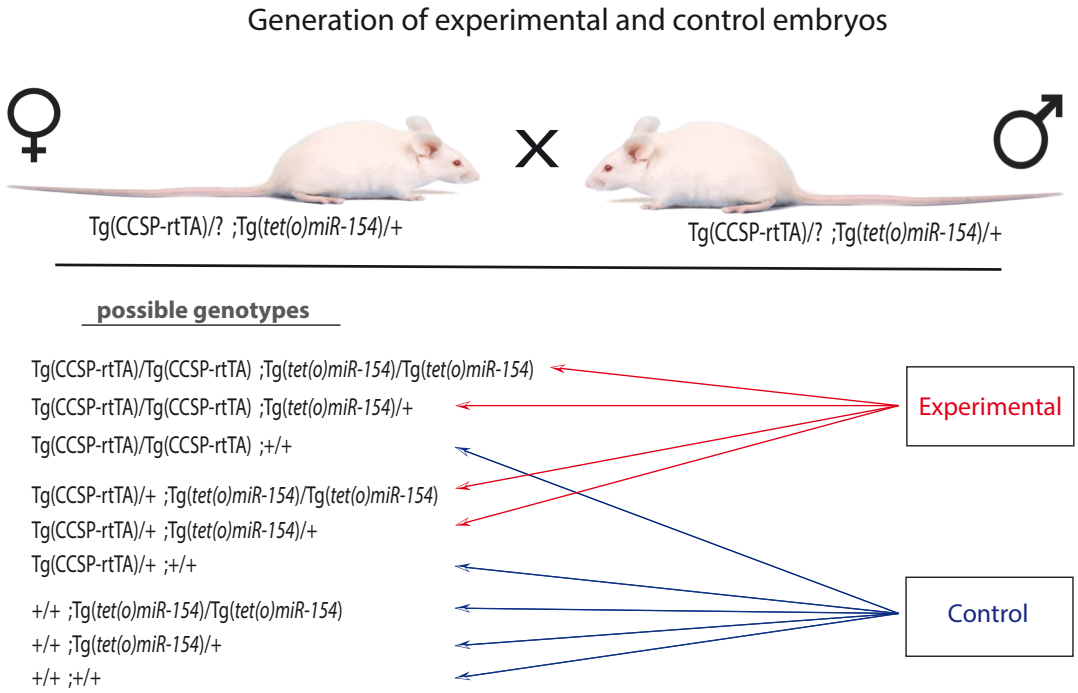

Figure 02. Design of mice crossing scheme.
(A) Two mice heterozygous for both the Tg(*CCSP-rtTA)* and *tet(O)mir-154* operon were identified as ideal mates for the generation of a preferably balanced litter. **(B)** List of possible pup genotypes sorted into experimental and control group.

As a vaginal plug was approved, embryonic life was set to E0.5. From E7.5 until the sacrifice at E18.5 the pregnant mice were fed with Doxycycline food (Altromin Spezialfutter, Lage, Germany). The food was exchanged every second day.
At E18.5 the lungs were harvested. Therefore, the abdomen and thorax of the pregnant mouse were opened and the embryos were removed within the amniotic sac. For the collection of embryonic lungs, the amniotic sac was opened and the mouse thorax was cut along the sternum and beneath the undermost ribs. The mediastinal organs, heart, lung, esophagus and thymus, were removed together by pulling the heart ventrally. Then heart, esophagus and thymus were separated neatly from the lung. The left lobe of each lung was separated for histology and therefore stored in 4% paraformaldehyde (PFA) for either 24 hours at room temperature or up to seven days at 4°C. For gene analysis, the remaining parts were placed in Eppendorf tubes filled with QIAzol (Qiagen, Hilden, Germany), which were temporary stored in liquid nitrogen and later at -80°C. The tip of each mouse tail was kept for genotyping analysis.

2.2 Genotyping

For the analysis of genotypes, we used the tissue of the collected animal tails. These were put into Eppendorf tubes with 200 µl Viagen (Viagen Biotech Inc, Los Angeles, CA 90010, USA) and 2 µl protein kinase K. The samples were incubated overnight at 56°C and 1400 rpm using the Thermomixer comfort (Eppendorf AG, Hamburg, Germany). The next day deactivation was run at 85°C for 45 minutes.
In order to detect the *Tg(tet(O)miR-154)* transgene, two primer sequences were used. The forward primer (SB034F) sequence reads: 5'-TGT TAC GGT GGG AGG CCT AT-3'. The reverse primer (SB034R) sequence is: 5'-GCG GGA TTT GGT ACT GAA AA-3'. The PCR protocol was run as described in the table (see below). Step two to four were repeated for a total of 30 cycles.

Each PCR tube contained 4,3 µl H20, 5,5 µl Qiagen Master Mix (Qiagen, Hilden, Germany), 0,1 µl of each primer and 1 µl DNA template.

For verification of the *CCSP-rtTa* allele three primers were used. The primer for the *CCSP* promoter (P1, SB009R) is: 5'-ACT GCC CAT TGC CCA AAC AC-3'; the primer for the *SP-C* promoter (P2, SB009F) reads: 5'-GAC ACA TAT AAG ACC CTG GTC A-3'; and the primer for the *rtTA* coding sequence (P3, SB009C) states: 5'- AAA ARC TTG CCA GCT TTC CCC-3'. A mix of 4,4 µl H20, 0,5 µl 25mM MgCL2, 0,1 µl 25 mM dNTPs, 5 µl Qiagen Master Mix, 0,1 µl taq polymerase, 0,1µl of each primer and 1µl DNA template were pipetted into the PCR tubes. The PCR was then carried out as shown in the table below. Step two to four were repeated 29 times, 30 cycles in total. PCRs were performed with Thermal Cycler C1000 (Bio Rad Labratories Inc, Hercules, California, USA). The samples were further analyzed via capillary electrophoresis with QIAxcel (Qiagen, Hilden, Germany), which also digitalized the gel electrophoresis results (see **figure 05**). Based on the genotyping the probes were divided into a Control and an Experimental group respectively.

Table 2

Examined alleles	Primers	PCR protocol		
Tet(O)-miR154	**forward**: 5'-TGT TAC GGT GGG AGG CCT AT-3' **reverse**: 5'-GCG GGA TTT GGT ACT GAA AA-3'	**Step**	**Temp.**	**Time**
		1	94	3 min
		2	94	30 sec
		3	57	30 sec
		4	72	1 min
		5	4	Hold
CCSP-rtTa	**P1:** 5'-ACT GCC CAT TGC CCA AAC AC-3' **P2**: 5'-GAC ACA TAT AAG ACC CTG GTC A-3' **P3**: 5'- AAA ARC TTG CCA GCT TTC CCC-3'	**Step**	**Temp.**	**Time**
		1	94	5 min
		2	94	30 sec
		3	58	30 sec
		4	72	30 sec
		5	72	5 min
		6	4	Hold

2.3 RNA isolation

After the harvest, the lung lobes were placed into QIAzol (Qiagen, Hilden, Germany) filled Eppendorf tubes, which were then frozen in liquid nitrogen and thereupon stored at -80°C. For RNA extraction, the lobes were thawed on ice, placed into gentleMac tubes (Miltenyi Biotec, Bergisch Gladbach, Germany) and covered with 700 µl QIAzol. The samples were homogenized using gentleMACS Dissociator (Miltenyi Biotec, Bergisch Gladbach, Germany) and centrifuged for 5 minutes at 2000 RPM. The supernatant was pipetted into new Eppendorf tubes and 140 µl Trichlomethan was added. The tubes were shaken strongly for 15 seconds. Afterwards the liquid was moved into Phase Lock tubes (5 Prime, Hilden, Germany), incubated for 3 minutes and then centrifuged at 4°C and 12RCF for 15 minutes. The phase above the Lock Gel was pipetted into RNeasy mini Columns (Qiagen, Hilden, Germany) meanwhile measuring the pipetted volume. The phase beneath the Lock Gel was discarded. 1.5 times of the previously dertermined volume was added to the samples in ethanol. Probes were then washed following the kit instructions of RNeasy Mini Kit (Qiagen, Hilden, Germany). The concentration of RNA was detected with nanodrop 2000c (Peqlab, VWR, Erlangen, Germany) using 1 µl of isolated RNA.

2.4 Reverse Transcription Quantitative PCR

2.4.1 Synthesis of cDNA

The RNA stored at -80°C was thawed on ice. Then genomic DNA elimination was carried out, using 2 µl DNA wipeout buffer, 2 µg of template RNA and 10 µl RNAse-free water. Probes were incubated for 2 minutes at 42°C, afterwards put on ice immediately. Further on 1µl of reverse transcriptase, 4µl RT buffer and1µl RT Primer Mix were added to the PCR tubes. Reverse transcription was carried out using QuantiTect Reverse Transcription Kit (Qiagen, Hilden, Germany). The material was incubated at 42°C for 50 minutes and 3 minutes at 95°C, which was performed by Thermal Cycler C1000 (Bio Rad Laboratories Inc, Hercules, California, USA). For qPCR, samples were diluted to a concentration of 3ng/µl with RNase free water and stored at -20°C.

2.4.2 Real time PCR

For qPCR, the SYBR green System (Invitrogen, life technologies, Carlsbad, USA) was used with a LightCycler 480 (Roche, Basel, Switzerland). The genes to be examined were pipetted in triplets using 2 µl cDNA and 18µl Mastermix. The Mastermix consists of 0,4 µl of each, forward and reverse, primer, 7.2 µl H2O and 10 µl SYBR green. *Hprt* was used as housekeeping gene. The LightCycler preformed 45 cycles consisting of pre-incubation (2 minutes at 55°C and 5 minutes at 95°C), amplification (5 seconds at 95°C, 10 seconds at 60°C and 10 seconds at 72°C) and melting curves. For further analysis, the cycle threshold values, or CT values, were entered into an Excel evaluation sheet, which calculated the p-values and standard deviation. Outliers within the triplets, which differed more than 2 cycles, were removed from calculations. For final results ddCT values were used. Also, T-test was calculated using Prism (Graphpad, La Jolla, CA 92037 USA).

For the analysis of gene expression of the Fgf10 and Tgf-ß signaling pathways, and for examination of epithelial cell and myofibroblast markers, the following mouse primers were used:

Table 3

Mouse primers: Fgf10 signaling		
Gene	**Forward sequence**	**Reverse sequence**
Hprt	CCTAAGATGAGCGCAAGTTGAA	CCACAGGACTAGAACACCTGCTAA
Fgf10	ATGACTGTTGACATCAGACTCCTT	CACTGTTCAGCCTTTTGAGGA
Fgfr2b	CCTACCTCAAGGTCCTGAAGC	CATCCATCTCCGTCACATTG
Fgfr1b	TGGGTCGGTGCGGAGATCGT	ACGGACAACAACAAACCAAACCCT
Etv4	CAGACTTCGCCTACGACTCA	GCCATAACCCATCACTCCAT
Etv5	GCAGTTTGTCCCAGATTTTCA	GCAGCTCCCGTTTGATCTT
Spry2	GAGAGGGGTTGGTGCAAAG	CTCCATCAGGTCTTGGCAGT
Spry4	GTGGAGCGATGCTTGTGAC	CACCAAGGGACAGGCTTCTA
Bmp4	GAGGAGTTTCCATCACGAAGA	GCTCTGCCGAGGAGATCA
N-myc	CCTCCGGAGAGGATACCTTG	TCTCTACGGTGACCACATCG

Table 4

Mouse primers: Epithelial markers		
Gene	**Forward sequence**	**Reverse sequence**
Nkx1.2	AAAACTGCGGGGATCTGAG	TGCTTTGGACTCATCGACAT
SpB	AACCCCACACCTCTGAGAAC	GTGCAGGCTGAGGCTTGT
SpC	GGTCCTGATGGAGAGTCCAC	GATGAGAAGGCGTTTGAGGT
Cc10	GATCGCCATCACAATCACTG	CAGATGTCCGAAGAAGCTGA
Epcam	TGTCATTTGCTCCAAACTGG	GTTCTGGATCGCCCCTTC
Aqp5	TAA CCT GGC CGT CAA TGC	GCC AGC TGG AAA GTC AAG AT

Table 5

Mouse primers: Tgf-ß signaling		
Gene	**Forward sequence**	**Reverse sequence**
Tgf-ß1	TGGAGCAACATGTGGAACTC	CAGCAGCCGGTTACCAAG
Tgf-ß3	GCAGACACAACCCATAGCAC	GGGTTVTGCCCACATAGTACA
Pai-1	AGGATAGGATCGAGGTAAACGAGAGC	GCGGGCTGAGATGACAAA
Smad7	AAGTGTTCAGGTGGCCGGATCTCAG	ACAGCATCTGGACAGCCTGCAGTTG
IL-1ß	TGTAATGAAAGACGGCACACC	TCTTCTTTGGGTATTGCTTGG

Table 6

Mouse primers: Myofibroblast markers		
Gene	**Forward sequence**	**Reverse sequence**
Pdgfr-α	TGCAAATTGACATAGAAGGAGAAG	GCCCTGTGAGGAGACAGC
Pdgf-a	TGAGGTTAGAGGAACACCTG	TCTCACCTCACATCTGTCTC
Elastin	CCACCTCTTTGTGTTTCGCT	CAAAAGAGCACACCAACAATCA
Acta2	ACTCTCTTCCAGCCATCTTTCA	TAGGTGGTTTCGTGGATGC
Fgf9	TGCAGGACTGGATTTCATTTA	CCAGGCCCACTGCTATACTG
Fgfr4	GGAAGGTGGTCAGTGGGAAG	CTCTTGCTGCTCCAGGATTG

2.5 Quantitative PCR for *miR154-3p/-5p*

Isolation of small RNAs was performed with a MirVana MiRNA Isolation Kit (Life Technologies, Carlsbad, USA). Thereupon retro transcription was performed with the Reverse Transcription Kit (Applied Biosystems, Foster City, California, USA) running the following program: 16°C for 30 minutes, 42°C for 30 minutes and 85°C for 5 minutes. 1 µl of each product of retro transcription was then used for Quantification of miRNA levels, based on TaqMan Micro RNA Assays (Life Technologies, Carlsbad, USA). *U6* expression levels functioned as reference gene. LightCylcer 480 run a program of 40 cycles each consisting of 10 minutes at 90°C, 15 seconds at 95°C, 60 seconds at 60°C and 30 seconds at 40°C.
Data were analyzed as described above.

2.6 Fixation of lungs

After the harvest the left lobes were placed into 4% PFA overnight at 4°C. The following day they were stored in phosphate-buffered saline (PBS) for 24 hours at 4°C. On the third day, the lobes were put into 30%, 50% and 70% ethanol for 2 hours each and overnight at 100% ethanol, all at room temperature. The lobes were then brought into Xylol until they became transparent (about 40 minutes). Afterwards, the samples were placed into Xylol-wax (Xylol to paraffin ratio was one-to-one) for 2 hours and in paraffin overnight, both at 60°C. The left lobes were then fixed in paraffin blocks with the Leica EG 1150 H embedding machine (Leica, Wetzlar, Germany). The paraffin blocks were cooled with Leica EG 1150 C (Leica, Wetzlar, Germany). For histological staining the blocks were cut in 5 µm sections using Leica RM 2235 (Leica, Wetzlar, Germany).

2.7 Immunohistochemistry/ Immunofluorescence

2.7.1 Hematoxylin Eosin staining

Slides with sections of 5 µm thickness were deparaffinized as following: The object carriers were dived into Xylol three times for 10min. Then plunged into 100%, 95%, 70%, 50% and 30% ethanol for 2 minutes each. Afterwards immersed into MiliQ for

another 2 minutes. The slides were then stained with Hematoxylin (Carl Roth, Karlsruhe, Germany) for 1-3 minutes and afterwards cleaned under running tap water. The staining intensity was controlled under the microscope.
The staining process continued by diving the slides into the Eosin resolution (Thermo Scientific, Kalamazoo, MI-USA) for 2 minutes. Finally, the slides were dipped 6 times into 80% and 100% ethanol each and cover slipped with Pertex (Histo Lab Products AB, Västra Frölunda, Sweden)

2.7.2 Acta2 staining

The deparaffination was carried out as mentioned above. Afterward the slides were washed three times for 5 minutes in PBST (PBS + 0,1% Tween20). The block mix consisting of PBS, 3% BSA (bovine serum albumin solution) and 0,4% Triton-X was applied. The samples were then incubated at room temperature for 60 minutes. As the block mix was discarded, the primary antibody was pipetted on the samples. The antibody concentration was 1:200. The probes were therefore incubated at room temperature for 60 minutes. Before covering the slides with ProLong Gold antifade reagent with DAPI (Life Technologies, Carlsbad, USA) they were washed three times for 10 minutes with PBST at the AT stirrer and once for 5 minutes with PBS.
Pictures were taken with Leica fluoresce microscope, Leica DM5500 B (Leica, Wetzlar, Germany). 5 images in 40x magnification per lung were analyzed for alveolar myofibroblast quantification with ImageJ (Wayne Rasband, NIH, Bethesda, Maryland, USA). Statistical evaluation was performed with Prism (Graphpad, La Jolla, CA 92037 USA).

2.8 Alveolar morphometry

A Leica DM600B microscope was used to generate total scans of hematoxylin and eosin (HE; see above) stained, 5mm thick, lung sections. The scans were then analyzed with Qwin V3 software (Leica, Wetzlar, Germany) in order to determine the mean linear intercept (MLI; in μm), mean air space (in %) and mean septal wall thickness (in μm). Tissue borders, as well as bronchi and blood vessels were manually marked and excluded from calculations. Non-stained areas were recognized as air space, whereas

stained parts were recorded as lung tissue. The average values for MLI, mean air space and septal wall thickness were statistically evaluated with Prism (Graphpad, La Jolla, CA 92037 USA).

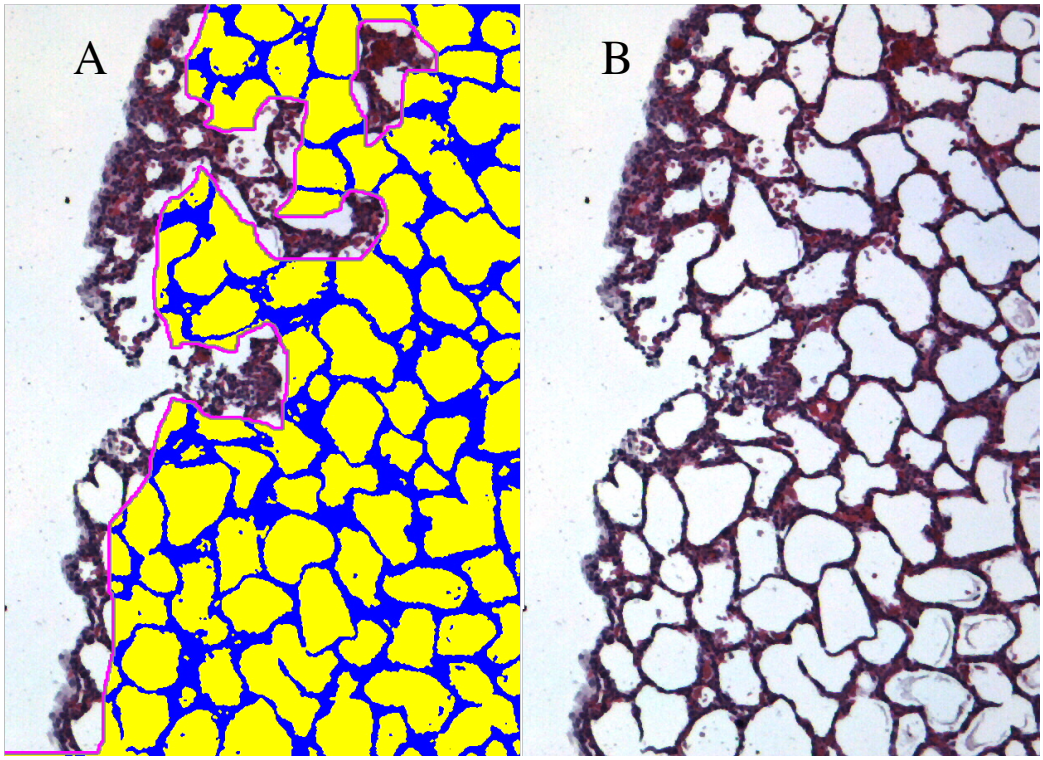

Figure 03. Methodical procedure alveolar morphometry at E18.5.
Scans of E18.5 lungs were uploaded into Leica's Qwin V3 software after Hematoxylin and Eosin staining. **(A)** E18.5 lung after manual exclusion of lung borders: yellow areas are registered as air space. Blue areas are recognized as septal lung tissue. **(B)** Lung at E18.5 before processing with Qwin V3.

2.9 In-vitro lung culture

Prior to the execution of the experiment, 50 µl Fetal Bovine Serum (ATCC *20-2030*, Manassas, USA) and 5 ml of Penicillin (10.000 U/ml)/Streptomycin (10 mg/ml) (PAN Biotech, *Cat-No. P06-07005,* Aidenbach, Germany) were added to DMEM medium which already contains glutamine.

WT E11.5 lungs were dissected under Leica M125 C microscope (Leica, Wetzlar, Germany) and placed in a glass petri dish with 10 µl of DMEM to keep them moisturized. Multi-well plates were prepared with 500 µl DMEM medium (Thermo Fisher Scientific, Waltham, USA) and Whatman Nuclepore membrane filters (GE Healthcare, Solingen, Germany). The explants were placed carefully on the membrane filters and treated either with Morpholino vivo *miR-154* (Gen Tools, Oregon, USA) or scrambled sequences (Geng at al. 2011). For the experimental group 4 µl of 0.5mM morpholino solution were added to 500 µl DMEM medium to obtain 4 µM end concentration of morpholino for the incubation of lung. 4 µl of scrambled sequences were added to the medium of the control group. Lungs were cultured on air-liquid interface at 37˚C for 72 hours. After 24 hours, 48 hours and 72 hours of culturing photos were taken with Leica MZ 125 (Leica, Wetzlar, Germany) and Spot imaging software (Diagnostic Instruments Inc, Sterling Heights, USA). Based on the images the buds were counted later on and p values were calculated using Prism (Graphpad, La Jolla, CA 92037 USA).

With completion of the 72 hours the lungs were collected, placed into QIAzol (Qiagen, Hilden, Germany) and stored at -80°C. For gene analysis RNA isolation and qPCR, as well as quantitative RT PCR were performed as described above.

3 Aims of the study

In the context of organogenesis research, microRNAs have gathered increasing interest in the recent decades. A substantial number of these small non-coding RNAs have already been linked to early lung development (Jiang et al. 2013; Carraro et al. 2009; Bhaskaran et al. 2009). One of those is *miR-154*, a member of the largest human microRNA cluster, which has previously been detected to be highly expressed in neonatal mouse lung (Williams et al. 2007). Until now however, only little is known about the effects of this specific microRNA. Therefore, we aimed to investigate the role of *miR-154* during the organogenesis of the lung. We approached this objective in two ways. First we overexpressed *miR-154* during E7.5 until E18.5 and secondly we blocked *miR-154* at E11.5 for 72 hours.

By means of our experimental inquiries we aimed to answer the following questions:

1.) Does *miR-154* overexpression during embryonic lung development lead to changes in gene expression and morphology of the lung?

2.) Does in-vitro blockade of *miR-154* during embryonic lung development lead to changes in gene expression and morphology of the lung?

4 Results

As only very little is yet understood about the role of *miR-154* in lung organogenesis, it was our main interest to examine the effects of this certain microRNA during the early developmental process of the lung. Therefore, we designed two experimental approaches, a gain and a loss of function model. In the first one, we overexpressed *miR-154* in a Tg(*CCSP-rtTA)/+;Tg(tet(O)miR-154)*/+ mouse model from E7.5 until E18.5, and analyzed the effects on morphology and gene expression. The second experimental setup was created in order to determine the effects of a blockade of *miR-154* during in vitro culture. Here wild type lungs were harvested at E11.5 and grown for 72 hours. Throughout the culture we used a Morpholino treatment to block *miR-154* in the experimental group.
In the following the results of both approaches will be presented. Therefore, the section is divided into two parts. At first, the observed effects of overexpressing *miR-154* during the time period of E7.5 until E18.5 will be presented. The second part deals with the blocking of *miR-154* from E11.5 for 72 hours.

4.1 Overexpression of *miR-154* in *Tg(CCSP-rtTA)/+;Tg(tet(O)miR-154)*/+ mice (E7.5 - E18.5)

The experimental set up for the gain of function model was designed to generate significantly increased epithelial expression levels of *miR-154* during the early stages of embryonic lung organogenesis. We aimed to raise *miR-154* expression from E7.5 until E18.5. This time period comprises the embryonic stage, the pseudoglandular stage (from E11.5 to 16.5), the canalicular stage (from 16.5 to 17.5) and partially the terminal saccular stage (beginning E17.5) of lung development.

For the implementation of our strategy, mice heterozygous for both *Tg(CCSP-rtTA)* and *Tg(tet(O)miR-154)* were crossed. **Figure 02** shows all possible genotypes that may result from this crossing. Also, the classification to either the Control or Experimental group is illustrated. The pictured mating was the one with the highest potential to

generate equal amounts of both experimental and control samples within the same litter. Thus, we could apply the exact same treatment to all of our samples.

The *miR-154* transgene, which we used, was previously analyzed by Gianni Carraro **Figure 04 A-C**. After installation into the mouse genome, the *miR-154* transgene is located adjacent to *Snx19*. Gianni Carraro proved, that in comparison with wild types, the mice carrying the *miR-154* gene showed no significant alteration of *Snx19* expression. Consequently, the installation of the *miR-154* transgene itself does not significantly affect the natural processes in our transgenic mice (**Figure 04**). The transgene comprises an tet(O) operon, the *miR-154* gene and a poly(A) tail. The presence of this transgene can be verified with gel electrophoresis. The corresponding band is located between 300 and 400 base pairs (**Figure 05**).

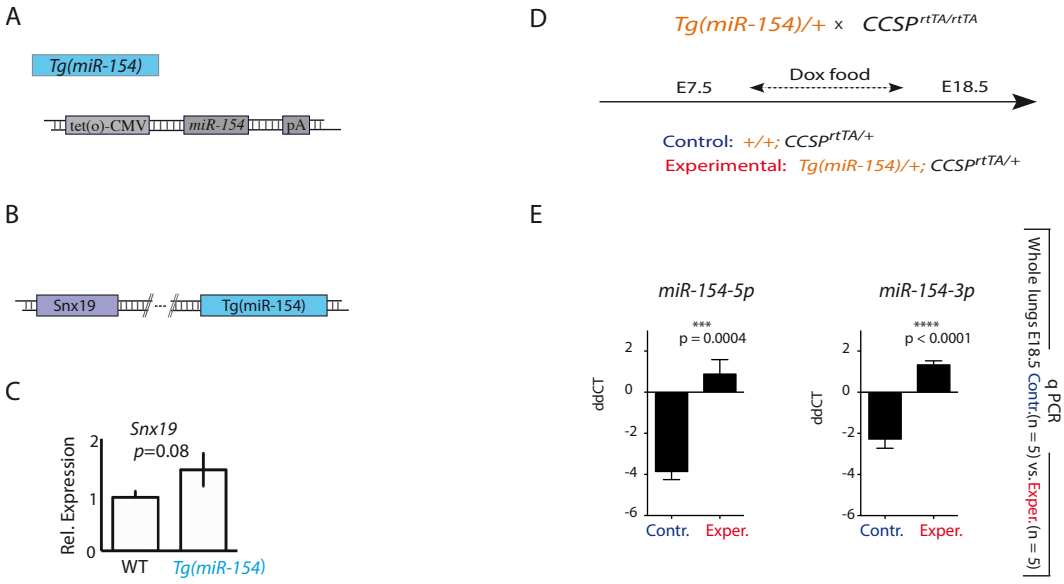

Figure 04. Design of transgenic mouse line.
(A) *MiR-154* transgene composes a tet(O) operon, the *miR-154* transgene and a poly A tail. **(B)** *MiR-154* transgene is located adjacent to *Snx19* in transgenic mice. **(C)** *Snx19* expression is not significantly altered due to gene insertion in transgenic mice. **(D)** Timeline of experimental set up: The pregnant mice were fed with doxycycline food from E7.5 to E18.5 in order to induce *miR-154* overexpression. **(E)** *MiR-154*-3p and *miR-154*-5p are both significantly overexpressed in the experimental group at E18.5.

The Tet-On system, we used, is designed to induce overexpression of target genes in the presence of an effector. The binding of doxycycline causes a conformational switch in the reverse-rtTA variant, which is then able to bind the tet operator (tet(O)). The following activation of the P-tet promoter allows the expression of the downstream located gene (Das, Tenenbaum, and Berkhout 2016). After the mating, the desired overexpression of *microRNA 154* is reached by feeding doxycycline food to the pregnant mother from E7.5 until E18.5.

4.1.1 Verification of miR-154 overexpression in transgenic mice

In our experimental set up all embryonic lungs were harvested at E18.5. Thereupon, we examined the genotype of every pup for the *CCSP-rtTA* and *miR-154* alleles. By selective gene amplification and gel electrophoresis, the *CCSP* promoter allele was detected at 500 base pairs. The alleles for *miR-154* could be verified at 465 base pairs for wild type and at 231 base pairs for the mutant genotype. On the basis of these results, all animals were classified as Control or Experimental. **Figure 05** shows an example of the genotyping of both Control and Experimental pups. All Controls are homozygous for the wild type alleles of either the *CCSP* promoter or the *Tg(tet(O)miR-154),* or both. Mice with these genotypes are unable to respond to the doxycycline food. In contrast, the animals within the Experimental group carry both transgenes. These animals might be homo- as well as heterozygous for *Tg(tet(O)miR-154)*.

In order to confirm the sufficient overexpression of *miR-154* at E18.5, we performed a quantitative PCR, using *U6* as housekeeping gene. Control as well as Experimental group comprised five animals (n=5). The experimental group showed highly significant expression levels for *miR-154-5p* ($p = 0.0004$). Likewise, *miR-154-3p* was significantly higher expressed ($p < 0.0001$) in the experimental group. In contrast, the expression of both *miR-154-3p* and *miR-154-5p* were attenuated in the control group. We therefore assumed a sufficient overexpression of *miR-154* (results shown in **Figure 04 E**).

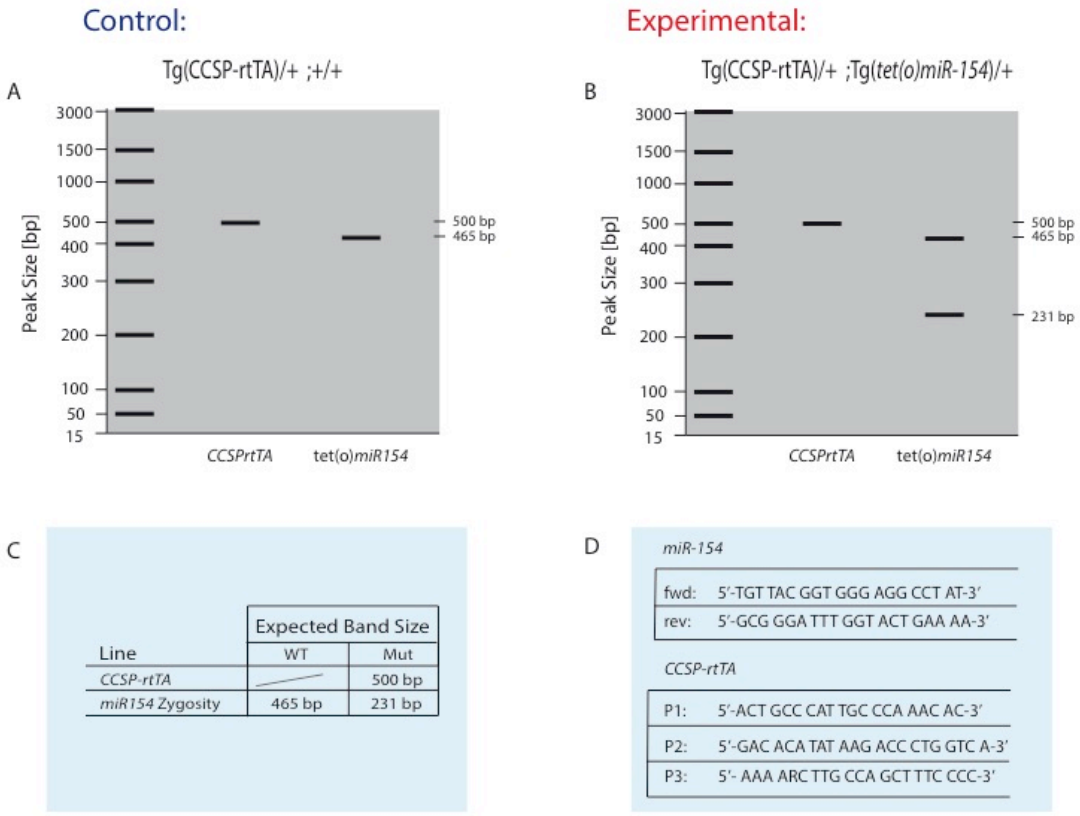

Figure 05. Exemplary genotyping of an experimental and a control mouse at E18.5. **(A)** Gel electrophoresis of a Control group mouse: Only one band was detected for the *CCSP-rtTA* transgene in WT mice. The presence of the *miR-154* wild type gene was detected with the band at 465 base pairs. **(B)** Gel electrophoresis of an Experimental group mouse (heterozygous): The mutant shows bands for the *CCSP-rtTa* transgene at 500 base pairs and a band for the *miR-154* transgene at 231 base pairs, as well as a band for the *miR-154* wild type gene. (**C**) Expected band sizes for *CCSP-rtTA* and *miR-154*. (**D**) Primer sequences for miR-154 and *CCSP-rtTA*.

4.1.2 Overexpression of miR-154 leads to thinning of alveolar septa and alveolar simplification

The explanted lungs showed no macroscopic differences in terms of size and number of lobes. Moreover the surface structure of all lungs appeared regular. As the experimental setting was confirmed with the quantitative RT-PCR, we subsequently focused on the microscopic differences in phenotype. Therefore, the Hematoxylin and Eosin (H&E) staining was carried out.

The first impression of the H&E staining was a distinct difference in lung structure. The epithelial overexpression of *miR-154* in the Experimental group appeared to lead to an emphysematous phenotype with thinned alveolar septa and extended alveoli. We thereupon aimed to objectify these observations by alveolar morphometry. For this more precise analysis of phenotypic differences, hematoxylin and eosin stained slides were scanned and uploaded to Qwin V3 software. Here the mean linear intercept (MLI, in µm), the airspace (in %) and mean septal wall thickness (in µm) could be determined. The MLI is a parameter of volume-to-surface ratio and reports the mean free distance in the airspaces. It may however not be considered as measure for “alveolar size” (Knudsen et al. 2010).

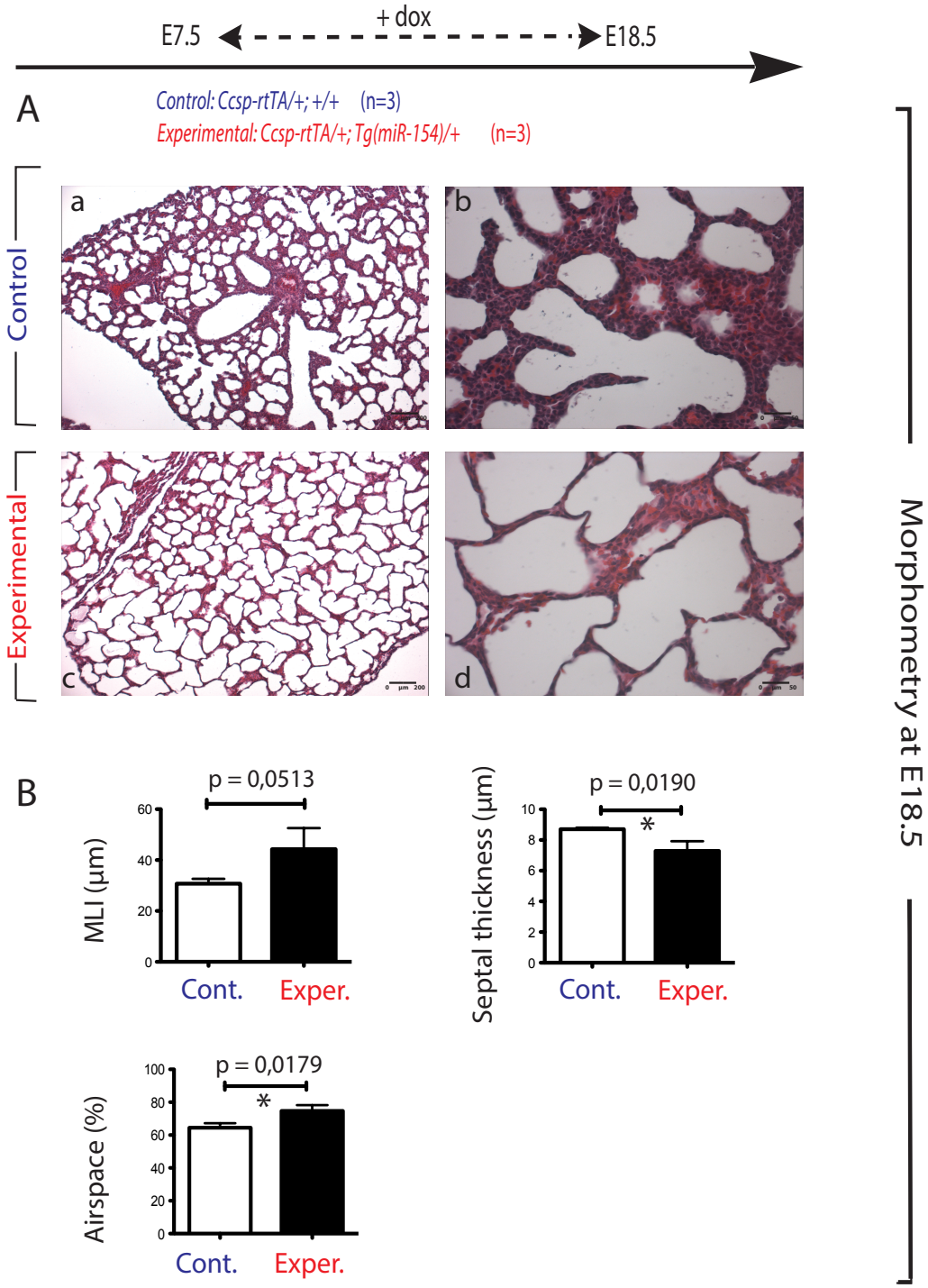

Figure 06. Overexpression of *miR-154* leads to altered lung morphology at E18.5

A) Overexpression of *miR-154* during E7.5 until E18.5 and related Hematoxylin/Eosin staining of control **(a, c)** and experimental lungs **(b, d)** at E18.5. **(B)** Corresponding alveolar morphometry at E18.5 discloses increased MLI **(a)**, significant elevation of airspace **(c)** and significantly decreased septal thickness **(b)**.

Congruently with our observations, the experimental group showed significantly reduced septal wall thickness ($p = 0.0190$) and significantly extended airspace ($p = 0.0179$) compared to the controls. The average septal thickness within the experimental group was 7.26 µm, the average airspace was 74.7%. Within the control group we measured an average septal thickness of 8.7µm and 64.4% average airspace. The mean linear intercept was almost significantly higher ($p = 0.0513$) in the experimental group, with an average of 44.3 µm compared to only 30.7 µm within the control group.

4.1.3 miR-154 overexpression causes down regulation of alveolar myofibroblast markers

To uncover the mechanism behind the observed phenotype, we performed several RT-qPCRs for gene analysis. Hereby we put our focus on Fgf10 and Tgf-ß signaling pathways, which are known to be orchestrating lung development. We also investigated the expression levels of epithelial cell markers, which would presumably give us an impression of tissue composition. Moreover, we were highly interested in the expression of alveolar myofibroblast (AMF) markers. These cells are known to be crucial for alveolar septation (Kim and Vu 2006). Each of our examined groups, Experimental and Control, comprised five animals ($n = 5$).

Fibroblast growth factor 10 (Fgf10) is known to have crucial impact on embryonic lung development. It mediates its effects mainly through transmembrane Tyrosine kinase receptors Fgfr2b and Fgfr1b. In the experimental group *Fgf10* and *Fgfr1b* are both down regulated, whereas *Fgfr2b* is slightly up regulated. *Etv4* and *Etv5*, both transcription factors acting downstream of Fgf10 are equally down regulated within the experimental group. Interestingly Fgf10 signaling modulators Spry2 and Spry4 are differently expressed. *Spry2*, which can be found in embryonic lung epithelium, is up regulated, whereas the mesenchymal located *Spry4* is down regulated. Moreover, we found *Bmp4*, a counter actor of Fgf10, up regulated. Also, *Nmyc*, another important gene in developing lung patterning, is up regulated.

Subsequently we analyzed the epithelial cell markers of the transgenic and wild type mice to draw an image of epithelial cell composition. We found elevated expression levels for *SpB*, a cell marker for alveolar epithelial cell type two (AECII) and an indicator for sufficient surfactant production. *SpC*, another marker for alveolar epithelial cell type two, as well as *Aqp5*, which is recognized as a marker for alveolar epithelial cell type one (AECI), were equally up regulated. The epithelial cell adhesion molecule (EpCam) is a transmembrane glycoprotein, which acts as cell-to-cell adhesion molecule in the epithelium. Interestingly, we found a highly significant up-regulation of *Epcam* ($p = 0.0031$), which might indicate a general increase of Epithelium, as well as an alteration of mesenchymal to epithelial ratio. *CC10*, the marker for secretory Club cells and *Nkx2.1*, an early marker of lung endoderm, were down regulated in the experimental group.

Furthermore, we were interested in potential changes of Tgf-ß signaling. This signaling pathway is a setscrew in numerous developmental processes including lung organogenesis. Signal mediating transforming growth factor beta 1 and 3 (*Tgf-ß*1; *Tgf-ß*3) were both down regulated in transgenic mice. Also, we found *Smad7*, an inducible antagonist of Tgf-ß signaling, down regulated. *Pai-1*, short for plasminogen activator inhibitor-1, is an important regulator of extra cellular matrix balancing (Kutz et al. 2001) and acts downstream of Tgf-ß. It is also it's strongest inducer and was found up regulated in our analysis. The same applies for *IL-1*, which codes for a pro inflammatory messenger substance and is therefore used as inflammatory marker.

Most strikingly, the examination of markers for alveolar myofibroblast revealed a general down-regulation. Within the experimental group, all of the investigated genes, apart from *Elastin*, showed this trend. This is particularly noteworthy, as alveolar myofibroblasts have a major impact on alveolar septation and therefore might be accountable for the observed phenotype.

Pdgf signaling, which is linked to lung organogenesis, usually shows high expression in fibroblasts and smooth muscle cells. Here we found Platelet-derived growth factor a, *Pdgf-a*, and *Pdgfr-α*, the related transmembrane Tyrosine kinase receptor, both significantly down regulated ($p = 0.0358$; $p = 0.0408$). *Alpha-actin-2* (*Acta2)*, also known as *alpha smooth muscle actin (α-SMA),* is a marker for smooth muscle cells and was slightly down regulated. Moreover, we detected a significant down regulation ($p = 0.0198$) of *Fgf9*, which is known to be involved in branching morphogenesis. The

expression levels of *Fgfr4*, a Fgf receptor, which has been linked to formation alveolar septa (Weinstein et al. 1998) presented itself equally down regulated within the experimental group. The only up regulated gene in this set was *Elastin*, the coding gene for the key component of elastic fibers.

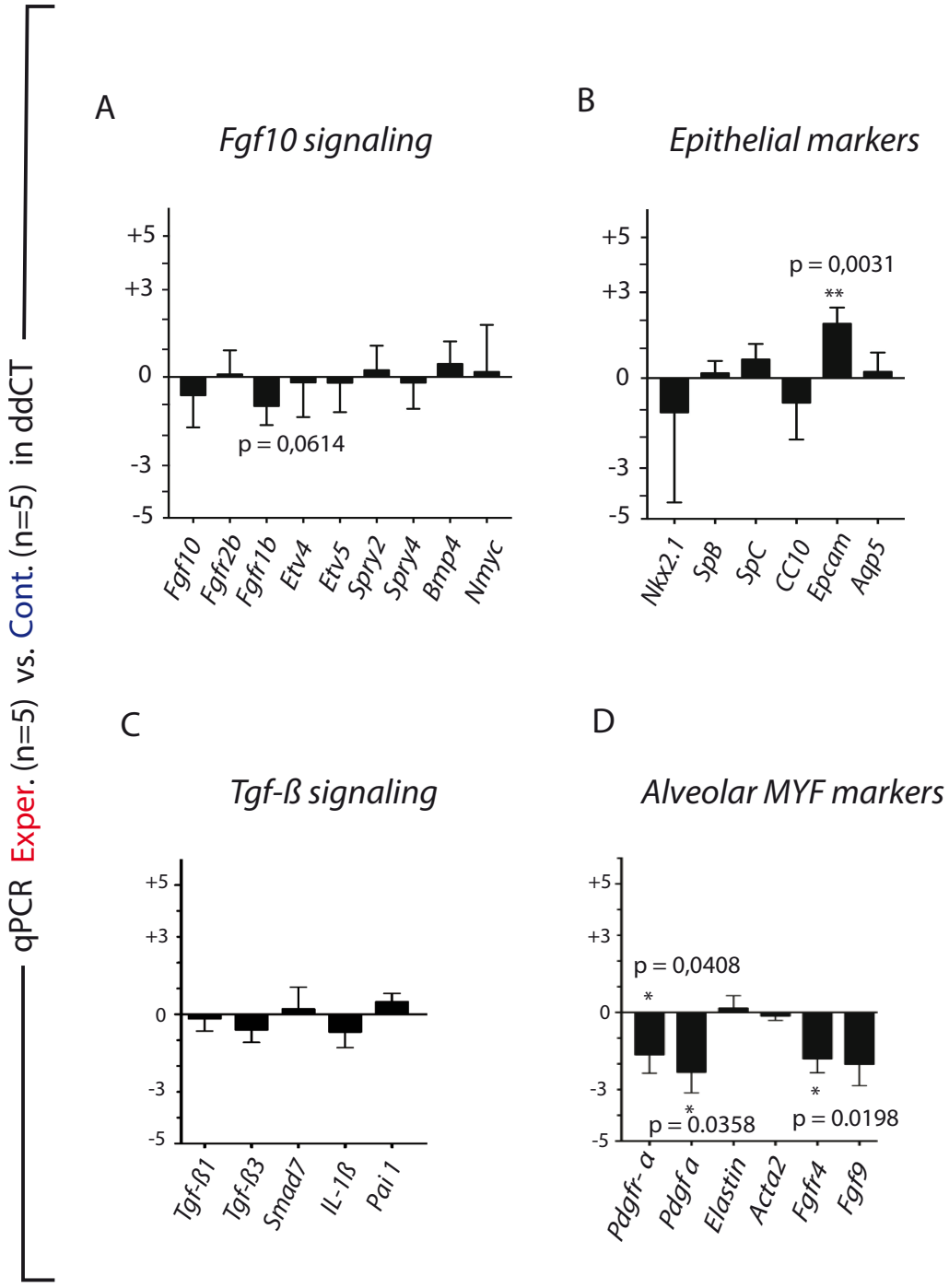

Figure 07. Overexpression of *miR-154* from E7.5 to E18.5 leads to changes in gene expression of *Fgf10*, epithelial markers, *Tgf*-ß signaling and AMF markers.
(A) In Fgf10 signaling five out of nine genes were found down regulated. These comprised *Fgf10*, *Fgfr1b*, *Etv4*, *Etv5* and *Spry4*. Contrary alterations were disclosed for *Fgfr2b*, *Spry2*, *Bmp4* and *Nmcy*. None of the observed changes were significant.
(B) The examination of epithelial markers revealed significantly higher expression levels for *Epcam* (p=0.0031), accompanied by elevated *SpB, SpC* and *Aqp5* expression. Only *Nkx1.2* and *Cc10* were found down regulated. **(C)** Most analyzed genes involved with Tgf-ß-signaling showed reduced expression. This applied for *Tgfß1*, *Tgfß3* and *Smad7*. Only *Pai-1* and inflammatory marker *IL-1b* were up regulated. **(D)** A concordant trend was found regarding the expression of alveolar myofibroblast markers. All genes, apart from *Elastin*, were found down regulated. The expression levels of *Pdgfr*-α (p=0.0408), *Pdgf-a* (p=0.0358) and *Fgf9* (p=0.0198) were significantly reduced.

4.1.4 The quantity of alveolar myofibroblasts is not altered by epithelial overexpression of miR-154 in E18.5 lungs

As we disclosed significant alterations of expression levels within the alveolar myofibroblast fraction, we decided to perform an Alpha-actin-2 (Acta2) staining. The quantification of the alveolar myofibroblasts (AMF) in both Experimental and Control group could potentially reveal further clarity. A changed presence of AMFs could be the cause of the phenotype in question. The Alpha-actin-2 protein is known to be a specific marker for alveolar myofibroblasts and also gives a hint to the location of muscle cells in blood vessels and bronchi. Thus the staining allowed us to evaluate any differences in AMF and smooth muscle presence.
At first sight there were no obvious alterations in smooth muscle actin expression. Control and Experimental group revealed equal occurrence of smooth muscle in bronchi and blood vessels. At higher magnification, we counted the stained alveolar myofibroblasts at the tip of alveolar septa. These are vital for secondary septation of

alveoli. The experimental group showed slightly more AMFs in average. The disparity of 19.25 AMFs in the Experimental group to only 17.25 in the Control group was however not significant.

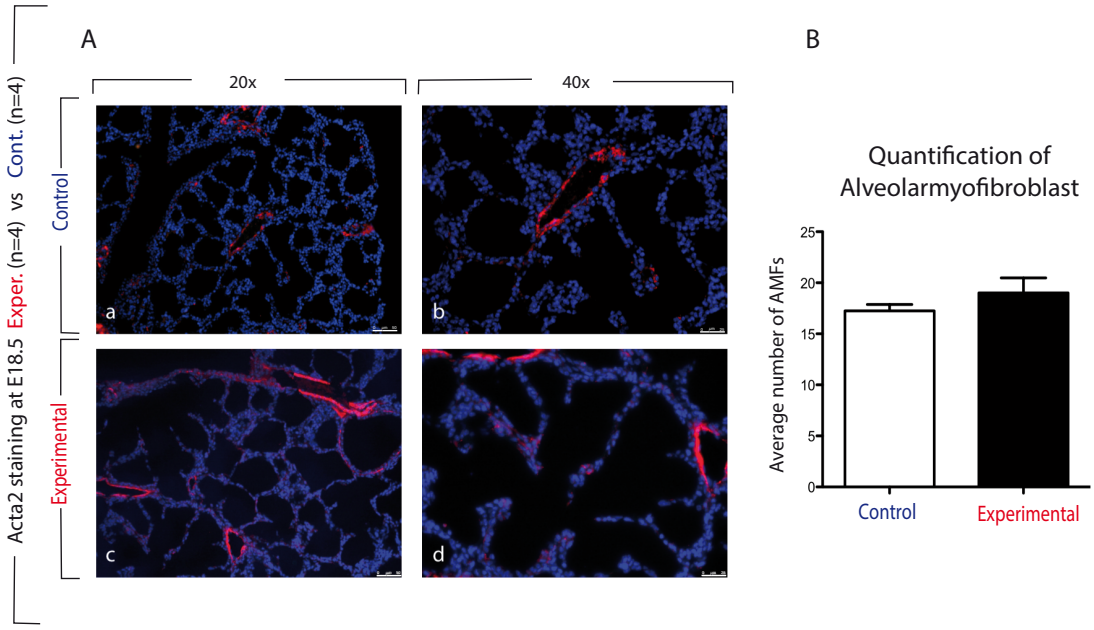

Figure 08. Presence of AMFs is not significantly altered in lungs with epithelial overexpressed *miR-154* at E18.5

(A) Alpha-actin-2 stained lungs at E18.5 in 20x and 40x magnification. Bronchi and vessels appear to contain similar amounts of muscle cells in Control **(a)** and Experimental **(c)** organs. The number of AMFs in alveolar areas of Control **(b)** and Experimental **(d)** lungs in 40x magnification did likewise show no differences at first sight. **(B)** The quantification of AMFs confirmed this assumption. The Control group showed 17.25 AMFs in average. The Experimental lungs contained slightly more: 19.25 AMFs in average.

4.2 Blockade of *miR-154* during in vitro lung culture

The remarkable changes in lung structure and gene expression, which we observed due to the overexpression of *miR-154*, further encouraged our interest in what potential alterations a loss of *miR-154* during early lung development might have. In our second experimental set up we therefore explanted wild type lungs at E11.5. These were cultured in two different treated groups on an air-liquid interface at 37°C for 72 hours. Thereby the Experimental group (n = 4) was treated with morpholino solution. This contains nucleic-acid analoga with the ability to block *miR-154*. The Control group (n = 4) was exposed to an equivalent amount of scrambled sequences. As with the first experimental approach, we focused on lung phenotype and genetic alterations. Therefore, we took pictures of the growing organs every 24 hours. These formed the basis for the analysis of lung phenotypes. After 72 hours, the organs were collected for further examination. We thereupon isolated the RNA of all cultured lungs for the examination of gene expression. The following **Figure 09** gives an overview of the experimental setup and different treatments of the harvested lungs.

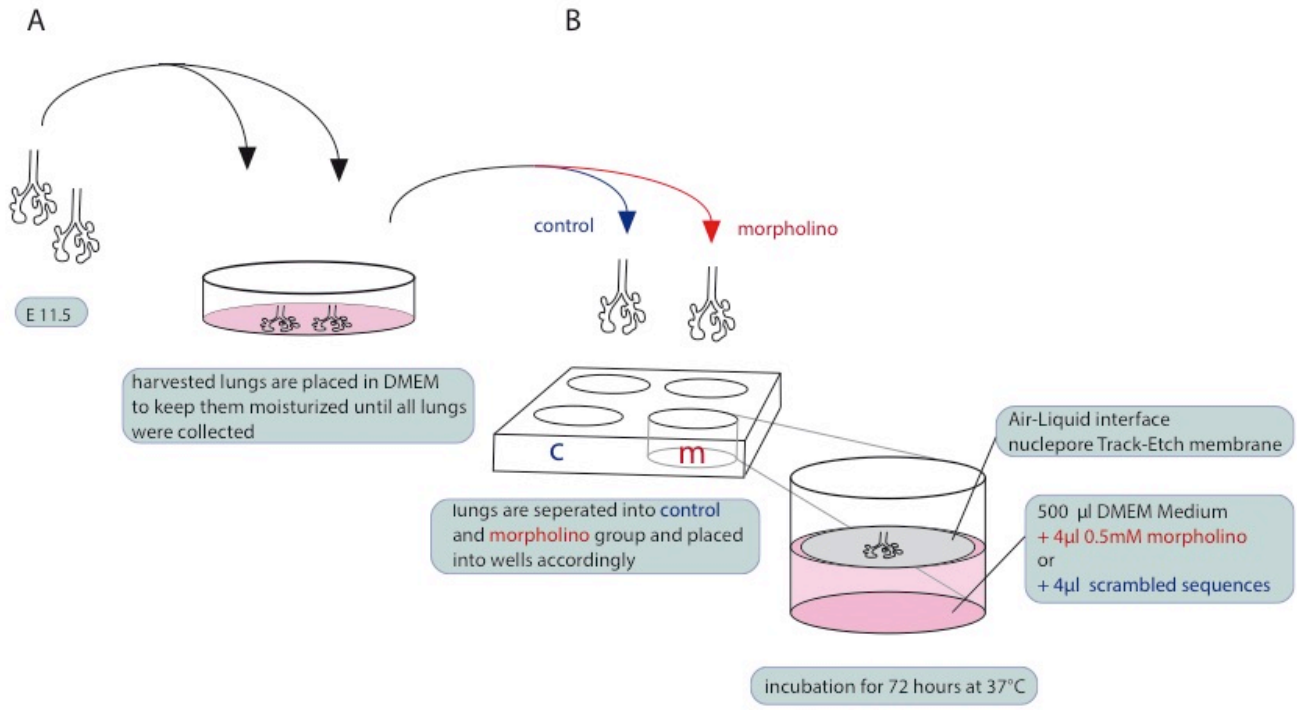

Figure 09. Experimental setup for lung culturing in vitro, starting from E11.5.
(A) Pups were collected from the mother at E11.5 and stored in PBS. Embryonic mice lungs were dissected under a microscope and placed in DMEM to keep them moisturized until all lungs were harvested. **(B)** Lungs were randomly separated into experimental and control group and thereafter placed on to an air-liquid interface. This way the explants had access to air and the nutritious medium simultaneously. Culturing was performed for 72 hours at 37°C.

4.2.1 Morpholino reduces miR-154 expression in embryonic mouse lung

For a start, we aimed to verify the functionality of the used morpholino solution. We therefore collected all lungs after 72 hours of culturing and isolated the RNA. Subsequently we performed a quantitative PCR in order to compare the expression levels of *miR-154*-3p and *miR-154*-5p in both Experimental (n =4) and Control group (n=4).

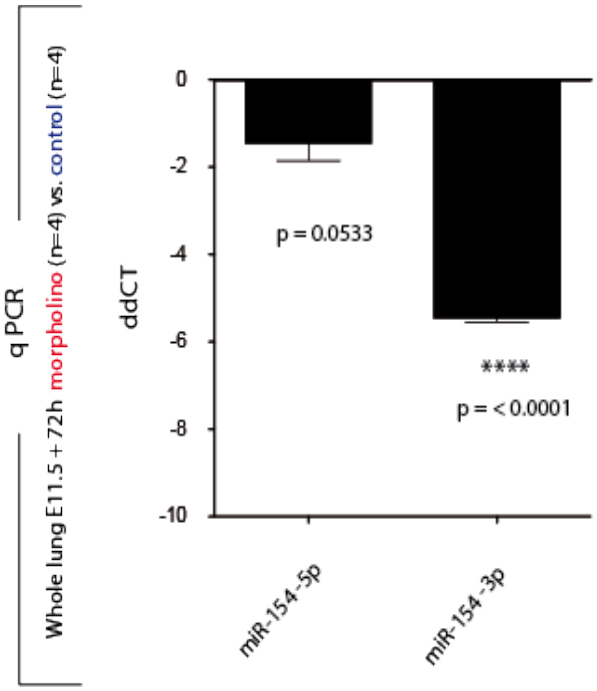

Figure 10. Expression of *miR-154* in in-vitro cultured lungs treated with morpholino vs. control from E11.5 for 72 hours.
Quantitative RT-PCR reveals diminished incidence of both strands of *miR-154* in the morpholino treated group. *MiR-154*-3p is significantly (p=0.0001) reduced in the experimental group. The presence of *miR-154*-5p is almost significantly decreased (p=0.0533).

Thereby *U6* was used as housekeeping gene. Strikingly, we discovered an almost significant attenuation of *miR-154*-5p expression and a highly significant reduction of *miR-154*-3p expression level (p = < 0.0001) in the morpholino treated group. These

results confirm the sufficient function of the morpholino solution and thus the blockade of *miR-154* in the Experimental group. Results are presented in **figure 10**.

4.2.2 Morpholino treatment causes reduced branching morphogenesis

As the reliability of the applied morpholino solution was proven, we concentrated on the morphological differences between both groups. Therefore, we analyzed the pictures taken in the course of the culturing. These were manufactured every 24 hours in 5x and 10x magnification.

At T0, immediately after the harvest, all lungs showed roughly 8 buds. After 24 hours (T1) we could determine the first changes in branching morphogenesis. The control group (n=4) had an average bud number of 14, whereas the morpholino group (n=4) had only 11.25 buds in average. At T2, 48 hours after the explant, the trend proceeded and we recognized significant ($p = 0.232$) differences in the number of buds. Here the average bud quantity within the control group was 25.25. The morpholino group only showed an average of 18.5 buds. Another 24 hours later (T3), 72 hours after the harvest, the control group had 35.5 buds in average. Whereas the morpholino treated lungs only developed an average number of 25.25 lung buds. This deviation is statistically significant with a p value of 0.0001.

lung culture E 11.5 + 72 hourrs morpholino (n=4) vs. Cont. (n=4)

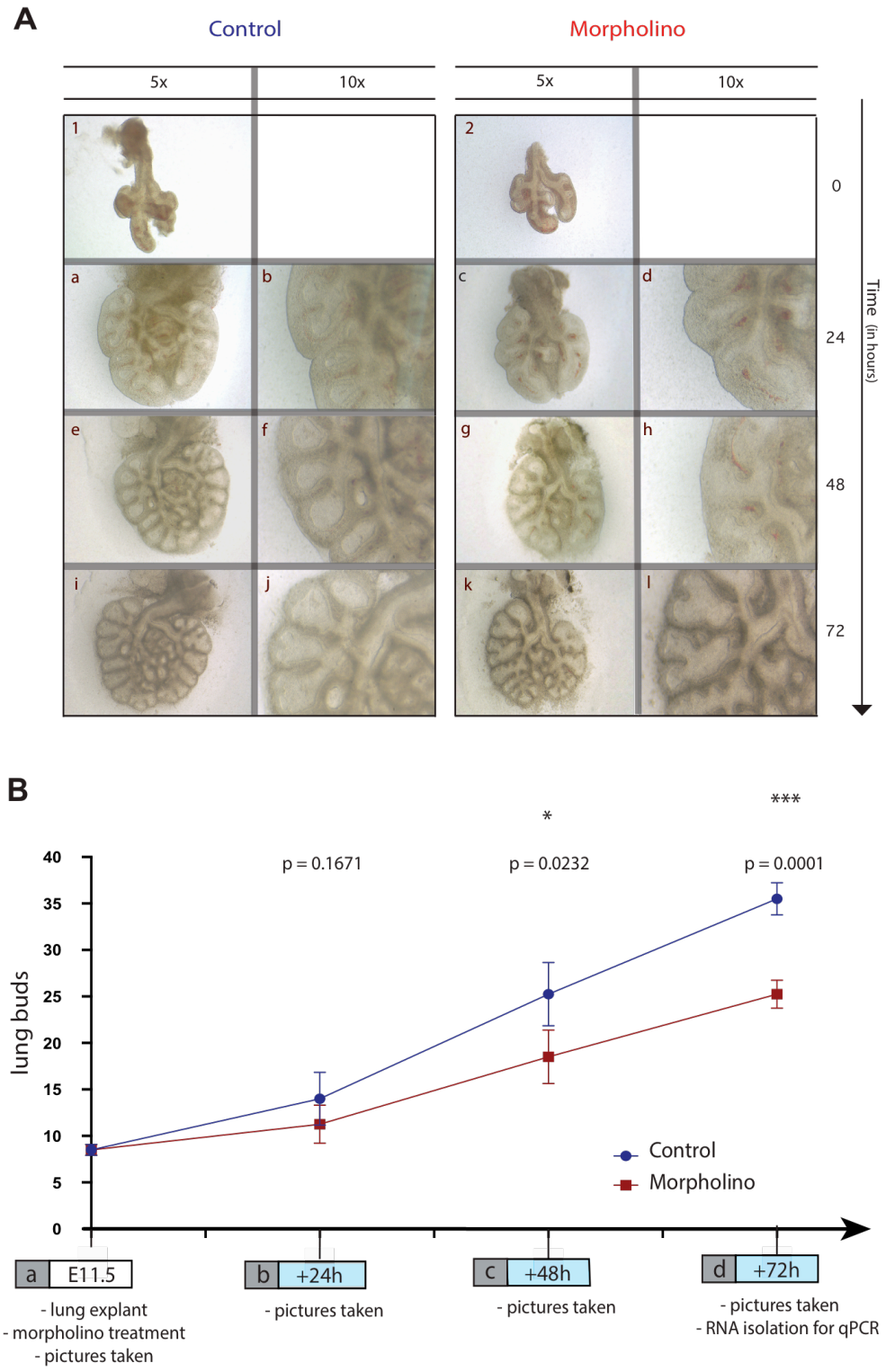

Figure 11. Analysis of in vitro lung culturing from E11.5 for 72 hours.

(A) Branching morphogenesis of cultured lungs.

(1,2) Images of explanted lungs in 5x magnification at E11.5 before treatment (0 hours cultured). Pictures of control **(a, b)** and morpholino **(c, d)** lungs in 5x and 10x magnification after 24 hours of in vitro culture. Control **(e, f)** and morpholino **(g, h)** captured in 5x and 10x magnification after 48 hours. **(i-l)** Lungs after 72 hours of in vitro culture. Images show control and morpholino lungs respectively in 5x and 10x magnification.

(B) Comparative presentation of lung growth (morpholino vs. control).

(a) At E11.5 both groups show lungs with eight lung buds in average. **(b)** After one day, the control lungs present 14 buds in average, whereas the morpholino treated lungs show only 11.25. **(c)** Another 24 hours later the differences become statistically significant (p= 0.0232). Here, the morpholino lungs count only 18.5 buds, whereas the controls grow 25.25 in average. **(d)** After 72 hours the trend reaches its peak with p=0.0001. Until now, the control lungs developed an average amount of 35.5 buds. In contrast the morpholino treated specimens grew only 25.25 buds over all.

The experimental group was treated with a *miR-154* blocking morpholino solution.

4.2.3 Blockade of miR-154 leads to increased expression of Fgf10 and Tgf-ß signaling as well as increased expression of epithelial and alveolar myofibroblast markers

The pertinent macroscopic and morphologic alterations caused by blocking of *miR-154* encouraged us to further investigate *miR-154* effects in detail. Therefore, we followed the approach we performed with the gain of function model and examined the gene expression of major signaling cascades and cell markers - Fgf10 and Tgf-ß signaling, along with the epithelial markers and markers for alveolar myofibroblasts after 72 hours (T3). Both Control and Experimental group comprised four animals (n = 4).

Interestingly, we observed a general overexpression of all genes linked to the Fgf10 signaling. The gene for the main ligand, *Fgf10* itself, was highly significant (p = 0.0074) up regulated. The tyrosine kinase receptors *Fgfr2b* and *Fgfr1b* (p = 0.0316; p =

0.053) and the transcription factors *Etv4* and *Etv5*, which act downstream of Fgf10, were also up regulated. The same applies for the genes of epithelial expressed Fgf10 modulator *Spry2* and Fgf10 antagonist *Bmp4*. Moreover, we observed an up regulation of *Nmyc*. Congruent with the up regulation of Fgf10 signaling, we determined an up regulation of all analyzed epithelial cell markers. *SpB*, the marker for alveolar epithelial cells type two (ACEII) and functioning surfactant production, was significantly ($p = 0.0005$) up regulated. In addition, the markers *Aqp5*, which represents the Pneumocytes type one, or AECI, and *SpC*, the primary marker for AECII, were up regulated. We also recognized a significant elevation of gene expression for the epithelial cell-to-cell adhesion molecule (Epcam; $p= 0.0465$) and the marker for protein secretory Club cells, *Cc10* ($p = 0.0497$).

The analysis of Tgf-ß signaling revealed an overexpression of most genes linked to the signaling pathway. Only *IL 1ß*, coding for an inflammatory signaling molecule, was significantly ($p= 0.0468$) down regulated. Remarkably, *IL-1ß* was the only gene of all 25 examined, which was reduced in expression. Apart from that, we found transforming growth factors beta 1 and 3 (*Tgf-ß1*; *Tgf-ß*3) up regulated, *Tgf-ß3* almost significant ($p = 0.0533$). Furthermore, the Tgf-ß antagonizing *Smad7*, as well as plasminogen activator inhibitor-1 (*Pai-1*) showed increased expression levels.

Just like the general overexpression of Fgf10 signaling associated genes, the overexpression of epithelial markers and the genes related to Tgf-ß signaling, the markers for alveolar myofibroblasts were likewise generally overexpressed in the morpholino treated group. Platelet-derived growth factor a, *Pdgf-a*, and *Pdgfr-α*, the transmembrane Tyrosinkinase receptor, were both up regulated. *Pdgf-a* was almost significantly ($p = 0.068$) and *Pdgfr-α* was in fact significantly ($p = 0.0478$) over expressed. Also, *Elastin* and *Acta2*, or alpha smooth muscle actin (α-SMA), were significantly up regulated ($p = 0.0026$; $p= 0.0211$). Furthermore, we found the Fgf signaling related genes *Fgf9* ($p = 0.0217$) and *Fgfr4* up regulated in the experimental group.

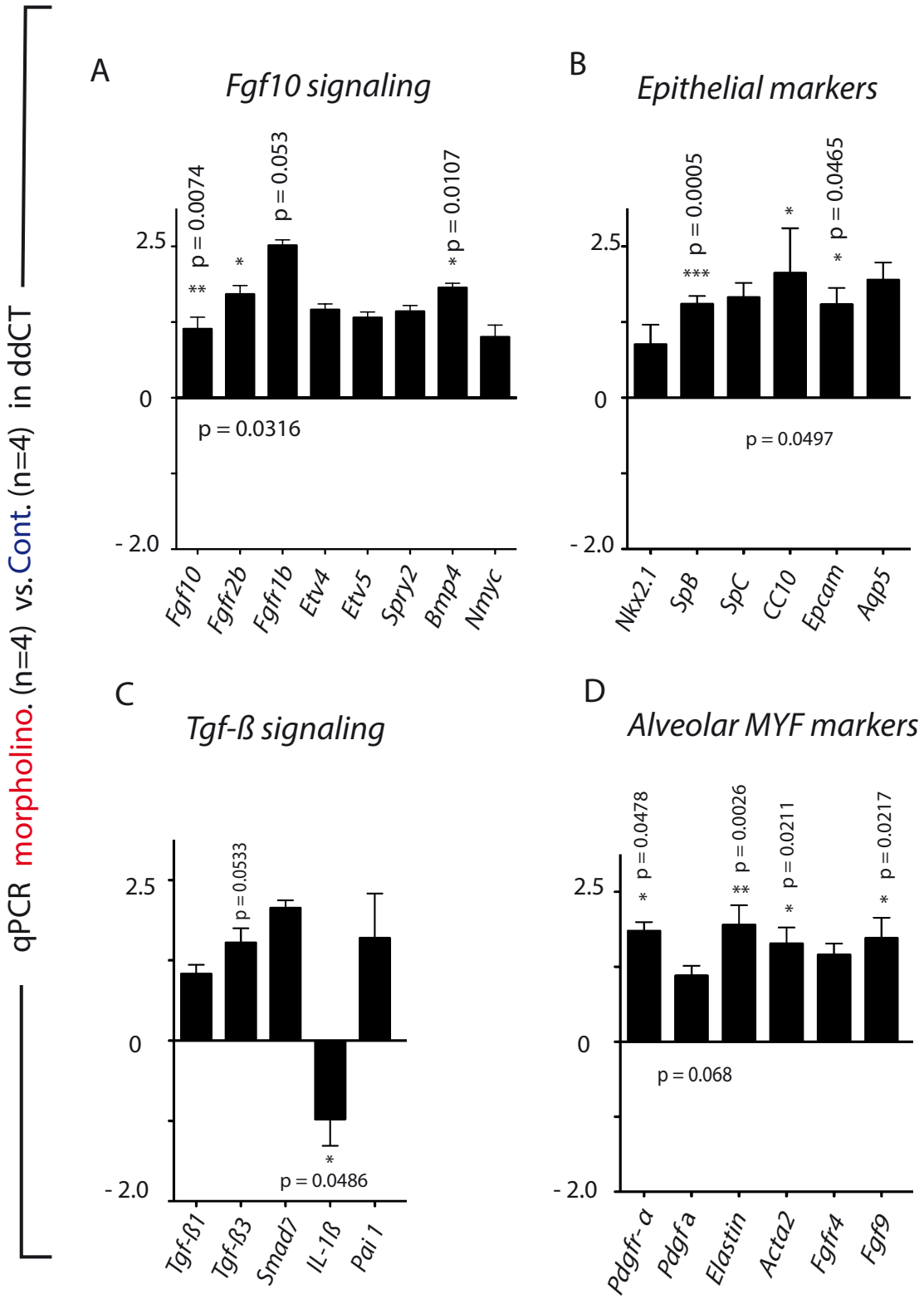
qPCR morpholino. (n=4) vs. Cont. (n=4) in ddCT
A
Fgf10 signaling
p = 0.0074
p = 0.053
p = 0.0107
p = 0.0316
Fgf10
Fgfr2b
Fgfr1b
Etv4
Etv5
Spry2
Bmp4
Nmyc
B
Epithelial markers
p = 0.0005
p = 0.0465
p = 0.0497
Nkx2.1
SpB
SpC
CC10
Epcam
Aqp5
C
Tgf-ß signaling
p = 0.0533
p = 0.0486
Tgf-ß1
Tgf-ß3
Smad7
IL-1ß
Pai 1
D
Alveolar MYF markers
p = 0.0478
p = 0.0026
p = 0.0211
p = 0.0217
p = 0.068
Pdgfr-α
Pdgfa
Elastin
Acta2
Fgfr4
Fgf9
2.5
0
- 2.0

Figure 12. Blockade of *miR-154* leads to up regulation of Fgf10 signaling, epithelial markers, Tgf-ß signaling and AMF markers after 72 hours of in vitro culture.

(A) Genetic analysis of Fgf10 signaling indicated a general up regulation of all investigated genes. *Fgf10* (p= 0.007), itself, *Fgfr2b* (p= 0.031) and antagonist *Bmp4* (p= 0.010) were significantly higher expressed. Not significant, but equally orientated were the expression levels of *Fgfr1b*, *Etv4*, *Etv5*, *Spry2* and *Nmyc*.

(B) All investigated epithelial markers showed elevated expression. *SpB* (p= 0.0005), *Cc10* (p= 0.049) and *Epcam* (p= 0.046) were significantly raised. *Nkx2.1*, *SpC*, and *Aqp5* were also higher expressed within the morpholino group.

(C) Apart from Il-1ß, which was significantly down regulated (p= 0.048), all other investigated genes, *Tgfß1*, *Tgfß3*, *Smad7* and *Pai-1*, involved with Tgf-ß signaling were overexpressed.

(D) The general trend of up regulation was also found with regard to the expression of alveolar myofibroblast markers. Unexceptional, all six genes were higher expressed in the morpholino treated lungs. *Pdgfr-α* (p= 0.047), *Elastin* (p= 0.002), *Acta2* (p= 0.021) and *Fgf9* (p= 0.021) were found significantly raised.

4.3 Summary of findings

The knowledge about miR-154's involvement in early lung development is still quite limited. Therefore, we developed two experimental approaches with the aim to answer the questions mentioned below:

1.) Does *miR-154* overexpression during embryonic lung development lead to changes in gene expression and morphology of the lung?

2.) Does in-vitro blockade of *miR-154* during embryonic lung development lead to changes in gene expression and morphology of the lung?

In both of our set ups we revealed severe alterations of lung phenotype. Due to the epithelial overexpression of *miR-154* from E7.5 to E18.5 the lungs presented thinned alveolar septa and extended sacculi. The alveolar morphometry revealed significant reduced septal thickness (in μm) and magnified percentage airspace in the Experimental group. The mean linear intercept was nearly significantly increased. Upon these observations, we scrutinized several groups of genes to detect changes explaining the phenotype. The most striking alterations were found amongst the alveolar myofibroblast markers. As an alteration of AMF presence and functionality could well be considered responsible for the appearance of the Experimental lungs, we decided to carry out an Acta2 staining. However, the count of relevant AMFs did not reveal significant differences between Experimental and Control lungs.
In order to answer the second question, we performed of a blocking of *miR-154*. In the course of a three-day culture the Experimental lungs grew significantly fewer lung buds. After we had proven the functionality of the applied morpholino solution, we took a closer look at gene expression. Notably, the expression of all genes belonging to the Fgf10 and Tgf-ß pathways were elevated. Moreover, the markers for epithelial cells and alveolar myofibroblasts were equally raised.
The answers to both of our questions suggest a vital role of *miR-154* during lung organogenesis. The alteration of *miR-154* presence was followed by changes in lung phenotype and gene expression levels in each of the two time periods.

5 Discussion

In this study, we were able to perceive *miR-154*'s impact during the process of early lung organogenesis in mice. This was approached following two concepts. On the one hand, we overexpressed *miR-154* during prenatal days E7.5 until E18.5 in the epithelium, on the other hand we reduced *miR-154* activity levels during the time period in between E11.5 + 72 hours in vitro.

The overexpression of *miR-154* led to strikingly altered lung morphology and gene expression levels. The experimental group presented lungs with significantly increased airspace, elevated mean linear intercept and thinned alveolar septa. On the genetic level, we found changes indicating *miR-154*'s influence on two pathways, which are known to be essential to lung organogenesis; the Fgf10 and Tgf-ß signaling pathways. Furthermore, the expression levels of epithelial and myofibroblast cell markers were affected, indicating a change in cell composition.

In our second approach - the blockade of *miR-154* in vitro - we also observed remarkably altered lung development. Here, too, genetic expression levels were modified. The Experimental group presented a general elevation of the genetic expression of Fgf10 and Tgf-ß signaling. The Epithelial- and myofibroblast cell markers were also higher expressed in these lungs compared to the Control group. Moreover, we could show increasing differences in the formation of lung buds throughout the lung culturing. Lungs lacking *miR-154* showed a significant reduction of lung bud outgrowth.

The interpretation and target-oriented development of our further strategy is quite a complex effort. As micro RNAs are regulatory molecules with the ability to regulate gene expression, the identification of potential targets is the main step towards a further understanding of the role of *miR-154*.

So far *miR-154* has been linked to several cancer entities. Although micro RNAs might play different roles in different organisms and biological processes, their molecular structure remains the same independent of their localization. Therefore, the targets identified in other studies should also be considered as potential targets of *miR-154* in

early lung development. The investigation of the current literature provided indications to some of these potential targets.

5.1 *MiR-154* might target Tgf-ß signaling and Smad7

So far *miR-154* has been subject to several studies on human carcinomas, but only little attention has been paid to its role during early lung development. However the studies on prostate-, colorectal-, hepatocellular -, skin squamous cell-, breast - and lung carcinoma, as well as glioblastoma have revealed different target genes and potential functions of *miR-154* (Zhu et al. 2013; Xin, Zhang, and Liu 2014; Pang et al. 2015; Chen and Gao 2018; Xu et al. 2016; Lin et al. 2016; Zhao et al. 2016).

Interestingly, several publications outline a relationship between *miR-154* and Tgf-ß signaling. Lin at al. determined ZEB2, Zinc finger E-box binding homeobox 2, as a direct target of *miR-154* in non-small cell lung cancer (NSCLC). The expression of ZEB2, which is known to be a regulator of epithelial-mesenchymal transition (EMT), was decreased on both messenger RNA and protein levels by overexpressing *miR-154*. Therefore the authors concluded that *miR-154* alters EMT by targeting ZEB2 (Lin et al. 2016). Strikingly, ZEB2 was initially characterized as a transcriptional regulator of the transforming growth factor (Tgf-ß) signaling pathway. It impedes Tgf-ß signaling, by interacting with Smad proteins (Verschueren et al. 1999; Postigo et al. 2003).

Previously to Lin et al. Gururajan et al. drew another connection between *miR-154* and the regulation of EMT and TGF-ß signaling. They investigated the role of *miR-154** and miR-379 in metastatic prostate cancer. Both members of the DLK1-DIO3 mega-cluster were found elevated in the serum of patients suffering from this disease. In the fate of the study both microRNAs could be identified as inducers of EMT in prostate cancer cells. Thus, an experimental knockdown of *miR-154** in cancer cells resulted in morphological, biochemical and functional EMT alterations. Strikingly, TGF-ß signaling was, among others, revealed as one of the target pathways, which were controlled by the investigated microRNAs. Also SMAD7, a known inhibitory regulator of the TGF-ß pathway, was identified as a target of *miR-154** (Gururajan et al. 2014).

Further reference for an interaction of *miR-154* and Tgf-ß signaling was indicated by a more recent investigation. Wang et al. described the mutual influence of Hdac3 (Histone deacetylase 3) and the miR-17-92 cluster on alveolar epithelial cell

remodeling. Due to a loss of Hdac3 in genetically modified mice, the authors observed an overexpression of several micro RNAs of the Dlk1-Dio3 cluster. Furthermore they identified the Tgf-ß pathway as one of the targets of both clusters (Wang, Frank, et al. 2016). Since miR-154 is a member of the investigated Dlk1-Dio3 cluster, these findings reinforce the assumption that *miR-154* targets Tgf-ß signaling.

5.2 *MiR-154* possibly alters lung organogenesis through targeting Tgf-ß signaling

With regard to branching morphogenesis and alveolarization the reciprocal communication between epithelium and mesenchyme via mediators, such as Tgf-ß, Wnt and fibroblast growth factors (Fgfs) has to be taken into account particularly (Morrisey and Hogan 2010).

The Tgf-ß signaling cascade itself is a recognized setscrew in both branching morphogenesis and late lung development. The right concentration at the right time is crucial and can easily lead to pathological developments if variations occur. As recognized in prior examinations, the down regulation of Tgf-ß signaling mediators Tgfßr2, Smad2, Smad3 or Smad4 led to enhanced branching morphogenesis in early lung development. Equal alterations were observed in cause of the overexpression of inhibitory *Smad7* (Zhao et al. 1996; Zhao et al. 1998; Zhao et al. 2000; Chen et al. 2008). Conversely, these findings suggest, that Tgf-ß signaling is inhibitory for early branching processes.

If we link this existing knowledge to the assumption, that miR-154 targets Tgf-ß signaling, a blockade of this specific microRNA should result in diminished lung branching. In our present study, we explanted mice lungs at E11.5, significantly reduced the presence of *miR-154*-3p through a specific morpholino treatment and cultured the specimens for 72 hours. In point of fact, the morpholino treated lungs presented significantly reduced lung bud outgrowth compared to the Control group. Our observations at the level of gene expression were concordant to this phenotype. Here, the *miR-154* blockade led to an overexpression of most *Tgf-ß* pathway genes.

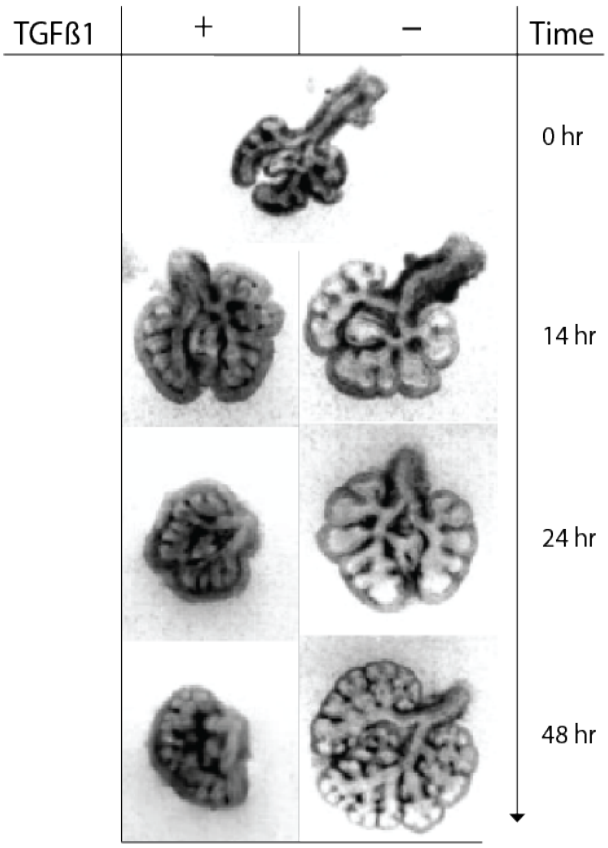

Figure 13. Branching morphogenesis of in vitro lung cultured lungs in the presence and absence of Tgf-ß1.

(+) Lungs were cultured in medium containing additional 100 ng Tgfβ1/ml.
(-) Samples were grown in medium without artificially added Tgf-ß.
Pictures of he growing lungs were taken at 0 hours, 14 hours 24 hours and 48 hours after the treatment.

In comparison with the controls, all lungs treated with Tgf-ß show diminished branching from hour 14 onwards (adapted from Serra, Pelton, and Moses 1994).

Moreover, our investigations go hand in hand with the studies of Serra, Pelton and Moses. The authors cultured E11.5 lungs in the presence and absence of Tgf-ß in different concentrations. Lungs cultured in a medium with and without artificial addition of 100 ng Tgf-β1/ml are shown in **Figure 13**. In comparison with the Control group, the lungs with artificially added Tgf-ß1 grew considerably less lung buds during the course of the examination (Serra, Pelton, and Moses 1994). The distinct similarity of phenotypes reinforces the assumption of a common underlying mechanism. Not only the arftificial addition of Tgf-ß, but also the blockade of *miR-154* seems to result in unphysiologically high levels of Tgf-ß and therefore diminished bud outgrowth.

At later stages of lung development Tgf-ß signaling plays a different role. Alejandre-Alcazar et al. found airway and alveolar epithelium formation, as well as the emergence of vascular and smooth muscle cells dependent on TGF-ß- signaling (Alejandre-Alcazar et al. 2008). In our gain of function approach *miR-154* was overexpressed in the epithelium from E7.5 to E18.5. Compared to the loss of function model, the genetically

and morphological analysis presented a similar situation. In both experimental approaches the expression of Tgf-ß signaling behaved equally dichotomous to the presence or absence of *miR-154*. Here, Tgf-ß1 and Tgf-ß3 expression were diminished in consequence of the epithelial overexpression of *miR-154*. Since the observed reduction of Tgf-ß signaling was relatively small, it could also be due to biological diversity and not the overexpressed *miR-154*. However, the thinned alveolar septa and increased airspaces can be considered as a precursor stage of impaired alveolarization. All the more so, since the emphysematous phenotype of our experimental group is comparable to results of other studies. Chen et al. analyzed lungs of mice with a deficiency for Smad3, an essential downstream mediator of Tgf-ß signaling. This reduction of Tgf-ß signaling led to similar emphysematous lung morphology with dysfunctional alveolarization (Chen et al. 2005). Therefore, an inhibitory function of miR-154 on Tgf-ß signaling seems to be plausible.

In conclusion, our experimental approaches showed equal effects on Tgf-ß signaling during lung organogenesis. In both experimental setups *miR-154* activity was found diametrically opposed to Tgf-ß expression and both approaches resulted in concomitant lung phenotypes. On the one hand, reduction of *miR-154* lead to increased expression of Tgf-ß signaling during early lung development and a congruent phenotype with impaired branching. On the other hand, the overexpression of *miR-154* in lung epithelium results in reduced Tgf-ß expression levels and a phenotype with thinned alveolar septa and increased airspace.

5.3 *MiR-154* might influence branching morphogenesis via alteration of Fgf10 and Bmp4 expression levels

As mentioned above, lung organogenesis is manly orchestrated by the crosstalk between mesenchyme and epithelium. One of the main facilitators is the fibroblast growth factor 10 signaling pathway. Fgf10 is an acknowledged key player in branching morphogenesis and has been intensively investigated over the past years. The outgrowth of lung buds during the organogenesis is crucially mediated by signaling between lung epithelium and its surrounding mesenchyme. Thereby mesenchymal expressed Fgf10

stimulates endoderm proliferation and bud formation by binding to epithelial expressed Fgfr2b (Bellusci, Grindley, et al. 1997). Moreover, Fgf10 was found able to guide the adjacent epithelium to bud outgrowth by chemo taxis (Park et al. 1998). Due to previous studies on Bmp4 and Fgf10 during lung organogenesis, Weaver, Dunn and Hogan established a model for the interplay of these two factors during branching morphogenesis. In short, this model suggests that mesenchymal expressed Fgf10 is responsible for proliferation and chemotaxis for the underlying epithelium and thus bud extension. In contrast Bmp4 inhibits lateral bud outgrowth and is therefore limiting the formation of further branching (Weaver, Dunn, and Hogan 2000).

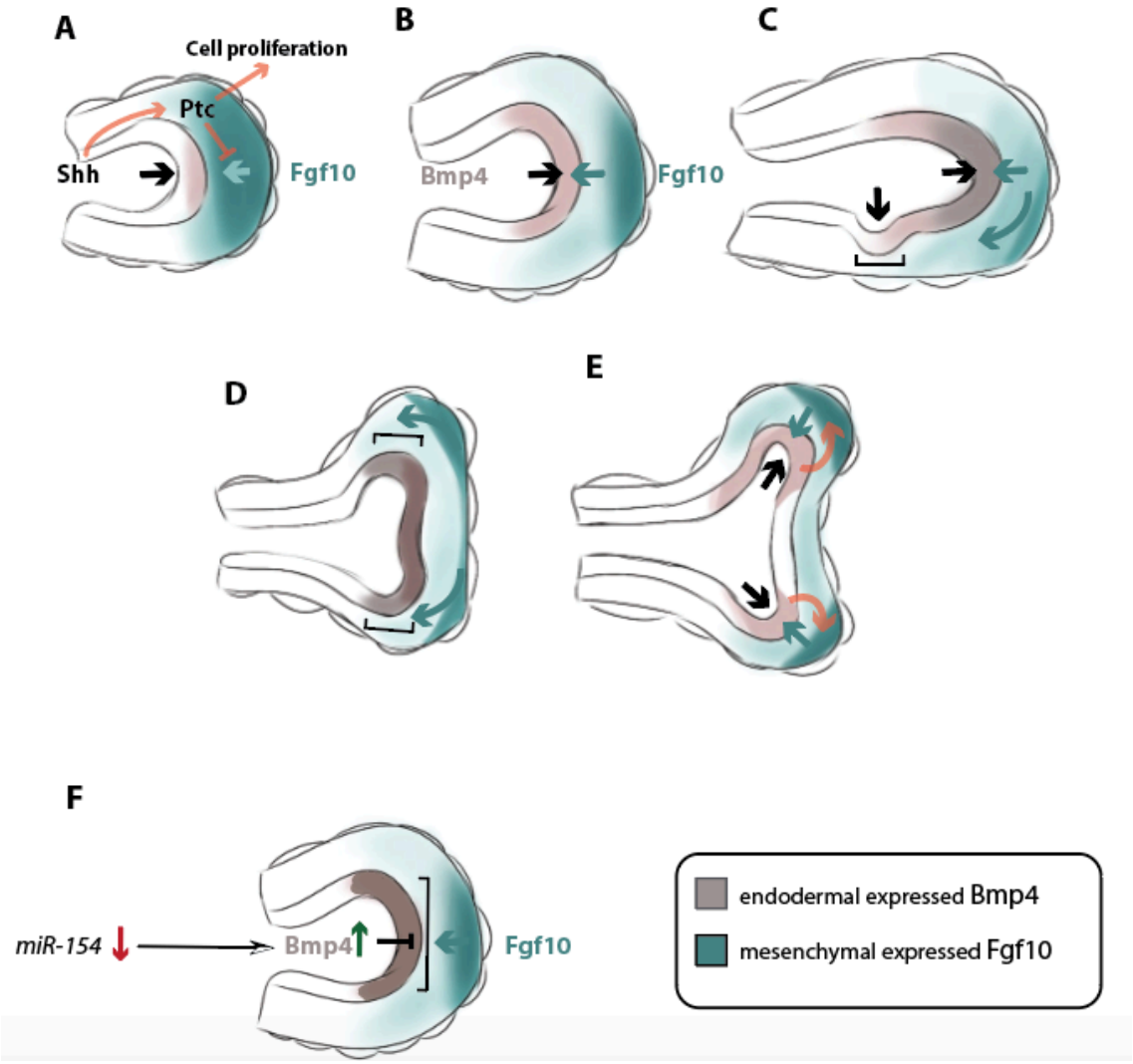

Figure 14. Model of growth factors orchestrating branching morphogenesis during early lung development

Pictured are the expression of Shh in the endoderm, Fgf10 in the mesenchyme (green) and Bmp4 (brown) in the distal endoderm. The black arrow represents the outgrowth and direction of movement of the endoderm. Fgf10 activity is depicted through the green arrow.
(A) In the early stages of bud outgrowth Bmp4 is only sparsely expressed in the distal endoderm, whereas Fgf10 is highly active in the opposing mesenchyme. The endodermally expressed Shh drives cell proliferation via Ptc1 (Patched1), but also attenuates Fgf10 expression (Bellusci, Furuta, et al. 1997). **(B)** Bmp4 expression intensifies in the further course of bud outgrowth. In contrast, Fgf10 expression is diminished and decentralized to more lateral areas of the mesenchyme. **(C)** The formation of a lateral bud (bracket) is induced by the lateralized Fgf10 expression and a lack of Bmp4 expression in the adjacent endoderm. **(D)** Further longitudinal outgrowth of the bud tip is impeded by the appreciably high expression of Bmp4 in the distal endoderm. **(E)** Further dichotomous branching is induced by the laterally enhanced expression of Fgf10 and will be limited by increasing activity of Bmp4 in the underlying endoderm (adapted from Weaver, Dunn, and Hogan 2000).
(**F**) Blockade of *miR-154* during in vitro lung culturing results in overexpression of *Bmp4*. Higher Bmp4 levels might therefore be accountable for reduced bud outgrowth and branching morphogenesis, as observed after 72 hours of culture.

The authors observed this reduction of branching through Bmp4 in cultured lungs during the exact same time period in which we performed the in vitro blockade of *miR-154*. Our treatment equally led to a constrained outgrowth of lung buds. Furthermore, we could disclose significantly elevated expression levels for *Bmp4* in the loss of function approach. Higher levels of Bmp4 seem to be a further conceivable reason for the limited budding in the experimental group. Interestingly, we also detected elevated expression levels for all other investigated genes linked to Fgf10 signaling. However, the localization of overexpressed *Fgf10* and *Bmp4* remains unknown, as the qPCR was performed on whole lungs. Current experiments on morpholino treated and in vitro

cultured lungs from E14.5 show lungs with elongated lung buds and a lack of branching. These, yet unpublished, data strengthen the assumption of *miR-154* being implicated in branching regulation via Fgf10 and Bmp4. An investigation of mesenchymal and epithelial expressed signaling molecules could potentially uncover more details about the impact of *miR-154* at different stages of lung development.

5.4 *MiR-154* might be involved in alveolarization through Pdgf-a expression and AMF functionality

The process of alveologenesis is closely related to Platelet-derived growth factor a (Pdgf-a), as could be shown by Bostrom et al. For their investigation, the authors created a mouse line with a complete lack of Pdgf-a. These mice developed increasing emphysematous lungs, with constantly narrowing septae, over the period from P4 to P19. By performing an α -Smooth muscle actin staining, the authors recognized a lack of alveolar myofibroblast, which was proven essential for the process of alveolar septation (Bostrom et al. 1996).

As the mouse line, we used is capable of the production of Pdgf-a, we did not expect any equally extreme phenotypes, as were found by Bostrom et al.. However, the overexpression of *miR-154* in the epithelium from E7.5 to E18.5 resulted in a phenotype, which likewise showed significantly reduced septal thickness and a significantly increased air space. Moreover, we revealed a significant reduction of *Pdgf-a* and *Pdgfr-*α expression levels and a reduction of *Acta2*, a marker for α-Smooth muscle cells. Although the thereupon-preformed α-SMA staining did not disclose any differences in alveolar myofibroblast presence, the functionality of the existing AMFs remains uncertain. Therefore a potential involvement of *miR-154* with Pgdf-a signaling and AMF quality should not be ignored, but subject to further exploration.

5.5 Limitations of Study

Although our investigation is based on a mature concept, there are obvious limits to the informative value and interpretability of our results. As limitations are a part of every scientific study, we will discuss some of ours in the following.

5.5.1 Limitations of loss of function approach

5.5.1.1 Potential toxic effect of morpholino solution

The significant difference in bud outgrowth we observed in our loss of function model has to be critically scrutinized. If the addition of a substrate to the culture medium leads to an impairment of organogenesis, its toxicity is always a possible reason. In spite of the elevated gene expression levels and the reduced levels of *miR-154*, a small uncertainty about the emergence of this phenotype remains.

5.5.2 Limitations of gain of function approach

5.5.2.1 Different extend of overexpression due to genotype

In our gain of function approach, we divided the animals into two groups. Depending on their ability to respond to the doxycycline food and therefore overexpress *miR-154,* the mice were either sorted into the Experimental or Control group. The genotypes examined were pivotal for this decision. All controls were equally unable to respond to the doxycycline and can therefore be considered as "identical". Animals within the Experimental group, in contrast, can be homozygous and heterozygous for the miR-154 transgene. The combination of alleles might however be determinant for the extent of *miR-154* expression. In 2013 Danopoulos et al. investigated the effects of Fgfr2b-ligand signaling on mouse limb development. The authors could show a dependency of gene dosage on the allelic constellation. Animals homozygous for the transgene presented a more pronounced phenotype, in this case diminished limb outgrowth, than the heterozygous animals (Danopoulos et al. 2013). Differences in gene expression within our Experimental group therefore seem imaginable.

5.5.2.2 Uncertain differentiation between effects of miR-154-3p and miR-154-5p

In both of our experimental setups, we observed interesting alterations of lung development on the presence of *miR-154*. Moreover, in both of our approaches we were able to show the sufficiency of our envisaged alterations of *miR-154* expression. Subsequently to the feeding of doxycycline *miR-154-3p* and *miR-154-5p* were significantly overexpressed. Likewise, *miR-154-3p* was significantly reduced during the lung culturing in our loss of function approach. Here we could also verify an almost significant reduction of *miR-154-5p*. However, these outcomes imply that our observations cannot be attributed to one or the other of the two *miR-154* molecules.

5.5.2.3 QPCR on whole lungs

In our gain of function approach, we successfully overexpressed miR-154 during the time period from E7.5 to E18.5. Due to the *Tg(CCSP-rtTA)* transgene this enhanced expression was restricted to the proximal and distal lung epithelium. For gene analysis, we performed a qPCR using the whole lungs collected at E18.5. In this way, we were able to analyze the effects of the epithelial overexpressed *miR-154* on the whole organ. However, no statement can be made about the distinct impacts of the overexpression on epithelium and mesenchyme.

5.5.3 Lack of investigations at the protein level

Our investigations allowed new insights to the role of *miR-154* in means of phenotype and gene expression. However, *miR-154's* impact on a protein level remain uncertain. To fully understand *miR-154*'s regulatory functions, an investigation of protein expression would be helpful. This is particularly advisable, as most micro RNAs are known to regulate gene expression in three different ways: mRNA target cleavage, mRNA deadenylation and translational repression. The identification of suppressed or enhanced expression of proteins could deliver further clarifications towards the interaction of *miR-154* with protein biosynthesis and the resulting phenotype.

5.5.4 Limited transferability from mouse to human

Besides the fundamental understanding of molecular biological processes, the higher goal of animal experiments is usually the transfer of this knowledge to humans. Animal experiments are therefore an integral part of research today, precisely because in many cases it is difficult to carry out comparable experiments on humans or with human tissue. In many cases this transfer of knowledge form animal to human has been successful and we benefit from it today. The establishment of blood transfections, but also the development of therapeutic approaches for Parkinson's disease and pacemakers are some of the most popular examples. Unfortunately, however, the transferability is often limited. More recently this has become an issue in lung research too. In early 2019 Danopoulos et al. published a paper dealing with the varying impacts of Fgf ligands on lung organogenesis between human and mouse. The authors investigated the expression of FGF7, FGF9 and FGF10 and the corresponding receptors in human lung tissue during fetal development. Moreover, they examined the effect of these ligands on the branching morphogenesis of in vitro cultured human lung tissue. All of these ligands have earlier been recognized as having a major effect on organ maturation. The human to mouse comparison revealed comparable results for FGF7 and FGF9. However, there were striking variations in the impact of FGF10 on mouse and human tissue. In mice, Fgf10 induces epithelial branching. Contrary to this, the authors determined expansion and formation of cysts in human lung explants as a result of FGF10 application (Danopoulos et al. 2019). The elaboration of these clear differences is an excellent example of the partially limited transferability of findings from animal experiments to humans, which may also apply for our own results.

5.6 Future perspectives

At this stage of research on *miR-154*, the knowledge about the exact mechanisms during lung development is still very limited. Thus, it is not entirely clear how *miR-154* might be regulated, or how the interactions with tightly regulated signaling pathways, such as Tgf-ß or Fgf10, take place.

It will be thrilling to further investigate *miR-154*'s role in early lung development and thereby identify further direct targets of this specific microRNA. A couple of future perspectives will be given in the following.

5.6.1 Further experimental approaches

In this study, we were able to highlight some of *miR-154*'s effects at two different time points of lung development. Taking in account, that the organogenesis of the lung as a dynamic process, during which *miR-154* is equally dynamically expressed (Williams et al. 2007), it would be instructive to repeat our experimental set up at different time stages. In this way, it will be possible to draw a continuous picture of the morphological and genetic alterations caused by overexpression or blocking of *miR-154*.

With regard to branching morphogenesis a further examination of both the Fgf10 and Bmp4 crosstalk, as well as Tgf-ß signaling appears to be crucial. Quantifying and locating Fgf10- and Bmp4- activity in the mesenchyme and epithelium could give further insight in the regulatory mechanisms of *miR-154* during branching morphogenesis. A qPCR on FACS sorted cells would be a knowledge-bringing method to begin with. In order to further evaluate *miR-154s* role in Tgf-ß signaling a phosphosmad staining for Smad signaling molecules would be useful.

To understand the formation of the phenotype we observed in the gain of function model, another look at the alveolar myofibroblasts could be informative. Although there were no significant differences in AMF presence, the high diversity in genetic expression of AMF markers might indicate yet undiscovered correlations. Therefore, it will be thrilling to further investigate the functionality of these cells, as they are known to have a high impact on alveolar septation.

As micro RNAs are recognized regulatory molecules of post-transcriptional gene expression (Chekulaeva and Filipowicz 2009), it would be highly interesting to examine the implications of *miR-154* on a protein level through western blotting. This could not only fortify the genetically observed changes, but also give further insight to the involvement with the mentioned signaling pathways or even give a hint to other direct targets of *miR-154*.

5.6.2 Identifying further miR-154 targets in early lung development

The potential range of *miR-154* targets seems to be wide. Therefore, a detection of Smad7 and Zeb2 proteins during lung development could be a starting point. This investigation might strengthen the hypothesis of *miR-154* equally targeting these inhibitory molecules during organogenesis, as was previously observed in cancer research (Gururajan et al. 2014; Lin et al. 2016).

A more recent study on *miR-154* identified it as tumor suppressive in glioblastoma. Zhao et al. did not only determine an inhibition of EMT by overexpressing *miR-154*, but also revealed the 3' untranslated region, 3'UTR, of Wnt5a as direct target of *miR-154* (Zhao et al. 2017). The Wnt/ß-catenin pathway is known to be involved in lung organogenesis at several stages (Cohen et al. 2008; Caprioli et al. 2015). Therefore, another regulatory function of *miR-154* during lung development through targeting Wnt-signaling is conceivable.

Recently our working group has also uncovered further, yet unpublished, details regarding the targets of *miR-154*. In a gain of function approach, we increased the proportion of *miR-154* in the cytoplasm of mouse epithelial lung cells (MLE12-cells) via transfection. These biotinylated microRNAs bound potential mRNA targets by base paring in the cytoplasm. Streptavidin magnetic beads then bound the "miR-target" complexes, which enabled the purification, washing and analysis of bound RNA molecules. The gene array identified 338 potential targets. In a second gain of function experiment, the overexpression of *miR-154* in transgenic mice, we could observe several down-regulated genes. The intersection of these two approaches narrowed the number of potential targets down to 37. These 37 refined targets comprised yet unexplored genes, but also well-known ones. Especially Caveolin-1 (Cav1) aroused our attention. It has previously been characterized as regulatory in Tgf-ß signaling against the background of idiopathic pulmonary fibrosis. The examinations of Cardenas et al. uncovered the role of miR-199-5a in bleomycin induced IPF. The authors revealed a Tgf-ß mediated activation of lung fibroblasts due to miR-199-5a targeting Cav1 (Lino Cardenas et al. 2013). This link between Cav1 and Tgf-ß signaling makes a further examination of this potential target of *miR-154* highly sensible, particularly as *miR-154* was awarded a profibroctic role in IPF (Milosevic et al. 2012).

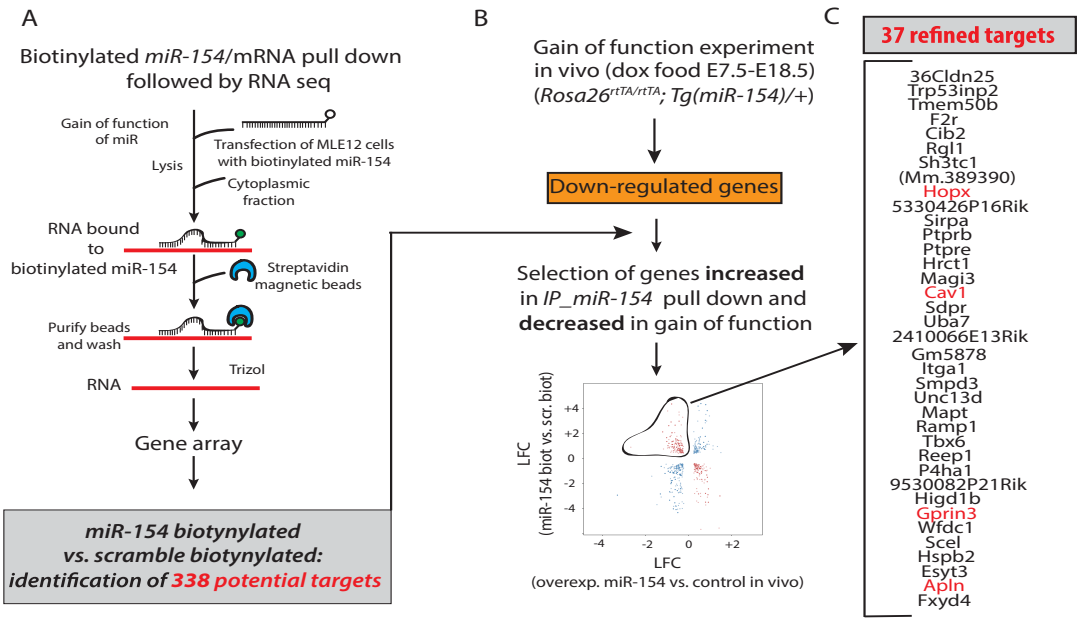

Figure 15. Genetic pull down of *miR-154* target genes.

(A) MLE-12 cells were transfected with biotinylated *miR-154*. These cytoplasmatic localized miRs base pair with target mRNAs and are marked with Streptavidin magnetic beads. These were purified, washed and analyzed via gene array. In total 338 potential targets were identified. **(B)** Overexpressed miR154 in transgenic mice led to down regulation of certain genes. The genes identified through the pulldown and those down regulated after overexpression revealed 37 intersecting potential target genes. **(C)** List of refined targets (Data generated by Gianni Carraro).

5.6.3 Regulation of miR-154

In our experimental set up *miR-154* was either unphysiologically strongly overexpressed or blocked completely, as in most approaches investigating the effects of microRNAs. Until now a lot of attention has been paid to the potential and actual targets of these regulatory RNA strands. In order to transfer the knowledge gained in the artificial context of studies to a physiological level, it will be equally necessary to understand how the specific microRNAs are regulated themselves. This way an induction or suppression of microRNAs in "naturally" living organisms could be achieved and maybe even be taken to clinical application.

6 Summary (English)

Since the discovery of the first regulatory RNA strands in 1993, the number of known *micro RNAs* has steadily increased. However, the function of the individual molecules is often unknown. The aim of our study was to investigate the role of *microRNA 154* in embryonic lung development. Our strategy included two opposing experimental approaches: A "gain of function" and a "loss of function" experiment. In both approaches, we analyzed the lung morphology and the changes at the genetic level.

For the gain of function approach, we designed a mouse line that overexpressed *miR-154* in the pulmonary epithelium upon doxycycline food application. We induced this process from embryonic day 7.5 until organ harvest (at E18.5). Using quantitative PCR we were able to prove the successful overexpression. As a consequence of epithelial *miR-154* overexpression a phenotype with thinned alveolar septa and elongated sacculi was observed microscopically. In alveolar morphometry we found a significant reduction of septal thickness (in μm) and a significant increase of airspace. The parameter for volume-to-surface ratio (MLI) was also increased. Searching for the genetic correlate for this phenotype, we focused on four gene groups related to lung development: The signal cascades of the cytokines Fgf10 and Tgf-ß, as well as the marker genes for epithelial cells and alveolar myofibroblasts (AMF). AMFs are important mediators of alveolar separation. In our analysis, their marker genes showed a significant down regulation. However, the subsequent Acta2 staining did not reveal any difference in AMF presence.

For the loss of function approach, we blocked *miR-154* with a morpholino solution. We explanted embryonic lungs at E11.5 and cultivated the organs in vitro for 72 hours. Morphologically, the lungs of the experimental group showed a significantly reduced formation of lung buds. Gene analysis of Fgf10 and Tgf-ß signaling, but also the gene markers of epithelial cells and AMFs showed a trend towards overexpression.

7 Zusammenfassung (Deutsch)

Seit der Entdeckung der ersten regulatorischen RNA-Stränge im Jahr 1993 nimmt die Anzahl bekannter Micro-RNAs stetig zu. Die Funktion der einzelnen Moleküle ist jedoch häufig unbekannt. Ziel unserer Studie war es die Rolle der *microRNA 154* in der frühen embryonalen Lungenentwicklung herauszuarbeiten. Unsere Strategie dabei umfasste zwei gegensätzliche experimentelle Herangehensweisen: Ein „Gain -" und ein „Loss of function" Experiment. In beiden Ansätzen analysierten wir die Morphologie der Lungen und die Veränderungen auf genetischer Ebene.

Für den „Gain of function" Ansatz designten wir eine Mauslinie, die *miR-154* bei Applikation von Doxycyclin-Nahrung im Lungenepithel überexpremierte. Wir induzierten diesen Prozess von Embryonaltag 7.5 bis zur Organentnahme (E18.5). Mittels quantitativer PCR konnten wir die erfolgreiche Überexpression beweisen. Als Folge der epithelialen *miR-154* Überexpression zeigte sich mikroskopisch ein Phänotyp mit verdünnten Alveolarsepten und elongierten Sacculi. Passend dazu fanden wir in der Alveolarmorphometrie signifikant verschmälerte alveoläre Septen (in µm) und einen signifikant erhöhten Anteil an Luft im Gewebe. Auch der Parameter für das Volumen-Oberflächen-Verhältnis (MLI) war erhöht. Auf der Suche nach dem genetischen Korrelat für den vorliegenden Phänotypen fokussierten wir vier Gengruppen, die im Zusammenhang mit der Lungenentwicklung stehen: Die Signalkaskaden der Zytokine Fgf10 und Tgf-ß, sowie die Markergene für Epithelzellen und Alveolarmyofibroblasten (AMF). AMFs sind als wichtige Mediatoren der Alveolarseparation bekannt. Die Expression dieser Genmarker war in unserer Analyse signifikant reduziert. Die anschließenden Acta2 Färbungen unterschieden sich jedoch nicht hinsichtlich der Anwesenheit der AMFs.

Für den „Loss of function" Ansatz blockierten wir die *miR-154* mit einer Morpholino-Lösung. Dazu explantierten wir embryonale Lungen an E11.5 und kultivierten die Organe für 72 Stunden in-vitro. Morphologisch zeigten die Lungen der Experimentalgruppe eine signifikant verminderte Ausbildung von Lungenknospen. Die Genanalyse des Fgf10 und Tgf-ß Signaling, aber auch die Genmarker der Epithelzellen und AMFs zeigte einen Trend zur Überexpression.

8 *References*

Uncategorized References

Abdollahi, A., M. Li, G. Ping, C. Plathow, S. Domhan, F. Kiessling, L. B. Lee, G. McMahon, H. J. Grone, K. E. Lipson, and P. E. Huber. 2005. 'Inhibition of platelet-derived growth factor signaling attenuates pulmonary fibrosis', *J Exp Med*, 201: 925-35.

Afrakhte, M., A. Moren, S. Jossan, S. Itoh, K. Sampath, B. Westermark, C. H. Heldin, N. E. Heldin, and P. ten Dijke. 1998. 'Induction of inhibitory Smad6 and Smad7 mRNA by TGF-beta family members', *Biochem Biophys Res Commun*, 249: 505-11.

Alejandre-Alcazar, M. A., M. Michiels-Corsten, A. G. Vicencio, I. Reiss, J. Ryu, R. R. de Krijger, G. G. Haddad, D. Tibboel, W. Seeger, O. Eickelberg, and R. E. Morty. 2008. 'TGF-beta signaling is dynamically regulated during the alveolarization of rodent and human lungs', *Dev Dyn*, 237: 259-69.

Ambros, V. 2001. 'microRNAs: tiny regulators with great potential', *Cell*, 107: 823-6.

Bagby, S. C., N. H. Bergman, D. M. Shechner, C. Yen, and D. P. Bartel. 2009. 'A class I ligase ribozyme with reduced Mg2+ dependence: Selection, sequence analysis, and identification of functional tertiary interactions', *RNA*, 15: 2129-46.

Bascom, C. C., J. R. Wolfshohl, R. J. Coffey, Jr., L. Madisen, N. R. Webb, A. R. Purchio, R. Derynck, and H. L. Moses. 1989. 'Complex regulation of transforming growth factor beta 1, beta 2, and beta 3 mRNA expression in mouse fibroblasts and keratinocytes by transforming growth factors beta 1 and beta 2', *Mol Cell Biol*, 9: 5508-15.

Beenken, A., and M. Mohammadi. 2009. 'The FGF family: biology, pathophysiology and therapy', *Nat Rev Drug Discov*, 8: 235-53.

Bellusci, S., Y. Furuta, M. G. Rush, R. Henderson, G. Winnier, and B. L. Hogan. 1997. 'Involvement of Sonic hedgehog (Shh) in mouse embryonic lung growth and morphogenesis', *Development*, 124: 53-63.

Bellusci, S., J. Grindley, H. Emoto, N. Itoh, and B. L. Hogan. 1997. 'Fibroblast growth factor 10 (FGF10) and branching morphogenesis in the embryonic mouse lung', *Development*, 124: 4867-78.

Bellusci, S., R. Henderson, G. Winnier, T. Oikawa, and B. L. Hogan. 1996. 'Evidence from normal expression and targeted misexpression that bone morphogenetic protein (Bmp-4) plays a role in mouse embryonic lung morphogenesis', *Development*, 122: 1693-702.

Benlhabib, H., W. Guo, B. M. Pierce, and C. R. Mendelson. 2015. 'The miR-200 family and its targets regulate type II cell differentiation in human fetal lung', *J Biol Chem*, 290: 22409-22.

Bentwich, I., A. Avniel, Y. Karov, R. Aharonov, S. Gilad, O. Barad, A. Barzilai, P. Einat, U. Einav, E. Meiri, E. Sharon, Y. Spector, and Z. Bentwich. 2005. 'Identification of hundreds of conserved and nonconserved human microRNAs', *Nat Genet*, 37: 766-70.

Bernstein, E., S. Y. Kim, M. A. Carmell, E. P. Murchison, H. Alcorn, M. Z. Li, A. A. Mills, S. J. Elledge, K. V. Anderson, and G. J. Hannon. 2003. 'Dicer is essential for mouse development', *Nat Genet*, 35: 215-7.

Bhaskaran, M., Y. Wang, H. Zhang, T. Weng, P. Baviskar, Y. Guo, D. Gou, and L. Liu. 2009. 'MicroRNA-127 modulates fetal lung development', *Physiol Genomics*, 37: 268-78.

Bohnsack, M. T., K. Czaplinski, and D. Gorlich. 2004. 'Exportin 5 is a RanGTP-dependent dsRNA-binding protein that mediates nuclear export of pre-miRNAs', *RNA*, 10: 185-91.

Bostrom, H., A. Gritli-Linde, and C. Betsholtz. 2002. 'PDGF-A/PDGF alpha-receptor signaling is required for lung growth and the formation of alveoli but not for early lung branching morphogenesis', *Dev Dyn*, 223: 155-62.

Bostrom, H., K. Willetts, M. Pekny, P. Leveen, P. Lindahl, H. Hedstrand, M. Pekna, M. Hellstrom, S. Gebre-Medhin, M. Schalling, M. Nilsson, S. Kurland, J. Tornell, J. K. Heath, and C.

Betsholtz. 1996. 'PDGF-A signaling is a critical event in lung alveolar myofibroblast development and alveogenesis', *Cell*, 85: 863-73.
Bragg, A. D., H. L. Moses, and R. Serra. 2001. 'Signaling to the epithelium is not sufficient to mediate all of the effects of transforming growth factor beta and bone morphogenetic protein 4 on murine embryonic lung development', *Mech Dev*, 109: 13-26.
Brown, E., and K. James. 2009. 'The lung primordium an outpouching from the foregut! Evidence-based dogma or myth?', *J Pediatr Surg*, 44: 607-15.
Cabrita, M. A., and G. Christofori. 2008. 'Sprouty proteins, masterminds of receptor tyrosine kinase signaling', *Angiogenesis*, 11: 53-62.
Caprioli, A., A. Villasenor, L. A. Wylie, C. Braitsch, L. Marty-Santos, D. Barry, C. M. Karner, S. Fu, S. M. Meadows, T. J. Carroll, and O. Cleaver. 2015. 'Wnt4 is essential to normal mammalian lung development', *Dev Biol*, 406: 222-34.
Carraro, G., A. El-Hashash, D. Guidolin, C. Tiozzo, G. Turcatel, B. M. Young, S. P. De Langhe, S. Bellusci, W. Shi, P. P. Parnigotto, and D. Warburton. 2009. 'miR-17 family of microRNAs controls FGF10-mediated embryonic lung epithelial branching morphogenesis through MAPK14 and STAT3 regulation of E-Cadherin distribution', *Dev Biol*, 333: 238-50.
Carraro, G., A. Shrestha, J. Rostkovius, A. Contreras, C. M. Chao, E. El Agha, B. Mackenzie, S. Dilai, D. Guidolin, M. M. Taketo, A. Gunther, M. E. Kumar, W. Seeger, S. De Langhe, G. Barreto, and S. Bellusci. 2014. 'miR-142-3p balances proliferation and differentiation of mesenchymal cells during lung development', *Development*, 141: 1272-81.
Carthew, R. W., and E. J. Sontheimer. 2009. 'Origins and Mechanisms of miRNAs and siRNAs', *Cell*, 136: 642-55.
Cazzoli, R., F. Buttitta, M. Di Nicola, S. Malatesta, A. Marchetti, W. N. Rom, and H. I. Pass. 2013. 'microRNAs derived from circulating exosomes as noninvasive biomarkers for screening and diagnosing lung cancer', *J Thorac Oncol*, 8: 1156-62.
Chao, C. M., F. Yahya, A. Moiseenko, C. Tiozzo, A. Shrestha, N. Ahmadvand, E. El Agha, J. Quantius, S. Dilai, V. Kheirollahi, M. Jones, J. Wilhem, G. Carraro, H. Ehrhardt, K. P. Zimmer, G. Barreto, K. Ahlbrecht, R. E. Morty, S. Herold, R. G. Abellar, W. Seeger, R. Schermuly, J. S. Zhang, P. Minoo, and S. Bellusci. 2017. 'Fgf10 deficiency is causative for lethality in a mouse model of bronchopulmonary dysplasia', *J Pathol*, 241: 91-103.
Chekulaeva, M., and W. Filipowicz. 2009. 'Mechanisms of miRNA-mediated post-transcriptional regulation in animal cells', *Curr Opin Cell Biol*, 21: 452-60.
Chen, C. Y., D. Zheng, Z. Xia, and A. B. Shyu. 2009. 'Ago-TNRC6 triggers microRNA-mediated decay by promoting two deadenylation steps', *Nat Struct Mol Biol*, 16: 1160-6.
Chen, H. Q., and D. Gao. 2018. 'Inhibitory effect of microRNA-154 targeting WHSC1 on cell proliferation of human skin squamous cell carcinoma through mediating the P53 signaling pathway', *Int J Biochem Cell Biol*.
Chen, H., J. Sun, S. Buckley, C. Chen, D. Warburton, X. F. Wang, and W. Shi. 2005. 'Abnormal mouse lung alveolarization caused by Smad3 deficiency is a developmental antecedent of centrilobular emphysema', *Am J Physiol Lung Cell Mol Physiol*, 288: L683-91.
Chen, H., F. Zhuang, Y. H. Liu, B. Xu, P. Del Moral, W. Deng, Y. Chai, M. Kolb, J. Gauldie, D. Warburton, H. L. Moses, and W. Shi. 2008. 'TGF-beta receptor II in epithelia versus mesenchyme plays distinct roles in the developing lung', *Eur Respir J*, 32: 285-95.
Chen, Y. G., A. Hata, R. S. Lo, D. Wotton, Y. Shi, N. Pavletich, and J. Massague. 1998. 'Determinants of specificity in TGF-beta signal transduction', *Genes Dev*, 12: 2144-52.
Chendrimada, T. P., R. I. Gregory, E. Kumaraswamy, J. Norman, N. Cooch, K. Nishikura, and R. Shiekhattar. 2005. 'TRBP recruits the Dicer complex to Ago2 for microRNA processing and gene silencing', *Nature*, 436: 740-4.
Claesson-Welsh, L., L. Ronnstrand, and C. H. Heldin. 1987. 'Biosynthesis and intracellular transport of the receptor for platelet-derived growth factor', *Proc Natl Acad Sci U S A*, 84: 8796-800.
Cohen, J. C., J. E. Larson, E. Killeen, D. Love, and K. Takemaru. 2008. 'CFTR and Wnt/beta-catenin signaling in lung development', *BMC Dev Biol*, 8: 70.
Colvin, J. S., B. Feldman, J. H. Nadeau, M. Goldfarb, and D. M. Ornitz. 1999. 'Genomic organization and embryonic expression of the mouse fibroblast growth factor 9 gene', *Dev Dyn*, 216: 72-88.

Colvin, J. S., A. C. White, S. J. Pratt, and D. M. Ornitz. 2001. 'Lung hypoplasia and neonatal death in Fgf9-null mice identify this gene as an essential regulator of lung mesenchyme', *Development*, 128: 2095-106.

Corcoran, D. L., K. V. Pandit, B. Gordon, A. Bhattacharjee, N. Kaminski, and P. V. Benos. 2009. 'Features of mammalian microRNA promoters emerge from polymerase II chromatin immunoprecipitation data', *PLoS One*, 4: e5279.

Cullen, B. R. 2011. 'Viruses and microRNAs: RISCy interactions with serious consequences', *Genes Dev*, 25: 1881-94.

Czech, B., and G. J. Hannon. 2011. 'Small RNA sorting: matchmaking for Argonautes', *Nat Rev Genet*, 12: 19-31.

Danopoulos, S., S. Parsa, D. Al Alam, R. Tabatabai, S. Baptista, C. Tiozzo, G. Carraro, M. Wheeler, G. Barreto, T. Braun, X. Li, M. K. Hajihosseini, and S. Bellusci. 2013. 'Transient Inhibition of FGFR2b-ligands signaling leads to irreversible loss of cellular beta-catenin organization and signaling in AER during mouse limb development', *PLoS One*, 8: e76248.

Danopoulos, S., M. E. Thornton, B. H. Grubbs, M. R. Frey, D. Warburton, S. Bellusci, and D. Al Alam. 2019. 'Discordant roles for FGF ligands in lung branching morphogenesis between human and mouse', *J Pathol*, 247: 254-65.

Das, A. T., L. Tenenbaum, and B. Berkhout. 2016. 'Tet-On Systems For Doxycycline-inducible Gene Expression', *Curr Gene Ther*, 16: 156-67.

Davis, B. N., A. C. Hilyard, G. Lagna, and A. Hata. 2008. 'SMAD proteins control DROSHA-mediated microRNA maturation', *Nature*, 454: 56-61.

De Moerlooze, L., B. Spencer-Dene, J. M. Revest, M. Hajihosseini, I. Rosewell, and C. Dickson. 2000. 'An important role for the IIIb isoform of fibroblast growth factor receptor 2 (FGFR2) in mesenchymal-epithelial signalling during mouse organogenesis', *Development*, 127: 483-92.

Diederichs, S., and D. A. Haber. 2007. 'Dual role for argonautes in microRNA processing and posttranscriptional regulation of microRNA expression', *Cell*, 131: 1097-108.

Farh, K. K., A. Grimson, C. Jan, B. P. Lewis, W. K. Johnston, L. P. Lim, C. B. Burge, and D. P. Bartel. 2005. 'The widespread impact of mammalian MicroRNAs on mRNA repression and evolution', *Science*, 310: 1817-21.

Forman, J. J., A. Legesse-Miller, and H. A. Coller. 2008. 'A search for conserved sequences in coding regions reveals that the let-7 microRNA targets Dicer within its coding sequence', *Proc Natl Acad Sci U S A*, 105: 14879-84.

Formosa, A., E. K. Markert, A. M. Lena, D. Italiano, E. Finazzi-Agro, A. J. Levine, S. Bernardini, A. V. Garabadgiu, G. Melino, and E. Candi. 2014. 'MicroRNAs, miR-154, miR-299-5p, miR-376a, miR-376c, miR-377, miR-381, miR-487b, miR-485-3p, miR-495 and miR-654-3p, mapped to the 14q32.31 locus, regulate proliferation, apoptosis, migration and invasion in metastatic prostate cancer cells', *Oncogene*, 33: 5173-82.

Gauldie, J., T. Galt, P. Bonniaud, C. Robbins, M. Kelly, and D. Warburton. 2003. 'Transfer of the active form of transforming growth factor-beta 1 gene to newborn rat lung induces changes consistent with bronchopulmonary dysplasia', *Am J Pathol*, 163: 2575-84.

Goetz, R., A. Beenken, O. A. Ibrahimi, J. Kalinina, S. K. Olsen, A. V. Eliseenkova, C. Xu, T. A. Neubert, F. Zhang, R. J. Linhardt, X. Yu, K. E. White, T. Inagaki, S. A. Kliewer, M. Yamamoto, H. Kurosu, Y. Ogawa, M. Kuro-o, B. Lanske, M. S. Razzaque, and M. Mohammadi. 2007. 'Molecular insights into the klotho-dependent, endocrine mode of action of fibroblast growth factor 19 subfamily members', *Mol Cell Biol*, 27: 3417-28.

Gregory, R. I., K. P. Yan, G. Amuthan, T. Chendrimada, B. Doratotaj, N. Cooch, and R. Shiekhattar. 2004. 'The Microprocessor complex mediates the genesis of microRNAs', *Nature*, 432: 235-40.

Griffiths-Jones, S., R. J. Grocock, S. van Dongen, A. Bateman, and A. J. Enright. 2006. 'miRBase: microRNA sequences, targets and gene nomenclature', *Nucleic Acids Res*, 34: D140-4.

Gururajan, M., S. Josson, G. C. Chu, C. L. Lu, Y. T. Lu, C. L. Haga, H. E. Zhau, C. Liu, J. Lichterman, P. Duan, E. M. Posadas, and L. W. Chung. 2014. 'miR-154* and miR-379 in the DLK1-DIO3 microRNA mega-cluster regulate epithelial to mesenchymal transition and bone metastasis of prostate cancer', *Clin Cancer Res*, 20: 6559-69.

Ha, T. Y. 2011. 'MicroRNAs in Human Diseases: From Lung, Liver and Kidney Diseases to Infectious Disease, Sickle Cell Disease and Endometrium Disease', *Immune Netw*, 11: 309-23.

Haigl, B., V. Vanas, U. Setinek, B. Hegedus, A. Gsur, and H. Sutterluty-Fall. 2014. 'Expression of microRNA-21 in non-small cell lung cancer tissue increases with disease progression and is likely caused by growth conditional changes during malignant transformation', *Int J Oncol*, 44: 1325-34.

Han, J., Y. Lee, K. H. Yeom, Y. K. Kim, H. Jin, and V. N. Kim. 2004. 'The Drosha-DGCR8 complex in primary microRNA processing', *Genes Dev*, 18: 3016-27.

Han, J., Y. Lee, K. H. Yeom, J. W. Nam, I. Heo, J. K. Rhee, S. Y. Sohn, Y. Cho, B. T. Zhang, and V. N. Kim. 2006. 'Molecular basis for the recognition of primary microRNAs by the Drosha-DGCR8 complex', *Cell*, 125: 887-901.

Harris, K. S., Z. Zhang, M. T. McManus, B. D. Harfe, and X. Sun. 2006. 'Dicer function is essential for lung epithelium morphogenesis', *Proc Natl Acad Sci U S A*, 103: 2208-13.

He, L., X. He, L. P. Lim, E. de Stanchina, Z. Xuan, Y. Liang, W. Xue, L. Zender, J. Magnus, D. Ridzon, A. L. Jackson, P. S. Linsley, C. Chen, S. W. Lowe, M. A. Cleary, and G. J. Hannon. 2007. 'A microRNA component of the p53 tumour suppressor network', *Nature*, 447: 1130-4.

Heldin, C. H. 1997. 'Simultaneous induction of stimulatory and inhibitory signals by PDGF', *FEBS Lett*, 410: 17-21.

Heldin, C. H., K. Miyazono, and P. ten Dijke. 1997. 'TGF-beta signalling from cell membrane to nucleus through SMAD proteins', *Nature*, 390: 465-71.

Hoffman, A. M., and E. P. Ingenito. 2012. 'Alveolar epithelial stem and progenitor cells: emerging evidence for their role in lung regeneration', *Curr Med Chem*, 19: 6003-8.

Hogan, B. L. 1996. 'Bone morphogenetic proteins in development', *Curr Opin Genet Dev*, 6: 432-8.

Huang, J., J. Wu, Y. Li, X. Li, T. Yang, Q. Yang, and Y. Jiang. 2014. 'Deregulation of serum microRNA expression is associated with cigarette smoking and lung cancer', *Biomed Res Int*, 2014: 364316.

Huang, P. J., W. C. Lin, S. C. Chen, Y. H. Lin, C. H. Sun, P. C. Lyu, and P. Tang. 2012. 'Identification of putative miRNAs from the deep-branching unicellular flagellates', *Genomics*, 99: 101-7.

Hutzinger, R., R. Feederle, J. Mrazek, N. Schiefermeier, P. J. Balwierz, M. Zavolan, N. Polacek, H. J. Delecluse, and A. Huttenhofer. 2009. 'Expression and processing of a small nucleolar RNA from the Epstein-Barr virus genome', *PLoS Pathog*, 5: e1000547.

Iwasaki, S., T. Kawamata, and Y. Tomari. 2009. 'Drosophila argonaute1 and argonaute2 employ distinct mechanisms for translational repression', *Mol Cell*, 34: 58-67.

Jankov, R. P., and A. Keith Tanswell. 2004. 'Growth factors, postnatal lung growth and bronchopulmonary dysplasia', *Paediatr Respir Rev*, 5 Suppl A: S265-75.

Jiang, Q., M. Lagos-Quintana, D. Liu, Y. Shi, C. Helker, W. Herzog, and F. le Noble. 2013. 'miR-30a regulates endothelial tip cell formation and arteriolar branching', *Hypertension*, 62: 592-8.

Jin, P., D. C. Zarnescu, S. Ceman, M. Nakamoto, J. Mowrey, T. A. Jongens, D. L. Nelson, K. Moses, and S. T. Warren. 2004. 'Biochemical and genetic interaction between the fragile X mental retardation protein and the microRNA pathway', *Nat Neurosci*, 7: 113-7.

Katoh, T., H. Hojo, and T. Suzuki. 2015. 'Destabilization of microRNAs in human cells by 3' deadenylation mediated by PARN and CUGBP1', *Nucleic Acids Res*, 43: 7521-34.

Katoh, T., Y. Sakaguchi, K. Miyauchi, T. Suzuki, S. Kashiwabara, T. Baba, and T. Suzuki. 2009. 'Selective stabilization of mammalian microRNAs by 3' adenylation mediated by the cytoplasmic poly(A) polymerase GLD-2', *Genes Dev*, 23: 433-8.

Ketting, R. F., S. E. Fischer, E. Bernstein, T. Sijen, G. J. Hannon, and R. H. Plasterk. 2001. 'Dicer functions in RNA interference and in synthesis of small RNA involved in developmental timing in C. elegans', *Genes Dev*, 15: 2654-9.

Khvorova, A., A. Reynolds, and S. D. Jayasena. 2003. 'Functional siRNAs and miRNAs exhibit strand bias', *Cell*, 115: 209-16.

Kim, N., and T. H. Vu. 2006. 'Parabronchial smooth muscle cells and alveolar myofibroblasts in lung development', *Birth Defects Res C Embryo Today*, 78: 80-9.

Kim, S. J., P. Angel, R. Lafyatis, K. Hattori, K. Y. Kim, M. B. Sporn, M. Karin, and A. B. Roberts. 1990. 'Autoinduction of transforming growth factor beta 1 is mediated by the AP-1 complex', *Mol Cell Biol*, 10: 1492-7.

Kim, V. N. 2005. 'MicroRNA biogenesis: coordinated cropping and dicing', *Nat Rev Mol Cell Biol*, 6: 376-85.

King, J. A., P. C. Marker, K. J. Seung, and D. M. Kingsley. 1994. 'BMP5 and the molecular, skeletal, and soft-tissue alterations in short ear mice', *Dev Biol*, 166: 112-22.

Knudsen, L., E. R. Weibel, H. J. Gundersen, F. V. Weinstein, and M. Ochs. 2010. 'Assessment of air space size characteristics by intercept (chord) measurement: an accurate and efficient stereological approach', *J Appl Physiol (1985)*, 108: 412-21.

Kresch, M. J., C. Christian, F. Wu, and N. Hussain. 1998. 'Ontogeny of apoptosis during lung development', *Pediatr Res*, 43: 426-31.

Krol, J., V. Busskamp, I. Markiewicz, M. B. Stadler, S. Ribi, J. Richter, J. Duebel, S. Bicker, H. J. Fehling, D. Schubeler, T. G. Oertner, G. Schratt, M. Bibel, B. Roska, and W. Filipowicz. 2010. 'Characterizing light-regulated retinal microRNAs reveals rapid turnover as a common property of neuronal microRNAs', *Cell*, 141: 618-31.

Krol, J., I. Loedige, and W. Filipowicz. 2010. 'The widespread regulation of microRNA biogenesis, function and decay', *Nat Rev Genet*, 11: 597-610.

Kulkarni, A. B., C. G. Huh, D. Becker, A. Geiser, M. Lyght, K. C. Flanders, A. B. Roberts, M. B. Sporn, J. M. Ward, and S. Karlsson. 1993. 'Transforming growth factor beta 1 null mutation in mice causes excessive inflammatory response and early death', *Proc Natl Acad Sci U S A*, 90: 770-4.

Kutz, S. M., J. Hordines, P. J. McKeown-Longo, and P. J. Higgins. 2001. 'TGF-beta1-induced PAI-1 gene expression requires MEK activity and cell-to-substrate adhesion', *J Cell Sci*, 114: 3905-14.

Lagos-Quintana, M., R. Rauhut, A. Yalcin, J. Meyer, W. Lendeckel, and T. Tuschl. 2002. 'Identification of tissue-specific microRNAs from mouse', *Curr Biol*, 12: 735-9.

Lanford, R. E., E. S. Hildebrandt-Eriksen, A. Petri, R. Persson, M. Lindow, M. E. Munk, S. Kauppinen, and H. Orum. 2010. 'Therapeutic silencing of microRNA-122 in primates with chronic hepatitis C virus infection', *Science*, 327: 198-201.

Lee, H. C., L. Li, W. Gu, Z. Xue, S. K. Crosthwaite, A. Pertsemlidis, Z. A. Lewis, M. Freitag, E. U. Selker, C. C. Mello, and Y. Liu. 2010. 'Diverse pathways generate microRNA-like RNAs and Dicer-independent small interfering RNAs in fungi', *Mol Cell*, 38: 803-14.

Lee, R. C., R. L. Feinbaum, and V. Ambros. 1993. 'The C. elegans heterochronic gene lin-4 encodes small RNAs with antisense complementarity to lin-14', *Cell*, 75: 843-54.

Lee, Y., C. Ahn, J. Han, H. Choi, J. Kim, J. Yim, J. Lee, P. Provost, O. Radmark, S. Kim, and V. N. Kim. 2003. 'The nuclear RNase III Drosha initiates microRNA processing', *Nature*, 425: 415-9.

Lee, Y., M. Kim, J. Han, K. H. Yeom, S. Lee, S. H. Baek, and V. N. Kim. 2004. 'MicroRNA genes are transcribed by RNA polymerase II', *EMBO J*, 23: 4051-60.

Li, H., X. Zhao, H. Shan, and H. Liang. 2016. 'MicroRNAs in idiopathic pulmonary fibrosis: involvement in pathogenesis and potential use in diagnosis and therapeutics', *Acta Pharm Sin B*, 6: 531-39.

Li, J., and G. W. Hoyle. 2001. 'Overexpression of PDGF-A in the lung epithelium of transgenic mice produces a lethal phenotype associated with hyperplasia of mesenchymal cells', *Dev Biol*, 239: 338-49.

Liang, H., C. Xu, Z. Pan, Y. Zhang, Z. Xu, Y. Chen, T. Li, X. Li, Y. Liu, L. Huangfu, Y. Lu, Z. Zhang, B. Yang, S. Gitau, Y. Lu, H. Shan, and Z. Du. 2014. 'The antifibrotic effects and mechanisms of microRNA-26a action in idiopathic pulmonary fibrosis', *Mol Ther*, 22: 1122-33.

Lin, X., Z. Yang, P. Zhang, Y. Liu, and G. Shao. 2016. 'miR-154 inhibits migration and invasion of human non-small cell lung cancer by targeting ZEB2', *Oncol Lett*, 12: 301-06.

Lin, X., Z. Yang, P. Zhang, and G. Shao. 2015. 'miR-154 suppresses non-small cell lung cancer growth in vitro and in vivo', *Oncol Rep*, 33: 3053-60.

Lindahl, P., L. Karlsson, M. Hellstrom, S. Gebre-Medhin, K. Willetts, J. K. Heath, and C. Betsholtz. 1997. 'Alveogenesis failure in PDGF-A-deficient mice is coupled to lack of distal spreading of alveolar smooth muscle cell progenitors during lung development', *Development*, 124: 3943-53.

Lino Cardenas, C. L., I. S. Henaoui, E. Courcot, C. Roderburg, C. Cauffiez, S. Aubert, M. C. Copin, B. Wallaert, F. Glowacki, E. Dewaeles, J. Milosevic, J. Maurizio, J. Tedrow, B. Marcet, J. M. Lo-Guidice, N. Kaminski, P. Barbry, T. Luedde, M. Perrais, B. Mari, and N. Pottier. 2013. 'miR-199a-5p Is upregulated during fibrogenic response to tissue injury and mediates TGFbeta-induced lung fibroblast activation by targeting caveolin-1', *PLoS Genet*, 9: e1003291.

Liu, J., F. V. Rivas, J. Wohlschlegel, J. R. Yates, 3rd, R. Parker, and G. J. Hannon. 2005. 'A role for the P-body component GW182 in microRNA function', *Nat Cell Biol*, 7: 1261-6.

Lu, J., K. I. Izvolsky, J. Qian, and W. V. Cardoso. 2005. 'Identification of FGF10 targets in the embryonic lung epithelium during bud morphogenesis', *J Biol Chem*, 280: 4834-41.

Lu, M. M., H. Yang, L. Zhang, W. Shu, D. G. Blair, and E. E. Morrisey. 2001. 'The bone morphogenic protein antagonist gremlin regulates proximal-distal patterning of the lung', *Dev Dyn*, 222: 667-80.

Lu, Y., J. M. Thomson, H. Y. Wong, S. M. Hammond, and B. L. Hogan. 2007. 'Transgenic over-expression of the microRNA miR-17-92 cluster promotes proliferation and inhibits differentiation of lung epithelial progenitor cells', *Dev Biol*, 310: 442-53.

Ma, E., I. J. MacRae, J. F. Kirsch, and J. A. Doudna. 2008. 'Autoinhibition of human dicer by its internal helicase domain', *J Mol Biol*, 380: 237-43.

Macklin, C. C. 1954. 'The pulmonary alveolar mucoid film and the pneumonocytes', *Lancet*, 266: 1099-104.

Mailleux, A. A., D. Tefft, D. Ndiaye, N. Itoh, J. P. Thiery, D. Warburton, and S. Bellusci. 2001. 'Evidence that SPROUTY2 functions as an inhibitor of mouse embryonic lung growth and morphogenesis', *Mech Dev*, 102: 81-94.

Marzi, M. J., F. Ghini, B. Cerruti, S. de Pretis, P. Bonetti, C. Giacomelli, M. M. Gorski, T. Kress, M. Pelizzola, H. Muller, B. Amati, and F. Nicassio. 2016. 'Degradation dynamics of microRNAs revealed by a novel pulse-chase approach', *Genome Res*, 26: 554-65.

Massague, J. 1998. 'TGF-beta signal transduction', *Annu Rev Biochem*, 67: 753-91.

Mathonnet, G., M. R. Fabian, Y. V. Svitkin, A. Parsyan, L. Huck, T. Murata, S. Biffo, W. C. Merrick, E. Darzynkiewicz, R. S. Pillai, W. Filipowicz, T. F. Duchaine, and N. Sonenberg. 2007. 'MicroRNA inhibition of translation initiation in vitro by targeting the cap-binding complex eIF4F', *Science*, 317: 1764-7.

McGowan, S. E., and J. S. Torday. 1997. 'The pulmonary lipofibroblast (lipid interstitial cell) and its contributions to alveolar development', *Annu Rev Physiol*, 59: 43-62.

McManus, M. T., B. B. Haines, C. P. Dillon, C. E. Whitehurst, L. van Parijs, J. Chen, and P. A. Sharp. 2002. 'Small interfering RNA-mediated gene silencing in T lymphocytes', *J Immunol*, 169: 5754-60.

Millan, F. A., F. Denhez, P. Kondaiah, and R. J. Akhurst. 1991. 'Embryonic gene expression patterns of TGF beta 1, beta 2 and beta 3 suggest different developmental functions in vivo', *Development*, 111: 131-43.

Milosevic, J., K. Pandit, M. Magister, E. Rabinovich, D. C. Ellwanger, G. Yu, L. J. Vuga, B. Weksler, P. V. Benos, K. F. Gibson, M. McMillan, M. Kahn, and N. Kaminski. 2012. 'Profibrotic role of miR-154 in pulmonary fibrosis', *Am J Respir Cell Mol Biol*, 47: 879-87.

Min, H., D. M. Danilenko, S. A. Scully, B. Bolon, B. D. Ring, J. E. Tarpley, M. DeRose, and W. S. Simonet. 1998. 'Fgf-10 is required for both limb and lung development and exhibits striking functional similarity to Drosophila branchless', *Genes Dev*, 12: 3156-61.

Minoo, P., G. Su, H. Drum, P. Bringas, and S. Kimura. 1999. 'Defects in tracheoesophageal and lung morphogenesis in Nkx2.1(-/-) mouse embryos', *Dev Biol*, 209: 60-71.

Mishina, Y., A. Suzuki, N. Ueno, and R. R. Behringer. 1995. 'Bmpr encodes a type I bone morphogenetic protein receptor that is essential for gastrulation during mouse embryogenesis', *Genes Dev*, 9: 3027-37.

Miyazono, K., H. Ichijo, and C. H. Heldin. 1993. 'Transforming growth factor-beta: latent forms, binding proteins and receptors', *Growth Factors*, 8: 11-22.

Mohammadi, M., S. K. Olsen, and O. A. Ibrahimi. 2005. 'Structural basis for fibroblast growth factor receptor activation', *Cytokine Growth Factor Rev*, 16: 107-37.

Molnar, A., F. Schwach, D. J. Studholme, E. C. Thuenemann, and D. C. Baulcombe. 2007. 'miRNAs control gene expression in the single-cell alga Chlamydomonas reinhardtii', *Nature*, 447: 1126-9.

Morrisey, E. E., and B. L. Hogan. 2010. 'Preparing for the first breath: genetic and cellular mechanisms in lung development', *Dev Cell*, 18: 8-23.

Mujahid, S., H. C. Nielsen, and M. V. Volpe. 2013. 'MiR-221 and miR-130a regulate lung airway and vascular development', *PLoS One*, 8: e55911.

Nadal, E., G. Chen, M. Gallegos, L. Lin, D. Ferrer-Torres, A. Truini, Z. Wang, J. Lin, R. M. Reddy, R. Llatjos, I. Escobar, J. Moya, A. C. Chang, F. Cardenal, G. Capella, and D. G. Beer. 2013. 'Epigenetic inactivation of microRNA-34b/c predicts poor disease-free survival in early-stage lung adenocarcinoma', *Clin Cancer Res*, 19: 6842-52.

Nakao, A., M. Afrakhte, A. Moren, T. Nakayama, J. L. Christian, R. Heuchel, S. Itoh, M. Kawabata, N. E. Heldin, C. H. Heldin, and P. ten Dijke. 1997. 'Identification of Smad7, a TGFbeta-inducible antagonist of TGF-beta signalling', *Nature*, 389: 631-5.

O'Donnell, K. A., E. A. Wentzel, K. I. Zeller, C. V. Dang, and J. T. Mendell. 2005. 'c-Myc-regulated microRNAs modulate E2F1 expression', *Nature*, 435: 839-43.

Ornitz, D. M., and N. Itoh. 2001. 'Fibroblast growth factors', *Genome Biol*, 2: REVIEWS3005.

Pang, X., K. Huang, Q. Zhang, Y. Zhang, and J. Niu. 2015. 'miR-154 targeting ZEB2 in hepatocellular carcinoma functions as a potential tumor suppressor', *Oncol Rep*, 34: 3272-9.

Park, W. Y., B. Miranda, D. Lebeche, G. Hashimoto, and W. V. Cardoso. 1998. 'FGF-10 is a chemotactic factor for distal epithelial buds during lung development', *Dev Biol*, 201: 125-34.

Pelosi, P., P. R. Rocco, D. Negrini, and A. Passi. 2007. 'The extracellular matrix of the lung and its role in edema formation', *An Acad Bras Cienc*, 79: 285-97.

Pelton, R. W., B. Saxena, M. Jones, H. L. Moses, and L. I. Gold. 1991. 'Immunohistochemical localization of TGF beta 1, TGF beta 2, and TGF beta 3 in the mouse embryo: expression patterns suggest multiple roles during embryonic development', *J Cell Biol*, 115: 1091-105.

Perl, A. K., L. Zhang, and J. A. Whitsett. 2009. 'Conditional expression of genes in the respiratory epithelium in transgenic mice: cautionary notes and toward building a better mouse trap', *Am J Respir Cell Mol Biol*, 40: 1-3.

Perry, M. M., I. M. Adcock, and K. F. Chung. 2015. 'Role of microRNAs in allergic asthma: present and future', *Curr Opin Allergy Clin Immunol*, 15: 156-62.

Pison, U., M. Max, A. Neuendank, S. Weissbach, and S. Pietschmann. 1994. 'Host defence capacities of pulmonary surfactant: evidence for 'non-surfactant' functions of the surfactant system', *Eur J Clin Invest*, 24: 586-99.

Postigo, A. A., J. L. Depp, J. J. Taylor, and K. L. Kroll. 2003. 'Regulation of Smad signaling through a differential recruitment of coactivators and corepressors by ZEB proteins', *EMBO J*, 22: 2453-62.

Ramasamy, S. K., A. A. Mailleux, V. V. Gupte, F. Mata, F. G. Sala, J. M. Veltmaat, P. M. Del Moral, S. De Langhe, S. Parsa, L. K. Kelly, R. Kelly, W. Shia, E. Keshet, P. Minoo, D. Warburton, and S. Bellusci. 2007. 'Fgf10 dosage is critical for the amplification of epithelial cell progenitors and for the formation of multiple mesenchymal lineages during lung development', *Dev Biol*, 307: 237-47.

Reddi, A. H., and A. Reddi. 2009. 'Bone morphogenetic proteins (BMPs): from morphogens to metabologens', *Cytokine Growth Factor Rev*, 20: 341-2.

Redfern, A. D., S. M. Colley, D. J. Beveridge, N. Ikeda, M. R. Epis, X. Li, C. E. Foulds, L. M. Stuart, A. Barker, V. J. Russell, K. Ramsay, S. J. Kobelke, X. Li, E. C. Hatchell, C. Payne, K. M. Giles, A. Messineo, A. Gatignol, R. B. Lanz, B. W. O'Malley, and P. J. Leedman. 2013. 'RNA-induced silencing complex (RISC) Proteins PACT, TRBP, and Dicer are SRA binding nuclear receptor coregulators', *Proc Natl Acad Sci U S A*, 110: 6536-41.

Reinhart, B. J., F. J. Slack, M. Basson, A. E. Pasquinelli, J. C. Bettinger, A. E. Rougvie, H. R. Horvitz, and G. Ruvkun. 2000. 'The 21-nucleotide let-7 RNA regulates developmental timing in Caenorhabditis elegans', *Nature*, 403: 901-6.

Rodriguez, A., S. Griffiths-Jones, J. L. Ashurst, and A. Bradley. 2004. 'Identification of mammalian microRNA host genes and transcription units', *Genome Res*, 14: 1902-10.

Roush, S. F., and F. J. Slack. 2009. 'Transcription of the C. elegans let-7 microRNA is temporally regulated by one of its targets, hbl-1', *Dev Biol*, 334: 523-34.

Saito, A., M. Horie, and T. Nagase. 2018. 'TGF-beta Signaling in Lung Health and Disease', *Int J Mol Sci*, 19.

Salzman, D. W., J. Shubert-Coleman, and H. Furneaux. 2007. 'P68 RNA helicase unwinds the human let-7 microRNA precursor duplex and is required for let-7-directed silencing of gene expression', *J Biol Chem*, 282: 32773-9.

Sanford, L. P., I. Ormsby, A. C. Gittenberger-de Groot, H. Sariola, R. Friedman, G. P. Boivin, E. L. Cardell, and T. Doetschman. 1997. 'TGFbeta2 knockout mice have multiple developmental defects that are non-overlapping with other TGFbeta knockout phenotypes', *Development*, 124: 2659-70.

Schwarz, D. S., G. Hutvagner, T. Du, Z. Xu, N. Aronin, and P. D. Zamore. 2003. 'Asymmetry in the assembly of the RNAi enzyme complex', *Cell*, 115: 199-208.

Seitz, H., H. Royo, M. L. Bortolin, S. P. Lin, A. C. Ferguson-Smith, and J. Cavaille. 2004. 'A large imprinted microRNA gene cluster at the mouse Dlk1-Gtl2 domain', *Genome Res*, 14: 1741-8.

Serra, R., R. W. Pelton, and H. L. Moses. 1994. 'TGF beta 1 inhibits branching morphogenesis and N-myc expression in lung bud organ cultures', *Development*, 120: 2153-61.

Sethi, P., and W. J. Lukiw. 2009. 'Micro-RNA abundance and stability in human brain: specific alterations in Alzheimer's disease temporal lobe neocortex', *Neurosci Lett*, 459: 100-4.

Shi, W., N. Heisterkamp, J. Groffen, J. Zhao, D. Warburton, and V. Kaartinen. 1999. 'TGF-beta3-null mutation does not abrogate fetal lung maturation in vivo by glucocorticoids', *Am J Physiol*, 277: L1205-13.

Shi, Y., and J. Massague. 2003. 'Mechanisms of TGF-beta signaling from cell membrane to the nucleus', *Cell*, 113: 685-700.

Song, J. J., S. K. Smith, G. J. Hannon, and L. Joshua-Tor. 2004. 'Crystal structure of Argonaute and its implications for RISC slicer activity', *Science*, 305: 1434-7.

Sountoulidis, A., A. Stavropoulos, S. Giaglis, E. Apostolou, R. Monteiro, S. M. Chuva de Sousa Lopes, H. Chen, B. R. Stripp, C. Mummery, E. Andreakos, and P. Sideras. 2012. 'Activation of the canonical bone morphogenetic protein (BMP) pathway during lung morphogenesis and adult lung tissue repair', *PLoS One*, 7: e41460.

Spooner, B. S., and N. K. Wessells. 1970. 'Mammalian lung development: interactions in primordium formation and bronchial morphogenesis', *J Exp Zool*, 175: 445-54.

Sporn, M. B., and A. B. Roberts. 1990. 'TGF-beta: problems and prospects', *Cell Regul*, 1: 875-82.

Suh, M. R., Y. Lee, J. Y. Kim, S. K. Kim, S. H. Moon, J. Y. Lee, K. Y. Cha, H. M. Chung, H. S. Yoon, S. Y. Moon, V. N. Kim, and K. S. Kim. 2004. 'Human embryonic stem cells express a unique set of microRNAs', *Dev Biol*, 270: 488-98.

Sun, J., H. Chen, C. Chen, J. A. Whitsett, Y. Mishina, P. Bringas, Jr., J. C. Ma, D. Warburton, and W. Shi. 2008. 'Prenatal lung epithelial cell-specific abrogation of Alk3-bone morphogenetic protein signaling causes neonatal respiratory distress by disrupting distal airway formation', *Am J Pathol*, 172: 571-82.

Suzuki, H. I., K. Yamagata, K. Sugimoto, T. Iwamoto, S. Kato, and K. Miyazono. 2009. 'Modulation of microRNA processing by p53', *Nature*, 460: 529-33.

Sylva, M., V. S. Li, A. A. Buffing, J. H. van Es, M. van den Born, S. van der Velden, Q. Gunst, J. H. Koolstra, A. F. Moorman, H. Clevers, and M. J. van den Hoff. 2011. 'The BMP antagonist follistatin-like 1 is required for skeletal and lung organogenesis', *PLoS One*, 6: e22616.

Szymczak, I., J. Wieczfinska, and R. Pawliczak. 2016. 'Molecular Background of miRNA Role in Asthma and COPD: An Updated Insight', *Biomed Res Int*, 2016: 7802521.

Tang, N., W. F. Marshall, M. McMahon, R. J. Metzger, and G. R. Martin. 2011. 'Control of mitotic spindle angle by the RAS-regulated ERK1/2 pathway determines lung tube shape', *Science*, 333: 342-5.

Tefft, D., M. Lee, S. Smith, D. L. Crowe, S. Bellusci, and D. Warburton. 2002. 'mSprouty2 inhibits FGF10-activated MAP kinase by differentially binding to upstream target proteins', *Am J Physiol Lung Cell Mol Physiol*, 283: L700-6.

Tefft, J. D., M. Lee, S. Smith, M. Leinwand, J. Zhao, P. Bringas, Jr., D. L. Crowe, and D. Warburton. 1999. 'Conserved function of mSpry-2, a murine homolog of Drosophila sprouty, which negatively modulates respiratory organogenesis', *Curr Biol*, 9: 219-22.

Topper, J. N., J. Cai, Y. Qiu, K. R. Anderson, Y. Y. Xu, J. D. Deeds, R. Feeley, C. J. Gimeno, E. A. Woolf, O. Tayber, G. G. Mays, B. A. Sampson, F. J. Schoen, M. A. Gimbrone, Jr., and D. Falb. 1997. 'Vascular MADs: two novel MAD-related genes selectively inducible by flow in human vascular endothelium', *Proc Natl Acad Sci U S A*, 94: 9314-9.

Vaccaro, C., and J. S. Brody. 1978. 'Ultrastructure of developing alveoli. I. The role of the interstitial fibroblast', *Anat Rec*, 192: 467-79.

van Rooij, E., L. B. Sutherland, X. Qi, J. A. Richardson, J. Hill, and E. N. Olson. 2007. 'Control of stress-dependent cardiac growth and gene expression by a microRNA', *Science*, 316: 575-9.

Vasudevan, S., Y. Tong, and J. A. Steitz. 2007. 'Switching from repression to activation: microRNAs can up-regulate translation', *Science*, 318: 1931-4.

Vencken, S. F., C. M. Greene, and P. J. McKiernan. 2015. 'Non-coding RNA as lung disease biomarkers', *Thorax*, 70: 501-3.

Verschueren, K., J. E. Remacle, C. Collart, H. Kraft, B. S. Baker, P. Tylzanowski, L. Nelles, G. Wuytens, M. T. Su, R. Bodmer, J. C. Smith, and D. Huylebroeck. 1999. 'SIP1, a novel zinc finger/homeodomain repressor, interacts with Smad proteins and binds to 5'-CACCT sequences in candidate target genes', *J Biol Chem*, 274: 20489-98.

Viswanathan, S. R., G. Q. Daley, and R. I. Gregory. 2008. 'Selective blockade of microRNA processing by Lin28', *Science*, 320: 97-100.

Wang, M., Y. Huang, Z. Liang, D. Liu, Y. Lu, Y. Dai, G. Feng, and C. Wang. 2016. 'Plasma miRNAs might be promising biomarkers of chronic obstructive pulmonary disease', *Clin Respir J*, 10: 104-11.

Wang, Y., D. B. Frank, M. P. Morley, S. Zhou, X. Wang, M. M. Lu, M. A. Lazar, and E. E. Morrisey. 2016. 'HDAC3-Dependent Epigenetic Pathway Controls Lung Alveolar Epithelial Cell Remodeling and Spreading via miR-17-92 and TGF-beta Signaling Regulation', *Dev Cell*, 36: 303-15.

Wang, Y., C. Huang, N. R. Chintagari, D. Xi, T. Weng, and L. Liu. 2015. 'miR-124 regulates fetal pulmonary epithelial cell maturation', *Am J Physiol Lung Cell Mol Physiol*, 309: L400-13.

Wang, Y., C. Huang, N. Reddy Chintagari, M. Bhaskaran, T. Weng, Y. Guo, X. Xiao, and L. Liu. 2013. 'miR-375 regulates rat alveolar epithelial cell trans-differentiation by inhibiting Wnt/beta-catenin pathway', *Nucleic Acids Res*, 41: 3833-44.

Warburton, D., L. Perin, R. Defilippo, S. Bellusci, W. Shi, and B. Driscoll. 2008. 'Stem/progenitor cells in lung development, injury repair, and regeneration', *Proc Am Thorac Soc*, 5: 703-6.

Weaver, M., N. R. Dunn, and B. L. Hogan. 2000. 'Bmp4 and Fgf10 play opposing roles during lung bud morphogenesis', *Development*, 127: 2695-704.

Weinstein, M., X. Xu, K. Ohyama, and C. X. Deng. 1998. 'FGFR-3 and FGFR-4 function cooperatively to direct alveogenesis in the murine lung', *Development*, 125: 3615-23.

Williams, A. E., S. A. Moschos, M. M. Perry, P. J. Barnes, and M. A. Lindsay. 2007. 'Maternally imprinted microRNAs are differentially expressed during mouse and human lung development', *Dev Dyn*, 236: 572-80.

Winter, J., S. Jung, S. Keller, R. I. Gregory, and S. Diederichs. 2009. 'Many roads to maturity: microRNA biogenesis pathways and their regulation', *Nat Cell Biol*, 11: 228-34.

Xin, C., H. Zhang, and Z. Liu. 2014. 'miR-154 suppresses colorectal cancer cell growth and motility by targeting TLR2', *Mol Cell Biochem*, 387: 271-7.

Xu, H., D. Fei, S. Zong, and Z. Fan. 2016. 'MicroRNA-154 inhibits growth and invasion of breast cancer cells through targeting E2F5', *Am J Transl Res*, 8: 2620-30.

Yang, L., Z. Yan, Y. Wang, W. Ma, and C. Li. 2016. 'Down-expression of miR-154 suppresses tumourigenesis in CD133(+) glioblastoma stem cells', *Cell Biochem Funct*, 34: 404-13.

Yi, R., Y. Qin, I. G. Macara, and B. R. Cullen. 2003. 'Exportin-5 mediates the nuclear export of pre-microRNAs and short hairpin RNAs', *Genes Dev*, 17: 3011-6.

Yin, Y., F. Wang, and D. M. Ornitz. 2011. 'Mesothelial- and epithelial-derived FGF9 have distinct functions in the regulation of lung development', *Development*, 138: 3169-77.

Yu, Y., J. Zuo, Q. Tan, K. Zar Thin, P. Li, M. Zhu, M. Yu, Z. Fu, C. Liang, and J. Tu. 2017. 'Plasma miR-92a-2 as a biomarker for small cell lung cancer', *Cancer Biomark*.

Zeng, Y., and B. R. Cullen. 2003. 'Sequence requirements for micro RNA processing and function in human cells', *RNA*, 9: 112-23.

Zhang, P. X., J. Cheng, S. Zou, A. D. D'Souza, J. L. Koff, J. Lu, P. J. Lee, D. S. Krause, M. E. Egan, and E. M. Bruscia. 2015. 'Pharmacological modulation of the AKT/microRNA-199a-5p/CAV1 pathway ameliorates cystic fibrosis lung hyper-inflammation', *Nat Commun*, 6: 6221.

Zhao, D., R. Wang, J. Fang, X. Ji, J. Li, X. Chen, G. Sun, Z. Wang, W. Liu, Y. Wang, G. Cheng, H. Zhen, C. Sun, and Z. Fei. 2016. 'MiR-154 Functions as a Tumor Suppressor in Glioblastoma by Targeting Wnt5a', *Mol Neurobiol*.

———. 2017. 'Retraction Note to: MiR-154 Functions as a Tumor Suppressor in Glioblastoma by Targeting Wnt5a', *Mol Neurobiol*, 54: 8460.

Zhao, J., D. Bu, M. Lee, H. C. Slavkin, F. L. Hall, and D. Warburton. 1996. 'Abrogation of transforming growth factor-beta type II receptor stimulates embryonic mouse lung branching morphogenesis in culture', *Dev Biol*, 180: 242-57.

Zhao, J., M. Lee, S. Smith, and D. Warburton. 1998. 'Abrogation of Smad3 and Smad2 or of Smad4 gene expression positively regulates murine embryonic lung branching morphogenesis in culture', *Dev Biol*, 194: 182-95.

Zhao, J., W. Shi, H. Chen, and D. Warburton. 2000. 'Smad7 and Smad6 differentially modulate transforming growth factor beta -induced inhibition of embryonic lung morphogenesis', *J Biol Chem*, 275: 23992-7.

Zhao, J., W. Shi, Y. L. Wang, H. Chen, P. Bringas, Jr., M. B. Datto, J. P. Frederick, X. F. Wang, and D. Warburton. 2002. 'Smad3 deficiency attenuates bleomycin-induced pulmonary fibrosis in mice', *Am J Physiol Lung Cell Mol Physiol*, 282: L585-93.

Zhao, Y., and D. U. Shah. 2000. 'Expression of transforming growth factor-beta type I and type II receptors is altered in rat lungs undergoing bleomycin-induced pulmonary fibrosis', *Exp Mol Pathol*, 69: 67-78.

Zhao, Y., and S. L. Young. 1995. 'Expression of transforming growth factor-beta type II receptor in rat lung is regulated during development', *Am J Physiol*, 269: L419-26.

Zhu, C., J. Li, G. Cheng, H. Zhou, L. Tao, H. Cai, P. Li, Q. Cao, X. Ju, X. Meng, M. Wang, Z. Zhang, C. Qin, L. Hua, C. Yin, and P. Shao. 2013. 'miR-154 inhibits EMT by targeting HMGA2 in prostate cancer cells', *Mol Cell Biochem*, 379: 69-75.

Zhuo, H. C., Y. F. Song, J. Ye, G. X. Lai, and D. L. Liu. 2016. 'MicroRNA-154 functions as a tumor suppressor and directly targets HMGA2 in human non-small cell lung cancer', *Genet Mol Res*, 15.

9 Acknowledgements

Finally, I would like to thank everyone who accompanied and supported me on my way to this doctoral thesis.

First of all I would like to thank Prof. Dr. Saverio Bellusci cordially for the opportunity to become part of his laboratory and thus gain a well-founded insight into basic research. His enthusiasm and passion encouraged and inspired me in my work. I also thank him for all the resources he has put at my disposal for the implementation of this project.

Secondly, I would like to thank Dr. Cho-Ming Chao, who has always been available to me as my project supervisor. His friendly leadership was irreplaceable for me during the realization.

My special thanks also go to Kerstin and Heike, as well as Amit, Alena, Jana, Mathew, Negah and Thomas who all belong to AG Bellusci and whose advice and actions I could often rely on. I really enjoyed the friendly and familiar atmosphere in the team. It was a pleasure to meet you all.
At this point I would also like to thank my colleagues Zvonimir, Volker, Fadi and Jamshid, with whom I could exchange information at any time and whose knowledge I was often allowed to profit from.

From my private environment I would like to thank especially my friends Zvonimir Rako, Alexander Häger and Volker Zimmermann, who helped me with the completion of the doctoral thesis and also privately in many respects.

Last but not least, I would like to thank the people who have always been at my side: My parents Christa and Ulrich, as well as my sisters Gesa and Anne. Your good will and unconditional support have made many things in my life easier.